

Université de Montréal

Investigation of Femtosecond Laser Technology for the Fabrication of Drug Nanocrystals in Suspension

par

Sukhdeep Kenth

Sciences pharmaceutiques

Faculté de pharmacie

Mémoire présenté à la Faculté des études supérieures
en vue de l'obtention du grade de Maître en sciences (M.Sc.)
en sciences pharmaceutiques
option technologie pharmaceutique

Décembre 2009

© Sukhdeep Kenth, 2009

Université de Montréal
Faculté des études supérieures et postdoctorales

Ce mémoire intitulé:

Investigation of Femtosecond Laser Technology for the Fabrication of Drug Nanocrystals
in Suspension

Présenté par :
Sukhdeep Kenth

a été évaluée par un jury composé des personnes suivantes :

Dr Grégoire Leclair, président-rapporteur
Dr Jean-Christophe Leroux, directeur de recherche
Dr Michel Meunier, co-directeur
Dr Sophie Dorothée-Clas, membre du jury

Résumé

La technique du laser femtoseconde (fs) a été précédemment utilisée pour la production de nanoparticules d'or dans un environnement aqueux biologiquement compatible. Au cours de ce travail de maîtrise, cette méthode a été investiguée en vue d'une application pour la fabrication de nanocristaux de médicament en utilisant le paclitaxel comme modèle. Deux procédés distincts de cette technologie à savoir l'ablation et la fragmentation ont été étudiés. L'influence de la puissance du laser, de point de focalisation, et de la durée du traitement sur la distribution de taille des particules obtenues ainsi que leur intégrité chimique a été évaluée. Les paramètres ont ainsi été optimisés pour la fabrication des nanoparticules. L'évaluation morphologique et chimique a été réalisée par microscopie électronique et spectroscopie infrarouge respectivement. L'état cristallin des nanoparticules de paclitaxel a été caractérisé par calorimétrie différentielle et diffraction des rayons X.

L'optimisation du procédé de production de nanoparticules par laser fs a permis d'obtenir des nanocristaux de taille moyenne (400 nm, polydispersité $\leq 0,3$). Cependant une dégradation non négligeable a été observée. La cristallinité du médicament a été maintenue durant la procédure de réduction de taille, mais le paclitaxel anhydre a été transformé en une forme hydratée.

Les résultats de cette étude suggèrent que le laser fs peut générer des nanocristaux de principe actif. Cependant cette technique peut se révéler problématique pour des médicaments sensibles à la dégradation. Grâce à sa facilité d'utilisation et la possibilité de travailler avec des quantités restreintes de produit, le laser fs pourrait représenter une alternative valable pour la production de nanoparticules de médicaments peu solubles lors des phases initiales de développement préclinique.

Mots-clés: paclitaxel, nanocristaux, laser femtoseconde, ablation, fragmentation

Abstract

Femtosecond (fs) laser ablation and fragmentation, a novel technique based upon the breakdown of material using laser energy was previously used for the production of fine gold nanoparticles in suspension. This technique has been newly investigated for the fabrication of paclitaxel nanocrystals in aqueous solution. In this work, we report the fabrication and characterization of paclitaxel nanocrystals generated by fs laser technology. Two distinct methods of this technology have been explored: ablation and fragmentation. The influence of the laser power, focusing position and treatment time on the particle size, size distribution and chemical integrity of the drug has been studied. Morphology and chemical composition of the finest paclitaxel nanocrystal formulation was studied by scanning electron microscopy and Fourier-transform infrared spectroscopy respectively. Differential scanning calorimetry and X-ray diffraction analyses were employed to evaluate the polymorphic state of the paclitaxel nanocrystals.

Optimal laser fabrication parameters have been established for the fabrication of uniformly small sized paclitaxel nanocrystals. Those optimal conditions generated finely-sized paclitaxel nanoparticles (400 nm, $PDI \leq 0.3$) with a considerable degradation. The drug remained crystalline upon nanonization at high power, though the anhydrous crystals were converted to a partially hydrated form.

These findings suggest that drug nanocrystals could be produced using the fs laser technology; however, this technique may be inappropriate for drugs sensitive to degradation. Moreover, the simple fabrication of drug nanocrystals using the fs laser fragmentation presents a great asset for the initial phases of preclinical development of many poorly soluble drug candidates, which are not as sensitive as paclitaxel.

Keywords: paclitaxel, nanocrystals, femtosecond, ablation, fragmentation

Table of Contents

RESUMÉ.....	i
ABSTRACT.....	ii
LIST OF TABLES	vi
LIST OF FIGURES.....	vii
ABBREVIATIONS.....	x
ACKNOWLEDGEMENTS.....	xiii
CHAPTER 1 : STRATEGIES TO ENHANCE DRUG SOLUBILITY.....	1
1.1. Introduction	2
1. 2. Salt formation	6
1.3. Complexation	7
1.4. Prodrugs	10
1.5. Cosolvents	13
1.6. Surfactants and Micelles	14
1.7. Emulsions, Microemulsions and Self-emulsifying delivery systems	16
1.8. Liposomes	17
1.9. Polymeric Solid dispersions	20
1.10 Size Reduction	21
1.11 References	24
CHAPTER 2: NANOCRYSTALS AND NANOSUSPENSIONS	28
2.1. Introduction	29
2.2. Methods of nanocrystal fabrication	31
2.2.1 Bottom-up strategies	31
2.2.2 Top-down strategies	33
2.3. Characterization of Nanocrystals	38
2.4. Administration routes	40
2.4.1 Oral	40
2.4.2 Parenteral	41

2.4.3	Ocular	41
2.4.4	Pulmonary	42
2.5	Marketed Nanocrystalline drugs	43
2.6	References	45
CHAPTER 3: LASER FABRICATION OF NANOCRYSTALS IN LIQUID		
	48
3.1	Introduction	49
3.2	Fabrication of inorganic nanosuspensions	52
3.3	Fabrication of organic nanosuspensions	56
3.4.	Fabrication of drug nanosuspensions	57
3.5	Research proposal and Objectives	59
3.6	References	63
CHAPTER 4: PRESENTATION OF ARTICLE		67
4.1	Absract	68
4.2	Introduction	69
4.3.	Experimental	72
	4.3.1 Materials	72
	4.3.2 Methods	72
	4.3.2.1 Preparation of paclitaxel tablet and suspension	72
	4.3.2.2 Fs-laser treatment	72
	4.3.2.3 Paclitaxel Assay.....	73
	4.3.2.4 Particle size and zeta potential measurements	74
	4.3.2.5 Scanning electron microscopy.....	74
	4.3.2.6 Thermal Analyses.....	75
	4.3.2.7 Spectroscopic Analyses.....	75
4.4.	Results and Discussion	77
4.5.	Conclusion	82
4.6.	Acknowledgements	83
4.7	References	96

CHAPTER 5: DISCUSSION	100
5.1 Optimization of laser ablation procedure	102
5.2. Optimization of fragmentation (following ablation)	106
5.3. Optimization of single-step fragmentation strategy	107
5.4. Optimization of fragmentation in larger volume	109
5.5 Characterization of paclitaxel nanocrystals	110
5.6 References	112
CHAPTER 6: CONCLUSION	115
References	118
APPENDIX I: Mononuclear phagocyte system.....	i
APPENDIX II: Degradation products of paclitaxel.....	ii
APPENDIX III: Optimization of HPLC assay.....	iii

List of tables

Table 1.1: Approved and marketed drug–cyclodextrin complexes in various world markets	9
Table 2.1: Summary of nanocrystalline products currently on the market	43
Table 4.1: Degradation of the paclitaxel colloidal suspensions generated by ablation at three focusing conditions. Mean \pm SD (n=3)	91
Table 4.2 : Chemical degradation, size distribution and surface charge of paclitaxel suspensions prepared by two-step fs-laser ablation and fragmentation. Mean \pm SD (n=3).....	92
Table 4.3 : Chemical degradation and size distribution of paclitaxel particles obtained by fragmentation (60 min) Mean \pm SD (n=3).....	93
Table 4.S1 : XRD peaks (angle 2θ) comparison of anhydrous paclitaxel, water-exposed paclitaxel, laser fragmented nanocrystals and dihydrate paclitaxel	95
Table 5.1: Degradation and size analysis of paclitaxel particles by ablation and fragmentation in two different surfactants at various concentrations n=1	106
Table 5.2: Degradation and size analysis of fragmented paclitaxel suspension, n=1.....	107
Table 5.3 : Scale-up of fragmentation process at 400mW, n=1.....	109

List of figures

Figure 1.1: Drug administration and transport in the body.....	3
Figure 1.2: The Biopharmaceutics Classification System (BCS).....	4
Figure 1.3: Chemical structure of a cyclodextrin molecule.....	7
Figure 1.4: Complexation of drug and cyclodextrin.....	8
Figure 1.5: An illustration of the prodrug concept.....	10
Figure 1.6: Paclitaxel prodrug strategies	11
Figure 1.7: Representation of micelle formation.....	15
Figure 1.8: Structure of a liposome.....	17
Figure 1.9: Classification of liposomes.....	19
Figure. 1.10. Dissolution velocity dc/dt and saturation solubility C_s as a function of the size of drug powders ranging from coarse to nanonized drugs	22
Figure 2.1: Comparison of plasma concentrations of active ingredient of EMEND [®] following oral administration in Beagle dogs of a conventional suspension and a NanoCrystal [®] dispersion formulation of MK-0869.....	29
Figure 2.2: schematic representation of the media milling process.....	34
Figure 2.3: High pressure homogenization technique: (right) forcing of drug suspension through narrow valve, (left) fabrication of drug nanocrystals due to generated forces.....	36

Figure 3.1: (left) Typical experimental set-up for laser ablation at solid-liquid interface and (right) laser fragmentation; irradiation of of suspension by laser 50

Figure 3.2. (A) Illustration of the production of drug nanoparticles by femtosecond laser ablation; B) Photography of a paclitaxel tablet immersed in a poloxamer 188 aqueous solution and irradiated by a femtosecond laser 60

Figure 3.3. (A) Size distribution of drug nanoparticles produced by femtosecond laser ablation before (■) and after (●) the second laser treatment step; (B) illustration of the fragmentation process during the second laser treatment step..... 60

Figure 4.1: Representation of fs-laser ablation (top) and fragmentation (bottom) methods. 84

Figure 4.2: Chemical Structure of paclitaxel (5 β ,20-epoxy-1,2 α ,4,7 β ,13 α -hexahydroxytax-11-en-9-one 4,10- diacetate 2-benzoate 13-ester with (2*R*,3*S*)-*N*-benzoyl-3-phenyllisoserine) 85

Figure 4.3 (top). Paclitaxel concentration of the suspensions prepared by fs-laser ablation at focusing positions of $z = 0$ mm (squares), 1 (circles) and 1.5 (triangles), at power ranging from 25 to 400 mW. Mean \pm SD ($n=3$). **(bottom)** Paclitaxel concentration of the colloidal suspensions prepared by fs-laser ablation at focusing positions $z = 1$, 150 mW, and time ranging from 10 to 60 min. Mean \pm SD ($n=3$)..... 86

Figure 4.4: Scanning electron micrographs of **(right)** water-exposed non fragmented paclitaxel and **(left)** laser fragmented paclitaxel nanocrystals (400 mW, 60 min). 87

Figure 4.5 :FTIR spectra of anhydrous paclitaxel (**d**), water exposed non-fragmented paclitaxel (**c**), laser fragmented nanocrystals (**b**) and dihydrate paclitaxel (**a**).....88

Figure 4.6 : DSC thermograph of anhydrous paclitaxel (**a**), water exposed non-fragmented paclitaxel (**b**) laser fragmented (400 mW, 60 min) nanocrystals (**c**) and dihydrate paclitaxel (**d**).89

Figure 4.7: XRD analysis of anhydrous paclitaxel (**d**), water exposed non-fragmented paclitaxel (**c**), laser fragmented (400 mW, 60 min) paclitaxel nanocrystals (**b**) and dihydrate paclitaxel (**a**). 90

Figure 4.S1: TGA thermograph of paclitaxel anhydrous powder (**a**), water exposed non-fragmented paclitaxel (**b**) laser fragmented (400 mW, 60 min) nanocrystals (**c**) and dihydrate paclitaxel (**d**). Weight percent is expressed in solid line and derivative weight percent is expressed as dashed line..... 94

Figure 4.S2: XRD analysis of milled paclitaxel (mill-PTX), dihydrate paclitaxel ($2\text{H}_2\text{O}\cdot\text{PTX}$) and anhydrous paclitaxel (PTX)..... 97

Figure 5.1: SEM images of craters formed with ablation ($z = 1\text{ mm}$, 20 min) on the surface of paclitaxel tablet at 50 mW (Left) and 250 mw (Right). 102

Figure A3: HPLC assay of paclitaxel and degradation products iii

Abbreviations

API	Active pharmaceutical ingredient
BCS	Biopharmaceutical Classification System
Bac	Baccatin III
CD	Cyclodextrin
CMC	Critical micelle concentration
DEPTX	10-Deacetyl-7-epipaclitaxel
DLS	Dynamic light scattering
DSC	Differential scanning calorimetry
DPH	Diphenylhydantoin
DPTX	10-Deacetylpaclitaxel
EPTX	7-Epipaclitaxel
Fs	Femtosecond
FT-IR	Fourier-transform infrared spectroscopy
HPMC	Hydroxymethylcellulose
HPLC	High performance liquid chromatography
GI	Gastrointestinal
LD	Laser diffractrometry
MPS	Mononuclear phagocyte system
ns	Nanosecond

PCS	Photon correlation spectroscopy
PDI	Polydispersity index
PEG	Poly (ethylene glycol
PLA	Pulsed laser ablation
PLD	Pulsed laser deposition
PTX	Paclitaxel
PTCDA	3,4,9,10-perylenetetracarboxylicdianhydride
PVP	Polyvinylpyrrolidone
RESS	Rapid expansion from supercritical solution
RESAS	Rapid expansion from supercritical aqueous solution
SAS	Supercritical anti-solvent
SEDDS	Self-emulsifying drug delivery systems
SEM	Scanning electron microscopy
TGA	Thermal gravimetric analysis
VOPc	Vanadyl phthalocyanine
XRD	X-ray diffraction

*For my wonderful mother, my representation
of strength, courage & patience*

Acknowledgements

First and foremost, I would like to express my sincerest gratitude to my supervisor, Dr Jean-Christophe Leroux, for presenting me the opportunity to work in his group, with the responsibility of conducting such an exciting and innovative research project. I appreciate his guidance and support throughout my research studies.

Secondly, I would like to thank my co-director, Dr Michel Meunier, for the giving me the opportunity to work in the laser processing laboratory at École Polytechnique. I am grateful for his valuable opinions and guidance.

Next, I would thank Dr. Jean-Philippe Sylvestre, for providing valuable advice and assistance for my laser experiments. Furthermore, I am grateful to all my lab colleagues for their guidance in the lab, and teaching me how to be a patient and vigilant researcher. I enjoyed working with such intelligent and friendly people. Special thanks to Dr. Jeanne Leblond, Dr. Geneviève Gaucher and Maud Pinier for their support and friendship throughout my graduate studies.

I am also thankful to *Fonds de la recherche en santé Québec* (FRSQ) for financial support and to Dr Grégoire Leclair and Dr Sophie-Dorothee Clas for taking the time to review my thesis.

Lastly, I would like to thank my wonderful friends and family, especially my parents for their love, support and care.

CHAPTER 1:

Strategies to Enhance Drug Solubility

1.1 Introduction

Pharmaceutical products may be administered through various routes, such as oral, nasal, dermal, intravenous, pulmonary, ocular, rectal, or vaginal delivery. However the oral route of administration is preferred, for its many advantages. When ingested orally, the drug is absorbed by the gastrointestinal (GI) tract and enters the hepatic system. Upon its passage through the GI tract, the drug encounters diverse environments with respect to pH, enzymes, electrolytes, fluidity, surface features, all of which may influence its absorption (Kwan 1997). Part of the orally administered dose may not be available for absorption as a consequence of chemical degradation in the GI tract, or it may be metabolized through the gut wall (Figure 1.1). Next, as the drug passes through the portal vein, it is carried to the liver before reaching systemic circulation, where it is distributed through the bloodstream to various tissues. The main problem here is that the liver metabolizes many drugs, and sometimes only a small fraction of active drug substance is available for distribution to the rest of the body. This phenomenon is known as the first pass effect, and greatly reduces bioavailability of some drugs. This effect is defined as the amount of ingested dose that reaches the systemic circulation (Mahota 2007). If administered intravenously the drug bypasses absorption and metabolism processes and is directly available in the bloodstream, and by definition bioavailability of a drug is 100%. The low oral bioavailability of drugs may be attributed to several factors, such as slow dissolution rate, poor solubility, metabolism by GI tract or liver due to first pass effect, chemical instability in the GI tract and/or poor permeability across intestinal membrane (Horter 2001). In addition, the absorption of the drug across the GI tract can highly depend upon membrane transport proteins (Rajendran 2010). Also known as drug transporters, these proteins allow for the active transport of many drug compounds across biological membranes (Lee 2009).

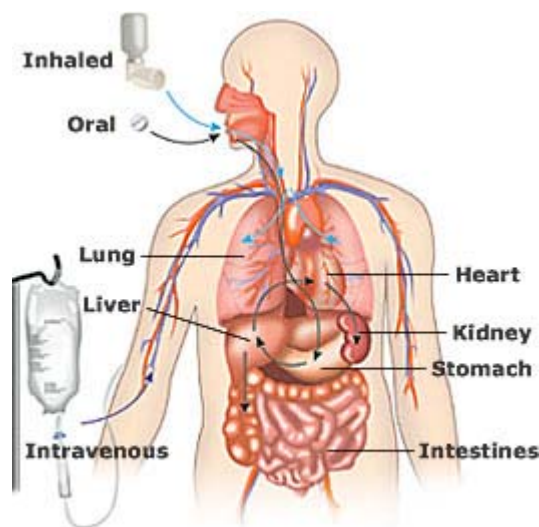


Figure 1.1: Drug administration and transport in the body.

(nihseniorhealth.gov/images/drug_admin1.jpg)

Pharmacological activity of a drug partly depends on its bioavailability, which subsequently depends on its solubility, dissolution rate permeability. Therefore a drug must have an adequate aqueous solubility for systemic absorption and therapeutic response. Solubility, a thermodynamic property, refers to the concentration of saturated drug in solution, whereas dissolution, a kinetic parameter, is the rate at which the drug dissolves (Yvonne 2010). The aqueous solubility of a drug is a prime determinant of its dissolution rate. As a result of its poor solubility, the dissolution of the drug is so slow that dissolution takes longer than the transit time past its absorptive sites, resulting in incomplete bioavailability when administered orally (Horter 2001). In the case of parenteral administration (when the drug is dissolved in an organic solvent or micelles), it bears the high risk of precipitation in the circulatory system thereby becoming lodged in capillaries and obstructing their blood flow. Permeability, solubility and dissolution are major determinants of GI drug absorption. Permeability is defined as the rate at which the drug molecule is transported across a

membrane (Urban 2007). It is an important factor controlling the absorption and thus the pharmacological activity of a drug (Yvonne 2010). The Biopharmaceutics Classification System (BCS) categorizes drugs based upon their solubility and permeability (Figure 1.2). The solubility classification is based upon the dose strength of the drug. A highly soluble drug has a high strength such that it is soluble in a volume of 250 ml or less of aqueous media over pH range 1-7.5. If the drug does not exhibit high dose strength, it is considered as poorly soluble (Yu 2002). The permeability classification of BCS is based upon the extent of intestinal absorption of a drug in humans. Class I consists of drugs that demonstrate both high permeability and solubility. Such drugs are appropriate for the development of immediate release dosage forms. Class II drugs exhibit low solubility and high permeability, and may have limited bioavailability. However by formulating such drugs through physical means (*eg.* micronization or use of cosolvents), their dissolution may be improved. Class III (low permeability and high solubility) and class IV drugs (low solubility and low permeability) are much more difficult to formulate (Yvonne 2010). By altering the chemical structure, the permeability and thus the bioavailability of such drugs may be improved.

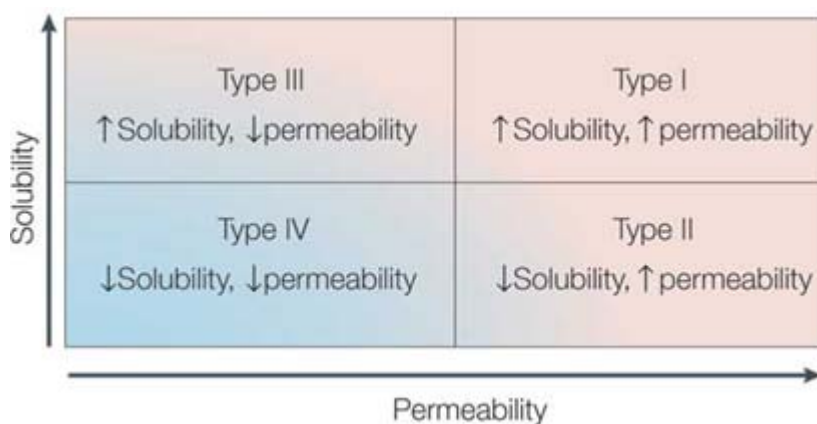


Figure 1.2: The Biopharmaceutics Classification System (BCS) (Davis 2004)

Over the years, progress in combinatorial chemistry, biology and genetics has lead to the steady increase in the number of drug candidates under development (Kesisoglou 2007). Drug design has attempted to explore new chemical species resulting in more complex molecules with higher hydrophobicities. This trend has often resulted in worsened aqueous solubility and intestinal permeability. Presently almost 40% of drugs in development pipelines and 60% of the drugs directly from synthesis are poorly water soluble (Lipinski 2002; Keck 2006). Such drugs typically display low bioavailability due to slow dissolution rate (Teeranachaideekul 2008).

Classic problems associated with poorly soluble drugs are low bioavailability and erratic absorption (Muller 2001). Innovative formulation approaches are continuously being investigated to increase bioavailability after oral administration or make available intravenously injectable forms (Keck 2006). Processes to improve solubility, dissolution and subsequent bioavailability of drugs include: (1) modification at the molecular level (*eg.* salt formation, prodrugs, co-solvents, complexation), (2) application of colloidal drug delivery systems (*eg.* micelles, emulsions, liposomes) and (3) modification of the drug properties at the particulate level (*eg.* nanosizing) (Yvonne 2010). These strategies are further discussed in detail in this chapter.

1.2 Salt formation

Salt formation is a very common and effective strategy for increasing the solubility, dissolution rate and ultimately the bioavailability of poorly soluble ionizable drugs. Salts of acidic and basic drugs generally have higher water solubility than their corresponding acid or base (Serajuddin 2007). The salt formation takes place by varying the pH and using a counterion, with a significantly different pKa value than that of the drug (Yvonne 2010). The sufficient difference in pKa allows for the pH of the solution to be altered and thus generate a salt form of the acidic or basic drug of interest. Potential drug compounds are becoming more and more insoluble and sometimes salt formation is not enough to increase their solubility (Serajuddin 2007). For instance, for a compound with solubility 1 $\mu\text{g/mL}$, even a 1000 fold increase in solubility by salt formation will give a concentration of only 1 mg/mL , which may not be adequate for the purpose of dosage form development. Under such circumstances, salt formation may be combined with other solubilization technique to obtain an optimal aqueous drug solubility. Furthermore, salt formation is only applicable to weakly acidic or basic drugs and not for neutral ones. In many cases, this technique does not achieve better bioavailability because under physiological conditions, the salt converts back into the acidic or basic form of the drug. This latter approach only works for weak acids and bases that ionize between pH 2 and pH 9 and that are chemically resistant to degradation and hydrolysis. Furthermore, an extreme pH can have biocompatibility issues such as tissue irritation (Narazaki 2007).

1.3 Complexation

Complexation, another approach to dissolve hydrophobic drugs has gained popularity in recent years. Inclusion complexes obtained with cyclodextrins (CDs) are able to solubilise certain poorly soluble drugs. CDs are cyclic oligosaccharides derived from starch, composed of 6-8 glucopyranose units joined through α -(1,4) glucosidic bonds (Figure 1.3) (Brewster 2007).

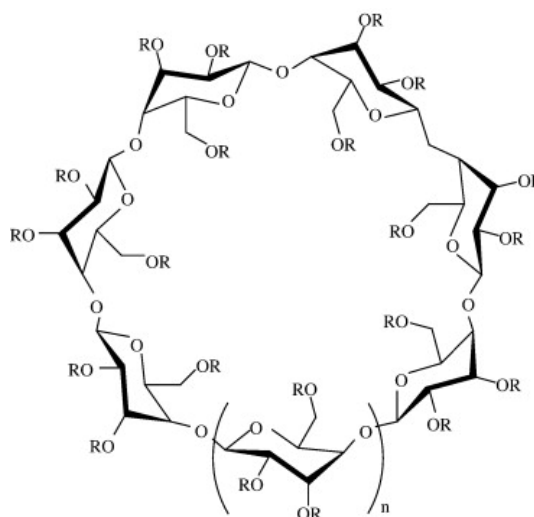


Figure 1.3 : Chemical structure of a cyclodextrin molecule (Brewster 2007)

The interior of the complex is relatively lipophilic whilst the exterior is hydrophilic, thus making it ideal for the inclusion of poorly water soluble drugs by non covalent interaction (Figure 1.4). There exist three natural CDs, α -, β -, and γ -CDs (with 6, 7, 8 units respectively), and they all differ in ring size and solubilisation properties. The use of CDs is often preferred for solubilisation of drugs (Stella 1997). For instance cosolvents such as alcohols and glycols will increase solubility of the poorly soluble drug in a non-linear way, with respect to the co-solvent concentration. For instance, a drug with solubility 0.1 mg/mL in water and 10 mg/mL in propylene glycol does not translate into 5 mg/mL solubility in a 50% mixture of water and propylene glycol. On

the other hand, CDs solubilize drugs as a linear function of their concentration, such that most drugs have a 1:1 complex with CD (Stella 1997). Hence the molecular weight of cyclodextrins becomes a limiting factor such that great amounts of cyclodextrin may be required for dissolve a small amount of drug.

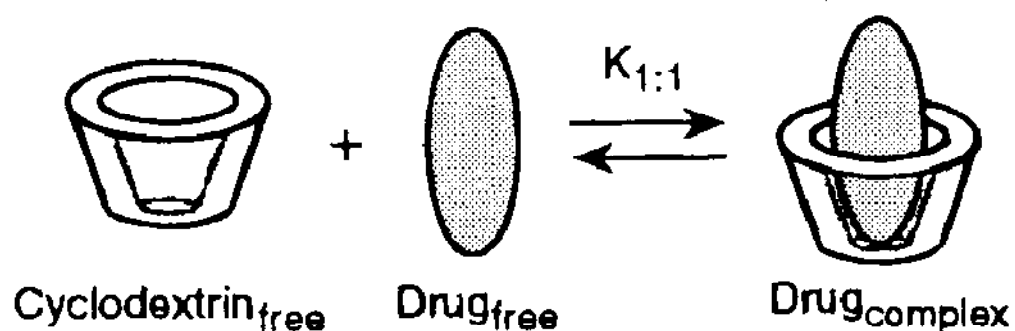


Figure 1.4: Complexation of drug and cyclodextrin (Stella VJ 1997)

Presently, there are over 35 different drugs marketed as solid or solution based CD complex formulations (Thorsteinn 2004). Both synthetic and natural CDs have been employed to enhance drug solubility and are administered *via* various routes (Table 1.1). In addition to enhancing solubility and dissolution rate of poorly water soluble drugs, CD complexes can reduce or prevent gastrointestinal and ocular irritation, prevent drug-drug or drug-additive interactions and convert oils and liquid drugs into microcrystalline or amorphous powders (Challa 2005).

Table 1.1 : Approved and marketed drug–cyclodextrin complexes in various world markets (Davis 2004)

Drug	Administration route	Trade name	Market
α-Cyclodextrin			
Alprostadil (PGE ₁)	Intravenous	Prostavastin, Caverject, Edex	Europe, Japan, United States
Cefotiam hexetil HCl	Oral	Pansporin T	Japan
Limaprost	Oral	Opalmon, Prorenal	
β-Cyclodextrin			
Benexate	Oral	Ulgut, Lonmiel	Japan
Dexamethasone	Dermal	Glymesason	Japan
Iodine	Topical	Mena-Gargle	Japan
Nicotine	Sublingual	Nicorette	Europe
Nimesulide	Oral	Nimedex, Mesulid	Europe
Nitroglycerin	Sublingual	Nitropen	Japan
Omeprazole	Oral	Omebeta	Europe
Dinoprostone (PGE ₂)	Sublingual	Prostarmon E	Japan
Piroxicam	Oral	Brexin	Europe
Tiaprofenic acid	Oral	Surgamyl	Europe
2-Hydroxypropyl-β-cyclodextrin			
Cisapride	Rectal	Propulsid	Europe
Hydrocortisone	Buccal	Dexocort	Europe
Indomethacin	Eye drops	Indocid	Europe
Itraconazole	Oral, intravenous	Sporanox	Europe, United States
Mitomycin	Intravenous	Mitozytrex	United States
Randomly methylated β-cyclodextrin			
17 β -Oestradiol	Nasal spray	Aerodiol	Europe
Chloramphenicol	Eye drops	Clorocil	Europe
Sulphobutylether β-cyclodextrin			
Voriconazole	Intravenous	Vfend	Europe, United States
Ziprasidone maleate	Intramuscular	Geodon, Zeldox	Europe, United States
2-Hydroxypropyl-γ-cyclodextrin			
Diclofenac sodium	Eye drops	Voltaren	Europe

1.4 Prodrugs

A common strategy to increase solubility of a drug is to redesign the molecule to a bioreversible, more water soluble derivative, called a prodrug. A prodrug is a pharmaceutical inactive compound that results from transient chemical modifications of a biologically active species and is designed to convert to biologically active species *in vivo* by a predictable mechanism (Xiaolong 2006). The drug is therapeutically inactive when administered, but becomes activated in the body when enzymatic or chemical processes break the promoiety linked to the drug (Figure 1.5) (Stella 2007).

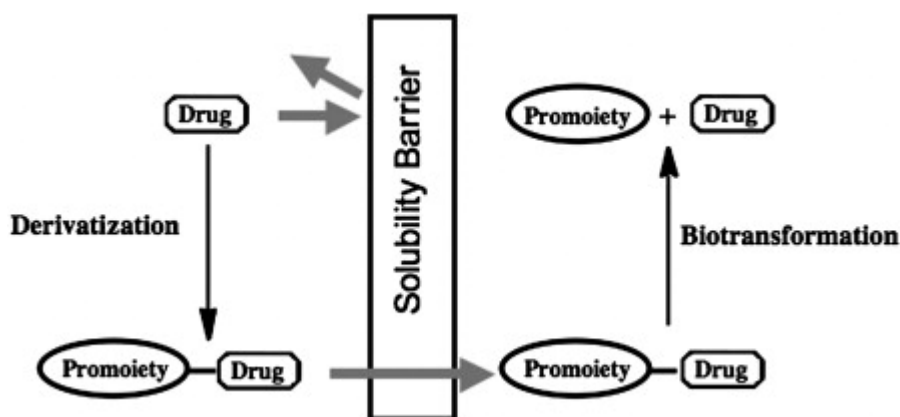


Figure 1.5: An illustration of the prodrug concept (Stella 2007).

The successful design of the prodrug is based upon the efficient transformation of the promoiety into the active drug *in vivo*. There are a variety of chemical structures, but most prodrugs are classified based upon their chemical linkage (eg. ester, amides and salts) (Fleisher 1996). Other prodrug approaches include conversion of promoieties into amines, imides, hydroxyls, thiols carboxyls and carbonyls. A variety of

paclitaxel prodrugs have been synthesized in which the promoiety is attached at position C2 or C7 (Figure 1.6) (Skwarczynski 2006).

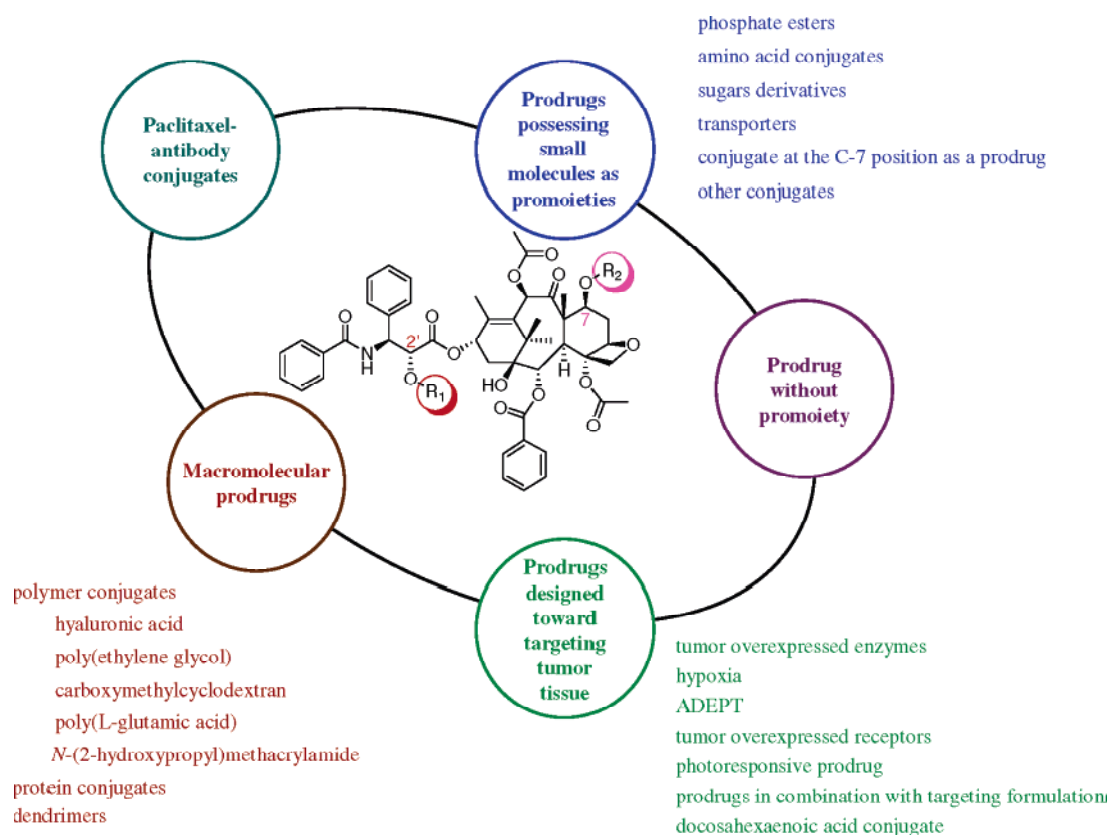


Figure 1.6 Paclitaxel prodrug strategies (Skwarczynski 2006).

Macromolecular prodrugs such as polymer-drug conjugates (polymeric prodrugs) are promising to enhance solubility of poorly water-soluble drugs (Duncan 2001). For instance, poly (ethylene glycol) (PEG), a water-soluble biocompatible polymer, dissolves in organic solvents quite readily. Its high solubility makes it a versatile candidate for polymer-drug conjugation (Peng 2008). Silybin, an antihepatotoxic agent used to treat liver and gall bladder has a solubility of 0.4 mg/mL. A soluble silybin prodrug conjugate with a linear PEG conjugated to the drug *via* a succinic

ester linkage enhanced the solubility to 800 mg/mL. Paclitaxel polymer prodrugs have also been reported. The first PEG prodrug of paclitaxel was reported by Greenwald *et al.* (Greenwald 1996). A water-soluble taxol 2'-PEG ester prodrug was designed and showed high solubility (660 mg/mL) (Skwarczynski 2006).

Prodrugs are not only used to enhance solubility of a drug, but offer other advantages as they increase drug stability, achieve sustained drug release, mask the taste of a drug and enable site specific drug delivery (Yvonne 2010). However, the use of the prodrug strategy is questionable due to the large costs and additional time needed to solve formulation and delivery problems (Stella 2007).

1.5 Cosolvents

The solubility of a drug may be enhanced by dissolving it in a cosolvent mixture, composed of water and a solvent (*eg.* ethanol, propylene glycol, glycerol and/or PEG) (Yvonne 2010). To achieve relatively high drug solubility, the concentration of the cosolvent mixture is usually high as well. Hence, upon dilution of the cosolvent mixture in the intravenous fluids or blood, the drug may easily precipitate (Singla 2002).

The use of cosolvent presents certain disadvantages such that an excess of solvent may be unsuitable and toxic for parenteral formulations. The intrinsic toxicity of cosolvent vehicles can be reduced by using a mixture of cosolvents or combining them with surfactants. Only few surfactants and organic cosolvents are regarded as safe for human use. Even fewer are compatible with injectable formulations possibly causing precipitation, pain, inflammation, and hemolysis. However, by raising the number of excipients in a given formulation, the risk of incompatibilities increases (Li 2007). Nonetheless, cosolvent strategies are explored to enhance solubility of many poorly water-soluble pharmaceutical agents. For instance, a cosolvent mixture of ethanol, polysorbate (Tween 80) and surfactant (Pluronic L64) in a 3:1:6 (v/v/v) ratio was used to formulate the poorly water-soluble drug paclitaxel (0.3 µg/mL). The drug concentration in the cosolvent formulation was reported at 5 mg/mL, but the formulation became unstable upon dilution with water (Singla 2002).

1.6 Surfactants and Micelles

Surfactants are amphiphilic agents with a hydrophilic head and hydrophobic tail. This specific nature of surfactants gives them unique activity at interfaces, wherein they significantly reduce the surface tension of water. At low concentrations, these molecules are freely dispersed in an aqueous environment, however as the concentration is increased, the free energy of the system augments as a result of unfavourable interactions between the hydrophobic regions and the surrounding water molecules (Gaucher, in press). At a precise concentration, the surfactant molecules arrange themselves to form aggregates called micelles, thereby minimizing the energy of the system (Figure 1.7) (Torchilin 2007). The minimum surfactant concentration at which micelles assemble is referred to as the critical micellization concentration (CMC). Micelles are in dynamic equilibrium with free molecules in solution, and so they are constantly dissociating and reforming (Torchilin 2007). The size of micelles varies and depends on the size, shape and number of surfactant monomers used. The formation of micelles is driven by the decrease of free energy in the system because of the removal of hydrophobic fragments from the aqueous environment and the re-establishing of the hydrogen bond network in water. Consequently, hydrophobic fragments of the amphiphilic molecules form the core and hydrophilic fragments form the shell (Torchilin 2007). Due to such a structure, micelles solubilise molecules of poorly soluble nonpolar drugs within its core and polar drug molecules may be adsorbed on the micelle surface (Jones 1999). Such solubilisation using micelle-forming surfactants results in an increased water solubility of poorly soluble drug and its improved bioavailability, and enhanced permeability across biological barriers (Torchilin 2001; Torchilin 2007).

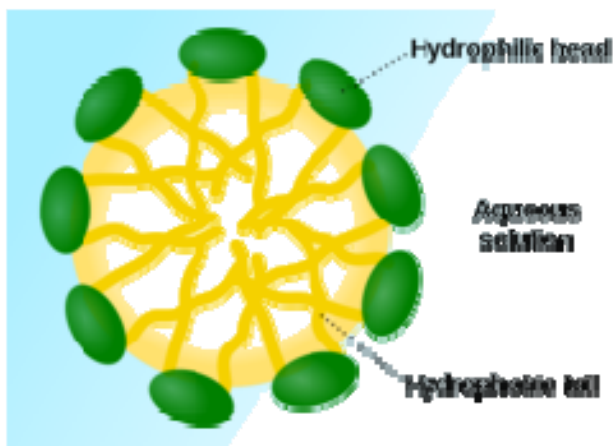


Figure 1.7: Representation of micelle formation at CMC (Wikipedia)

Polymeric micelles have attracted much attention over the years. Polymeric micelles are formed by block co-polymers consisting of hydrophilic and hydrophobic monomer units with the length of a hydrophilic block exceeding to some extent that of a hydrophobic one (Gaucher 2005). Similar to micelles formed by the conventional surfactants, block copolymer micelles assume a core-shell structure where the core is comprised of hydrophobic blocks, and is stabilized by the corona composed of hydrophilic chains (Gaucher, in press). In comparison to the conventional micelles, polymeric micelles form at lower CMC and are more stable upon dilution accordingly protecting the incorporated drug from fast degradation (Devalapally 2007). Genexol – PM is a methoxy-PEG-poly (D-L-lactide) micelle formulation of paclitaxel that obtained a pre-market approval in Korea in 2006. *In vivo* studies demonstrated that the antitumor efficacy of this formulation is better than the current market formulation of paclitaxel, Taxol[®] (Yvonne 2010).

1.7 Emulsions, microemulsions and self-emulsifying delivery systems

An emulsion is composed of a minimum of two immiscible liquid phases (*eg.* oil and water), where a dispersed phase (dispersed globules) is in a continuous phase (liquid phase) and the whole system is stabilized by an emulsifying agent (Mahato 2007). Depending on which phase is dispersed into the other, either an oil-in-water (o/w) or water-in-oil (w/o) emulsion is obtained. Micron or submicron sized droplets are formed upon applying high energy to the system (Yvonne 2010). Microemulsions; much smaller one-phase systems are more stable colloidal solutions. Microemulsions contain appropriate mixture of oil (polar lipids) water and surfactants, and the oil component is used to deliver the poorly soluble drug. In addition, whereas emulsions are composed of spherical droplets, microemulsions range from droplet-like micellular structures to bicontinuous structures. Self-emulsifying drug delivery systems (SEDDS), composed of an isotropic mixture of drug, lipid and surfactants, are used to deliver hydrophobic drugs. SEDDS form fine emulsion droplets (50-100 nm) upon dilution in physiological fluids (Tang 2008). Thus, the hydrophobic drug remains in solution and is delivered to the gut. SEDDS exist as solutions or are made into solid dosage forms. A few of the marketed o/w emulsion products include Diazepam[®], Etomidate[®] and Propofol[®] (Muller 2005).

1.8 Liposomes

Liposomes are spherical vesicles composed of phospholipids self-assembled in aqueous medium (Rawat 2006). Due to their amphiphilic nature, lipids in excess of water spontaneously self-associate above a concentration called the critical aggregation concentration, which is in the order of 10^{-10} M. The self-assembly process is spontaneous and cooperative (Mahato 2007). The lipid moieties spontaneously orient in water, and the lipid chains orient inward, giving rise to bilayer structures (Figure 1.8). The aggregation phenomenon is a result of both the polar interactions between the hydrophilic heads of the phospholipids, and the hydrophobic effect of the aliphatic chains (Simard 2007).

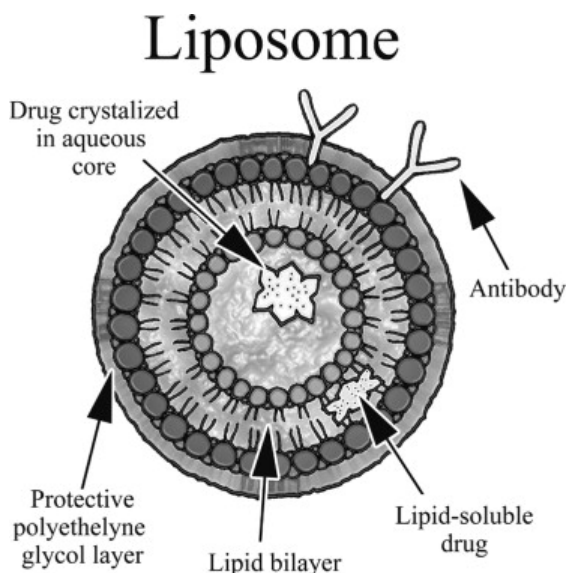


Figure 1.8: Structure of a liposome (Devalapally 2007)

Liposomes range from 50 nm to a few micrometers in diameter (Haley 2008). They consist of one or more concentric lipid bilayers separated by water compartments. The rationale of using liposomes as drug delivery systems to the cells was originally based upon the possibility of fusion of the liposome to the target cell membrane.

Hence, the preparation of liposomes had to be prepared from natural lipids found in cell membrane, such as glycerolipids, sphingolipids and sterols (Simard 2007). Synthetic lipids that mimic the structure and physicochemical properties of natural lipids may also be used to fabricate liposomes. Furthermore, these liposomes offer greater advantage such that they may be altered for improved properties. In comparison to other colloidal drug delivery systems, liposomes have the ability to encapsulate both hydrophilic (inside the aqueous region) and lipophilic drugs within the bilayer regions.

Liposomes are classified and described according to their size, the number of bilayers, or their preparation method. Multilamellar vesicles (MLV) are usually 1-5 μm in diameter, whereas unilamellar vesicles (UV) range from 40 nm to 1 μm . There exist four major types of liposomes: conventional, sterically stabilized, targeted and cationic (Simard 2007). Conventional liposomes are either neutral or negatively charged, and are composed of phospholipids, glycolipids, and/or cholesterol. Such liposomes have a limited circulation lifetime because they are removed by cells from the mononuclear phagocyte system (MPS) (Appendix I) (Janoff 1999). These liposomes are mainly used for passive targeting to the phagocytic cells of the MPS, localizing predominantly in the liver and spleen.

Sterically stabilized liposomes have a polymer coating to obtain prolonged circulation times. PEGylated (polyethylene glycol) lipids reduce the uptake of the liposomes by the MPS and subsequently circulation time of the vesicle is greatly increased. By residing in the bloodstream for a longer time, PEGylated liposomes (also known as STEALTH[®] liposomes) could localize into tumours and most inflammation sites (Mahato 2007). Targeted liposomes usually have a biological moiety attached to enable recognition by a specific receptor at the site of interest. Targeting ligands include monoclonal antibodies (generating an immunoliposome), vitamins or specific antigens. Most of the targeting liposomes are also PEGylated, and so are able to target nearly any cell type in the body and deliver drugs. Finally, cationic liposomes

are positively charged and are mainly used for the delivery of nucleic acids (Papahadjopoulos 1991). The positively charged liposomes interact with the negatively charged backbone of DNA or RNA, and lead to neutralization.

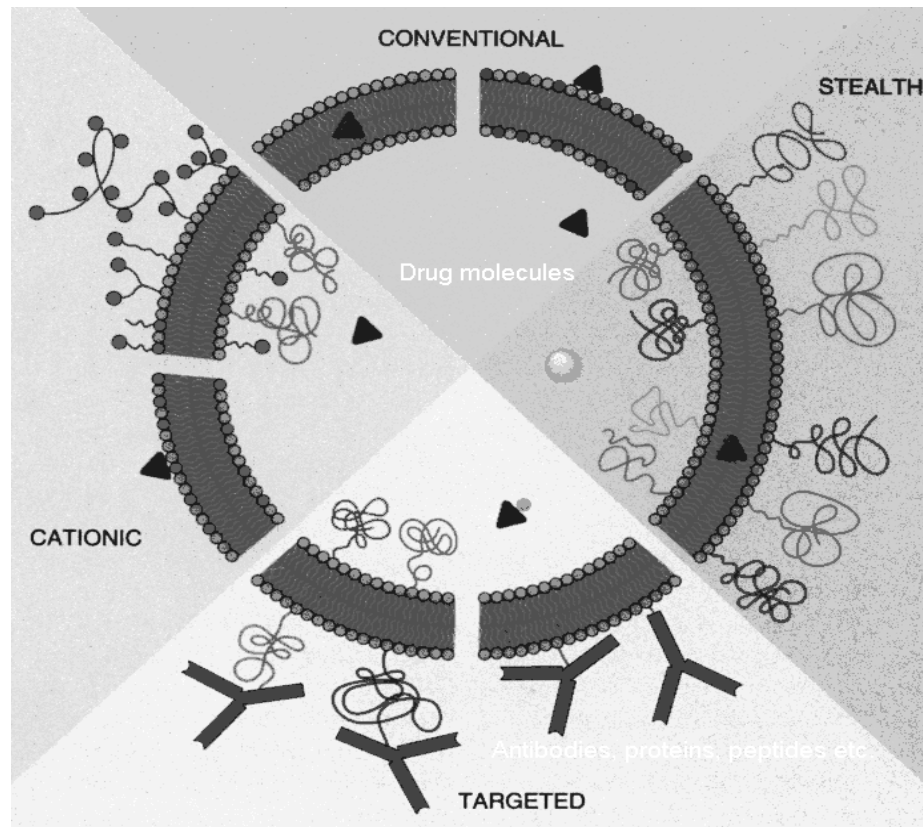


Figure 1.9: Classification of liposomes

(www.imcr.uzh.ch/static/onkwww/images/lipos4.gif)

Liposomes were one of the first drug delivery system to be approved for clinical use, and today there exists many liposomal formulations. One very popular formulation is Doxil[®], which encapsulates the poorly soluble drug Doxorubicin in 80-100 nm-sized liposomes of PEGylated distearoyl phosphatidyl ethanolamine, hydrogenated soy phosphatidylcholine and cholesterol (Yvonne 2010).

1.9 Polymer Solid dispersions

As discussed earlier, polymers play a vital role in solubilising poorly soluble drugs. Alternative applications of polymers include their use in solid dispersions as a strategy to improve solubility of poorly soluble drugs (Leuner 2000).

Solid dispersions consist of molecularly or physically dispersing drug in a water-soluble carrier (*eg.* PEG or PVP) or a water insoluble carrier (Sivert 2009). Drug dissolution can be improved by molecularly dispersing a drug in a hydrophilic polymer matrix *via* preparation processes such as solvent evaporation or hot-melt extrusion. Polymers have been used quite extensively to generate solid dispersions, because they make amorphous solid dispersions. Solubility of a given solid is a sum of crystal packing energy, cavitation and solvation energy. Different solid-state forms of a material have different crystal packing energy. The amorphous form, due to absence of an ordered crystal lattice requires minimal energy provides the maximal dissolution advantage as compared to the crystalline and hydrated forms of a drug (Vasconcelos 2007). Polymers used include both synthetic (PEG, polymethacrylates), and natural polymers such as hydroxymethylcellulose (HPMC), ethylcellulose and CDs (Vasconcelos 2007). When the solid dispersion is exposed to an aqueous milieu, the carrier dissolves allowing the release of the incorporated drug.

Due to the intensive work involved in the optimization of solid dispersions, the latter are rarely considered as a viable option to formulating poorly-water soluble drugs. In addition, the amorphous form of the drug within the solid dispersion may undergo crystallization over time.

1.10 Size reduction

A much more classical method to increase drug dissolution rate is through size reduction (Keck 2006). The Noyes-Whitney equation (equation 1), where dW/dt is

$$\text{Equation 1} \quad \frac{dW}{dt} = \frac{DA(C_s - C)}{L}$$

the rate of dissolution, A is the surface area of the solid, C is the concentration of the solid in the bulk dissolution medium, C_s is the concentration of the solid in the diffusion layer surrounding the solid, D is the diffusion coefficient, and L is the diffusion layer thickness explains that dissolution rate may be readily improved by reducing the size of the drug particle, and thereby increasing surface area available for dissolution (Figure 1.10) (Merisko-Liversidge 2003; Muller 2004). The size reduction also decreases the thickness of the diffusion layer around each particle, thus further promoting the dissolution. The surface area may be adjusted by altering the particle size (*eg.* micronization). Micronization, which involves coarse drug powder milled into an ultrafine powder of particle size distributions in the range of 1 - 25 μm , is a common method used to improve bioavailability of the poorly soluble drug (Merisko-Liversidge 2003).

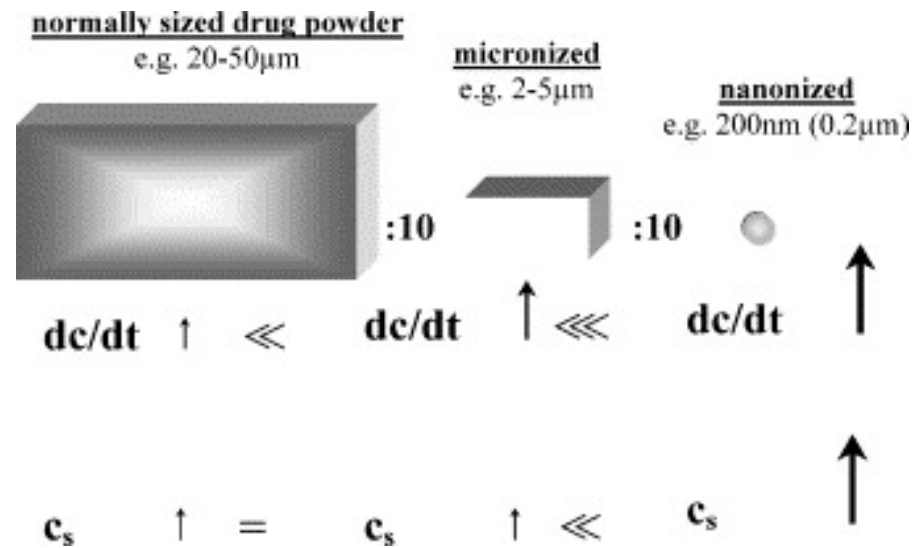


Fig. 1.10. Dissolution velocity dc/dt (or dW/dt) and saturation solubility C_s as a function of the size of drug powders ranging from coarse to nanonized drugs (Muller 2004)

Many of the new drugs exhibit such a low solubility that micronization is insufficient to increase the surface area of the drug to a large extent. At very low solubility, the achieved increase in dissolution rate is not significant enough to lead to high enough bioavailability. Though micronization increases dissolution rate, it does not change the saturation solubility of the poorly soluble drug and consequently desired therapeutic blood levels are not attained. Hence, the next approach involves further reduction of the drug particles, down to the nanoscale. Moreover, according to the Ostwald-Freundlich equation (equation 2),

$$\text{Equation 2} \quad \frac{RT\rho}{M} \ln \frac{S_1}{S_2} = 2\sigma \left(\frac{1}{r_1} - \frac{1}{r_2} \right),$$

where R is the gas constant, T is the absolute temperature, M the molecular weight of the solid in solution, σ is the interfacial tension between the solid and liquid, ρ is the density of the solid, and S_1 and S_2 are the solubilities of particle of radius r_1 and r_2 ,

respectively, the equilibrium solubility of particles increases with decreasing particle size. Particularly size reduction in the range below ca. 1 μm is accompanied by an increase in saturation solubility (Borm 2006).

Though many textbooks and articles follow this theory, the validity of the Oswald-Freundlich equation to describe the relationship between the size of a particle and its solubility is controversial (Godec 2009, Nancollas 2009). Experimental observations have shown that Oswald ripening is not due to the increased solubility of smaller crystals but rather to a negative tension between a solid and a solution (Wu 1998). Oswald stated that the driving force for ripening is the variation in solubility between large and small particles. However, the alternative mechanism concludes that the ripening is due to a thermodynamically unstable interface between the solid and solution. Wollaston and Curie assumed the hypothesis that finely divided solids should have larger solubilities than coarser ones in the late 19th century. Later Oswald and Freundlich used similar arguments to establish the equation above and prove that solubility of finely sized crystals is a function of particle size. However, when the first experimental investigations were made to test the supersaturation, particle size and solid-liquid interfacial tensions, limitations were encountered and the Oswald-Freundlich equation was subjected to criticism (Wu 1998). Despite the controversy, many believe that particle size reduction does indeed lead to enhanced dissolution rate.

Nanosizing is the reduction of the active pharmaceutical ingredient (API) particle size down to the sub-micrometer range (Kesisoglou 2007). By definition, drug nanocrystals are nanoparticles of pure crystalline drug without any matrix material typically ranging from 200 – 500 nm in size (Muller 2001). The following chapter comprehensively describes the advantages, methods of fabrication and applications of drug nanocrystals.

1.11 References

Borm P, Klaessig FC, *et al*, Wood S 2006. Research Strategies for Safety Evaluation of Nanomaterials, Part V: Role of Dissolution in Biological Fate and Effects of Nanoscale Particles. *Toxicol Sci* 90:23-32.

Breitenbach, J. (2002). Melt extrusion: from process to drug delivery technology. *Eur J Pharm Biopharm*, 54: 107-117.

Brewster, M., Loftsson T. (2007). Cyclodextrins as pharmaceutical solubilizers. *Adv Drug Deliver Rev*, 59: 645-666.

Challa, R., Ahuja A., *et al*. (2005). Cyclodextrins in drug delivery: An updated review. *AAPS PharmSciTech*, 6: E329-E357.

Davis ME, Brewster ME 2004. Cyclodextrin-based pharmaceuticals: past, present and future. *Nat Rev Drug Discov* 3(12):1023-1035

Devalapally, H., Chakilam A. *et al*. (2007). Role of nanotechnology in pharmaceutical product development. *J Pharm Sci*, 96: 2547-65.

Duncan, R., Gac-Breton S. *et al*. (2001). Polymer-drug conjugates, PDEPT and PELT: basic principles for design and transfer from the laboratory to clinic. *J Control Release*, 74: 135-146.

Gaucher G., Dufresne M.-H, *et al*. (2005). Block copolymer micelles: preparation, characterization and application in drug delivery. *J Control Release*, 109: 169-188.

Godec A, Gaberšček M, Jamnik J 2009. Comment on the Article “A New Understanding of the Relationship between Solubility and Particle Size” by W. Wu and G.H. Nancollas. *J Sol Chem* 38:135-146.

Haley B., Frenkel E. (2008). Nanoparticles for drug delivery in cancer treatment. *Urol Oncol-Semin Ori*, 26 :57-64.

Horter, D., Dressman J. B. (2001). Influence of physicochemical properties on dissolution of drugs in the gastrointestinal tract. *Adv Drug Deliv Rev*, 46 :75-87.

Janoff, A. S. (1999). Liposomes: Rational Design. New York, Marcel Dekker Inc.

- Jones, M.-C., Leroux J.-C. (1999). Polymeric micelles - a new generation of colloidal drug carriers. *Eur J Pharm Biopharm*, 48: 101-111.
- Keck, C. M., Muller R. H. (2006). Drug nanocrystals of poorly soluble drugs produced by high pressure homogenisation. *Eur J Pharm Biopharm*, 62: 3-16.
- Kesisoglou, F., Panmai S., *et al.* (2007). Nanosizing--oral formulation development and biopharmaceutical evaluation. *Adv Drug Deliv Rev*, 59: 631-44.
- Kwan, K. C. (1997). Oral Bioavailability and First-Pass Effects. *Drug Metab Dispos*, 25: 1329-1336.
- Lee EJD, Lean CB, Liment LMG 2009. Role of membrane transporters in the safety profile of drugs. *Expert Opinion on Drug Metabolism & Toxicology* 5(11):1369-1383.
- Leuner, C., Dressman J. (2000). Improving drug solubility for oral delivery using solid dispersions. *Eur J Pharm Biopharm*, 50: 47-60.
- Li P., (2007). Developing early formulations: practice and perspective. *Int J Pharm*, 34: 1-19.
- Lipinski, C. (2002). Poor Aqueous Solubility – an Industry Wide Problem in Drug Discovery. *Am Pharm Rev*: 5: 82
- Mahato, R. I. (2007). *Pharmaceutical Dosage Forms and Drug Delivery*. Boca Raton, Florida, CRC Press, Taylor & Francis Group, LLC.
- Merisko-Liversidge, E., Liversidge G. G., *et al.* (2003). Nanosizing: a formulation approach for poorly-water-soluble compounds. *Eur J Pharm Sci*, 18: 113-20.
- Muller, R. H., Peters K, (1998). Nanosuspensions for the formulation of poorly soluble drugs: I. Preparation by a size-reduction technique. *Int J Pharm*, 160: 229-237.
- Muller, R. H., Jacobs, C. *et al.* (2001). Nanosuspensions as particulate drug formulations in therapy. Rationale for development and what we can expect for the future. *Adv Drug Deliv Rev*, 47: 3-19.
- Nancollas G, Wu W 2009. Response to “Comment on “A New Understanding of the Relationship between Solubility and Particle Size” by Godec, A., Jamnik, J., and Gaderšček, M. *J Sol Chem* 38:147-148.

Narazaki, R., Sanghvi, R., *et al.* (2007). Estimation of Drug Precipitation upon Dilution of pH & Cosolvent Solubilized Formulations. *Chem Pharm Bull*, 55:1203-1206.

Papahadjopoulos D., Gabizon A. T., *et al* (1991). Sterically stabilized liposomes: improvements in pharmacokinetics and antitumor therapeutic efficacy. *Proc Natl Acad Sci U SA*. 84:11460-4.

Peng, Z., Y. Hai, *et al.* (2008). Water soluble poly(ethylene glycol) prodrug of silybin: Design, synthesis, and characterization. *J Appl Polym Sci*, 107: 3230-3235.

Rajendran L, Knolker H-J, Simons K (2010). Subcellular targeting strategies for drug design and delivery. *Nat Rev Drug Discov* 9:29-42.

Simard P., Leroux J.-C., *et al* (2007). Nanoparticles for Pharmaceutical Applications,. Valencia, American Scientific Publishers

Sivert A., Bérard, V. *et al.* (2009). New binary solid dispersion of indomethacin with surfactant polymer: From physical characterization to in vitro dissolution enhancement. *J Pharm Sci*, 99: 1399-1413.

Rasenack, N., Muller B. W. (2004). Micron Size Drug Particles: Common and Novel Micronization Techniques. *Pharm Dev Technol*, 9: 1-13.

Rawat, M., Singh D., *et al.* (2006). Nanocarriers: promising vehicle for bioactive drugs. *Biol Pharm Bull* 29: 1790-8.

Serajuddin, A. (2007). Salt formation to improve drug solubility. *Adv Drug Deliv Rev* , 59: 603-616.

Singla, A. K., Garg A., *et al.* (2002). Paclitaxel and its formulations. *Int J Pharm* 235: 179-92.

Stella, V. J., Nti-Addae K. W. (2007). Prodrug strategies to overcome poor water solubility. *Adv Drug Deliv Rev* 59: 677-694.

Stella V.J, (1997). Cyclodextrins: their future in drug formulation and delivery. *Pharm Res*, 5: 556-567.

Stevens, P., Sekido M., *et al.* (2004). A Folate Receptor–Targeted Lipid Nanoparticle Formulation for a Lipophilic Paclitaxel Prodrug. *Pharm Res*, 21 2153-2157.

Teeranachaideekul V., Junyaprasert V. B., *et al.* (2008). Development of ascorbyl palmitate nanocrystals applying the nanosuspension technology. *Int J Pharm*, 354: 227-234.

Thorsteinn, L., Marcus B., *et al.* (2004). Role of Cyclodextrins in Improving Oral Drug Delivery. *Am J Drug Del* 2: 261-275.

Torchilin, V. (2007). Micellar Nanocarriers: Pharmaceutical Perspectives. *Pharm Res*, 24 : 1-16.

Torchilin, V. P. (2001). Structure and design of polymeric surfactant-based drug delivery systems. *J Control Release* 73: 137-172.

Vasconcelos, T., Sarmiento B., *et al.* (2007). Solid dispersions as strategy to improve oral bioavailability of poor water soluble drugs. *Drug Discov Today* 12 :1068-1075.

Wu W, Nancollas GH 1998. A New Understanding of the Relationship Between Solubility and Particle Size. *J Sol Chem* 27:521-531.

Xiaolong Li (2006). Design of Controlled Release Drug Delivery Systems. New York, McGraw Hill.

Yu LX, Amidon GL, Polli JE, Zhao H, Mehta MU, Conner DP, Shah VP, Lesko LJ, Chen M-L, Lee VHL, Hussain AS 2002. Biopharmaceutics Classification System: The Scientific Basis for Biowaiver Extensions. *Pharmaceutical Research* 19(7):921-925.

Yvonne P., T. R. (2010). *Pharmaceutics- Drug Delivery and Targetting*. London, UK, Pharmaceutical Press

nihseniorhealth.gov/images/drug_admin1.jpg (retrieved December 1st 2009)

www.imcr.uzh.ch/static/onkwww/images/lipos4.gif (retrieved December 2nd 2009)

CHAPTER 2:

Nanocrystals and Nanosuspensions

2.1 Introduction

Whilst reduction in particle size has been applied in the pharmaceutical field for several decades, newer technologies and the deeper understanding of colloidal drug systems has allowed for the production of nanoscale drug particles. Drug nanocrystals are composed of pure crystalline drug devoid of polymeric or lipidic carriers and may be sized from few nanometers up to 400 nm. Nanosuspensions are dispersions of the nanocrystals in a liquid media, which are stabilized by surfactants or polymeric stabilizers (Junghanns 2008). Nanosuspensions overcome the delivery issues of poorly soluble compounds by obviating the use of potentially harsh vehicles, such as pH-buffers or cosolvents, thereby reducing toxicity and increasing efficacy (Rabinow 2004).

As presented section 1.10, a significant feature of drug nanocrystals is the increase in dissolution velocity (subsequently in bioavailability). Another exceptional feature of nanosuspensions is the increased adhesiveness compared to microparticles which is an additional factor for improving the oral absorption of poorly soluble drugs (Junghanns 2008). As a result of this phenomenon, nanocrystals remain in contact with the gut wall for longer time, thereby enhancing bioavailability of the drug upon oral administration (Gao 2008).

Being physically stable and displaying increased dissolution rate, a nanocrystal formulation greatly enhances biological performance of poorly soluble drugs (Merisko-Liversidge 2003).

By increasing the dissolution rate, nanonization enhances the rate and extent of absorption of drugs administered orally so that the bioavailability is less affected in the fed/fasted state. For instance, by nanosizing the active ingredient (MK-0869) of the drug EMEND[®], previously FDA approved for prevention of chemotherapy-induced nausea, the advantages of a nanocrystalline formulation over a conventional dosage form were confirmed (Figure 2.1) (Wu 2004). Additionally, owing to their small size, stable drug nanocrystals may be injected by the intravenous (*i.v.*) route

without the risk of embolic complications. More importantly, the total drug amount in the formulation may be adjusted to high levels, allowing usage of smaller administration volumes.

In this chapter, various methods of nanocrystal production, their characterization and applications are discussed in detail.

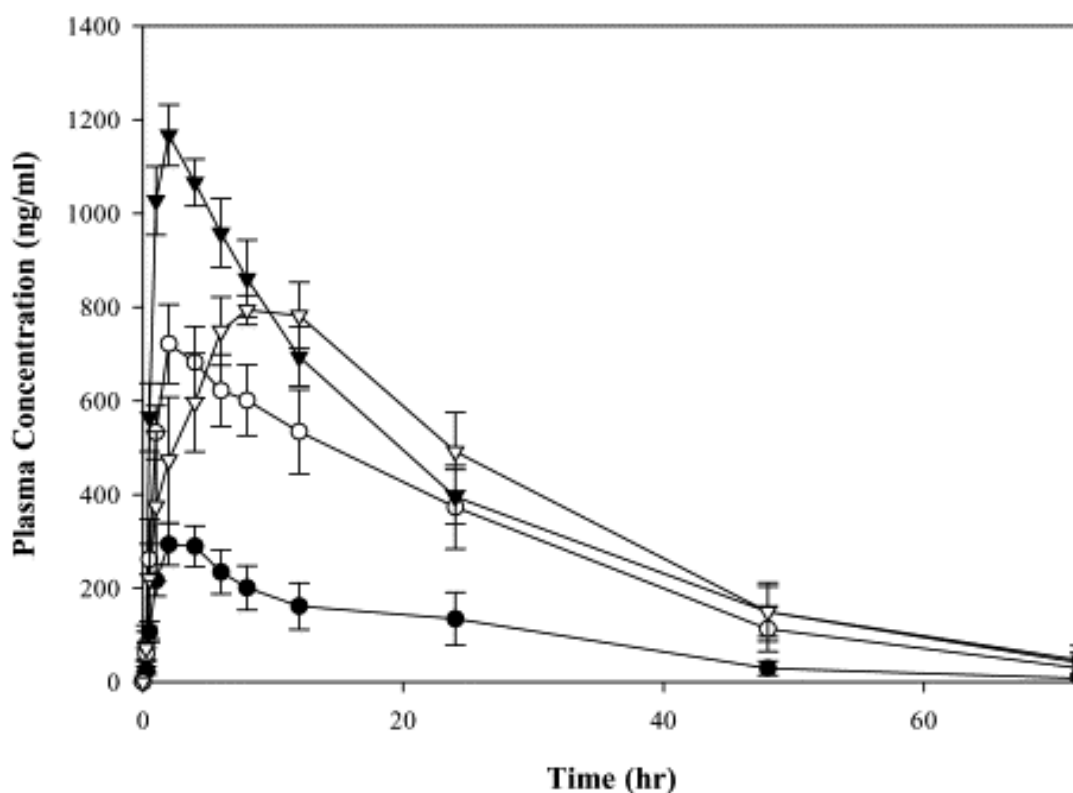


Figure 2.1: Comparison of mean (\pm S.E.) plasma concentrations of MK-0869 (active ingredient of EMEND®) following oral administration in Beagle dogs ($N = 5$) of a conventional suspension (●, fasted; ○, fed) and a NanoCrystal® dispersion formulation (▼, fasted; ▽, fed) of MK-0869 at a dose of 2 mg/kg (Wu 2004).

2.2 Methods of nanocrystal fabrication

Methodologies for the generation of drug nanocrystals are mainly categorized as “bottom-up” or “top-down” methods (Van Eerdenbrugh 2008). The first is based upon the strategy of growing drug nanocrystals, whereas the latter breaks down coarse drug powder into nanoparticles.

2.2.1 Bottom-up strategies

Precipitation techniques and supercritical fluid technology are the commonly used bottom-up approaches to fabricate drug nanocrystals.

The precipitation technique consists of dissolving the poorly soluble drug in a solvent (usually organic) and adding this solution to an anti-solvent (*eg.* water) under agitation (Kesisoglou 2007). This leads to a supersaturation which results in rapid nucleation of the drug, thereby forming nanoparticles (Gao 2008). Several parameters such as stirring rate, volume ratio of anti-solvent/ solvent and drug content require optimization for the production of uniformly sized nanoparticles. A faster stirring rate generates smaller particles and a greater anti-solvent/solvent ratio brings about a faster nucleation. The drug content should be adjusted to a moderate level, because very large drug quantities may cause uncontrolled agglomeration of the nanocrystals. The drug nanocrystals are further processed for removal of organic solvent.

The principle advantage of the precipitation technique is that it is relatively simple and inexpensive, however this technique does have its disadvantages. It is known that the particle size is not always controlled using this method because growth of the crystals is not hindered, and microcrystals are very often generated (Keck 2006). In order to avoid spontaneous agglomeration and subsequent formation of microcrystals, stabilizers are used. Another limitation of this technique is that the drug must be soluble in a solvent which is miscible with the anti-solvent. This poses difficulties

because most poorly soluble drugs needing to be nanosized, are poorly soluble in both aqueous and organic solvent, thus making them unsuitable candidates for the precipitation technique (Grau 2000). Amorphous drug content often is generated during the precipitation process. Though this state of a drug is more soluble and exhibits a higher dissolution than the crystalline state, it is not as stable and converts to crystalline over time (Gao 2008). Despite its limitations, liquid precipitation is low cost method offering convenient processing of nanocrystals (Zhang 2009). This bottom-up technology is marketed by DowPharma (Midland, MI, USA) and by BASF Pharma Solutions (Florham Park, NJ, USA) (Kesisoglou 2007).

Supercritical fluid based technologies, such as rapid expansion from supercritical solutions (RESS), rapid expansion from supercritical aqueous solutions (RESAS), and supercritical anti-solvent methods (SAS), have been investigated as an alternative bottom-up strategy for the fabrication of drug nanocrystals (Date 2004). This approach requires complex operating conditions and induces high costs (Zhang 2009).

The RESS method consists of dissolving the drug in a supercritical fluid (*eg.* CO₂) at a programmed temperature and pressure. The drug solution is introduced into a precipitation unit and allowed to expand rapidly through a capillary into a region of lower pressure and temperature (Date 2004). This phenomenon results in the dissolved drug precipitating rapidly as a finely sized powder, thus generating nanocrystals. The shortcoming of this method is that only drugs exhibiting solubility in supercritical fluids could be used. Similar to the liquid precipitation technique, generation of microcrystals are also obtained, resulting in large size distribution. The RESAS is an evolution of the RESS method, such that an aqueous solution containing stabilisers is used in addition to the supercritical fluid. Though size is better controlled, this technique displays similar concerns because of the use of solvents. The SAS method consists of dissolving the drug in an appropriate organic solvent or co-solvent, and then atomizing it into an excess flowing continuum of supercritical

CO₂, thus forming nanoparticles in a dried state. Hydrophobic drugs with poor solubility in supercritical fluids may be processed using the SAS procedure, however broad particle size distribution is obtained.

2.2.3 Top-down strategies

Top-down methods are more widely employed for the production of drug nanocrystals. This specific strategy relies on mechanical attrition to break down large crystalline particles into nanoparticles (Kesisoglou 2007). Such technologies include high-pressure homogenization and media milling.

Media milling (or wet milling) is based upon an attrition procedure in which micrometer sized drug crystals are milled in the presence of grinding media and stabilizers (Rabinow 2004). This patent protected technology was developed in 1990 by Liversidge *et al.* (Merisko-Liversidge 2008). In this process, a nanocrystal suspension is generated by high shear milling equipment composed of a milling chamber, milling beads (or grinding media), a rotor and a recirculation chamber (Figure 2.2).

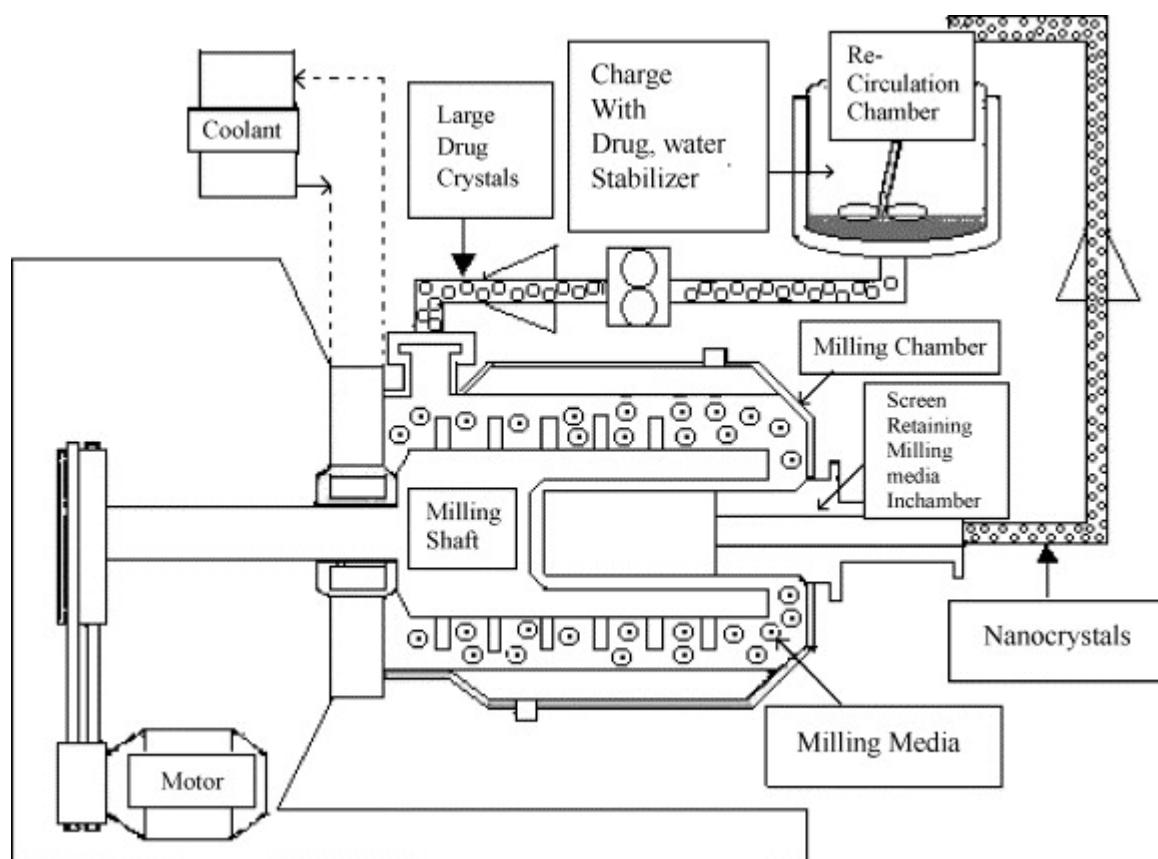


Figure 2.2: Schematic representation of the media milling process (Date 2004).

The poorly soluble drug is dispersed in an aqueous surfactant solution, and the resulting suspension is wet-milled with the grinding media (Gao 2008). The grinding material spherical in form, is typically composed of zirconium oxide, zirconium silicate or other media such as glass, titania, alumina (Hu 2004). The stabilizers (or surface modifiers) used comprise of various polymers, low molecular weight oligomers, natural products and surfactants. During the milling process, the generated shear forces and those created during impaction of the milling media with the solid drug provide high energy to break the drug crystals into nanoparticles (Merisko-Liversidge 2003). Particle size is determined by stress intensity (which is a function of kinetic energy of the grinding beads), number of contact points (which

may be increased by using smaller grinding media), and the time of milling (Rabinow 2004). The optimization of the following parameter: drug content, amount of grinding or milling pearls, milling speed and time are important for the generation of desirable nanosuspensions. Liversidge *et al.* reported that particles of Naproxen, a poorly soluble drug were reduced to 270 nm, from an average initial size of 20-30 μm over a period of 5 days of wet milling. PVP K-15 was used as the stabilizer (5:3 drug to stabilizer ratio) and the nanosuspension remained physically and chemically stable for up to 4 weeks at 4°C (Hu 2004).

Though the wet-milling procedure enables the production of stable drug nanosuspensions, there are a few drawbacks to this technique. Not only is it time consuming, but there have been reports on the contamination of the product by grinding material (Muller 2001). Erosion of the grinding material may contaminate the final drug product. In addition, wet-milling is a batch process; therefore batch-to-batch variations may be detected in the quality of the dispersion, processing time, degree of drug crystallinity and particle size distribution. Such variations affect the drug particle size and the efficiency of the delivery system. Moreover milling over several days may also bring risks of microbiological problems, particularly when performing the process at 30°C or using a dispersion media providing nutrition to bacteria (Gao 2008). Regardless of these limitations, this mechanical method of producing nanocrystals is successfully marketed as the NanoCrystal[®] technology (Élan) (Merisko-Liversidge 2008). Four oral products generated *via* the NanoCrystal[®] technology are currently marketed in the US and other countries: Rapamune[®], Emend[®], TriCor 145[®] and MegaceES[®] (section 2.5).

Another top-down method, known as high pressure homogenization, was invented by Muller *et al.* in the mid 1990s (Muller 1998). Homogenization involves the forcing of a drug suspension under pressure through a valve with a narrow aperture (Figure 2.3). Therefore, the formation of the nanosuspension is based on the cavitation energy generated in the high pressure homogeniser (*eg.* the piston-gap homogenizer).

In this process, the poorly soluble drug is dispersed in an aqueous surfactant solution *via* high speed stirring, and the resultant suspension is passed through a high pressure homogeniser (gap width of approximately 25 μm) at a pressure of 1500 bar over 3- 20 homogenization cycles (Hu 2004; Rabinow 2004). Due to the narrowness of the gap, the streaming velocity of the drug suspensions and the dynamic fluid pressure increase. Furthermore the static pressure of the fluid decreases below the boiling point of water (at room temperature), and as a consequence the water boils and gas bubbles form which implode when the fluid leaves the homogenization gap (Muller 2001). The generated cavitation forces are very strong and break the drug particles, forming nanocrystals of approximately 40 – 500 nm. The size is dependent upon the hardness of the drug substance and may be controlled by adjusting the processing pressure and the number of cycles applied (Hu 2004).

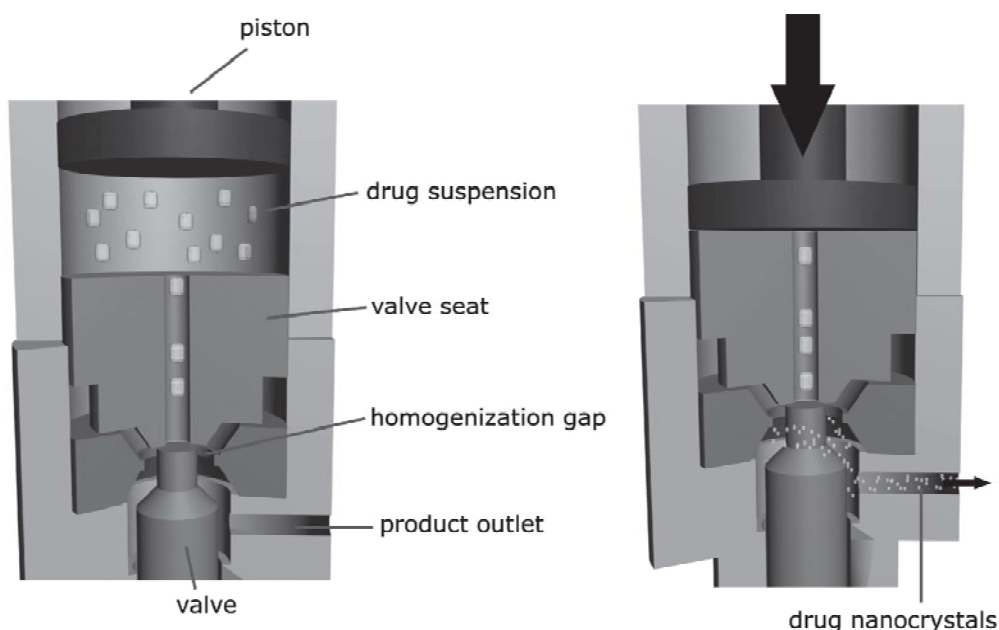


Figure 2.3: High pressure homogenization technique: (right) forcing of drug suspension through narrow valve, (left) fabrication of drug nanocrystals due to generated forces (Junghanns 2008).

This process also is time-consuming as it takes several cycles to reduce particle size which highly depends on the pressure in the homogenizer. Moreover, the drug

powder requires micronization prior to homogenization in order to avoid blockage of the narrow valve. Changes in drug crystallinity have been reported with this process. A portion of drug nanoparticles was reported as amorphous, and in some cases, complete transformation to amorphous state was observed (Muller 2001). In comparison to the milling procedure, high pressure homogenization displays much less contamination due to erosion of the equipment. Muller *et al.* investigated the contamination of nanosuspensions produced under harsh conditions (*eg.* 20 cycles and pressure of 1500 bar), and found iron contamination to be under 1 ppm, low enough to not pose health issues (Krause 2000).

DissoCube[®] was the first high pressure homogenization technology to be marketed. It involved the fabrication of nanocrystals in water. Shortly after, Nanopure[®] technologies was developed which involved homogenization in non-aqueous media or mixtures of water and immiscible substances (*eg.* PEG). The company Baxter developed a combined technology known as NANOEDGE[®] system in which homogenization procedure is combined with the precipitation technique discussed earlier. The homogenization step is used to avoid growth of the drug particles after precipitation takes place (Gao 2008).

2.3 Characterization of Nanocrystals

The essential characterization parameters for nanosuspensions include evaluation of size and size distribution, zeta potential, crystalline state, dissolution velocity and saturation solubility, surface hydrophilicity/hydrophobicity (Patravale 2004). Other tests include chemical investigation such as evaluation of possible degradation products and evaluation of moisture of nanocrystals (for lyophilized API) (Rabinow 2004).

The mean size and size distribution (polydispersity index) are important parameters because they govern properties such as saturation solubility, dissolution velocity, physical stability, and certain biological performances. Photon correlation spectroscopy (PCS) or dynamic light scattering technique (DLS) are employed, but limited to measuring sizes of 3 nm to 3 μm , therefore laser diffractometry (LD) is used to detect aggregates of drug nanocrystals. LD is able to measure particles of 0.05 μm to 2000 μm (Muller 2001). Scanning (or transmission) electron microscopy (SEM, TEM) may also be used for size evaluation. The polydispersity index (PDI) is an important index of physical stability of the nanocrystal. PDI values vary between 0 (monodisperse particles) to 1 (broad distribution), however lower values (≤ 0.3) are usually more appreciable for long-term stability of the nanosuspension.

Surface charge is an important parameter also governing the stability of the nanosuspensions. It is measured by means of electrophoresis and is expressed as electrophoretic mobility or converted to zeta potential. This measurement allows for the prediction of storage stability of the nano-dispersions. Usually the particles with sufficient zeta potential are less likely to aggregate. Literature states that a zeta potential of at least -30 mV for electrostatic and -20 mV for sterically stabilized nanoparticles is desirable for physically stable suspensions (Gao 2008).

Evaluation of crystalline character is required to ensure that crystallinity of the drug has been retained upon nanonization because fabrication procedures may alter the polymorphic state of the drug. For instance high pressure homogenization may generate nanocrystals with amorphous fraction (Muller 2001). Differential scanning

calorimetry (DSC) and X-ray diffraction analysis (XRD) may be used to evaluate the polymorphic state.

Dissolution velocity and saturation solubility need to be evaluated in comparison to the traditional dosage forms of the drug. The determination of such parameters also helps to anticipate the *in vivo* performance (eg. blood profiles, plasma peaks and bioavailability) of the nanocrystal formulation (nonetheless *in vivo* experiments should be followed). Shaking experiments at various temperatures in an artificial medium such as saline, may be used to assess solubility. The dissolution rates are determined using specific methods described in the Pharmacopoeia (Gao 2008).

Characterization of surface properties is essential as it provides insight of the *in vivo* performance of the generated nanocrystals. In the case of intravenous injection, the *in vivo* behaviour of the drug depends on organ distribution, which in turn depends on its surface properties such as hydrophobicity and interactions with plasma proteins (Patravale 2004). Hydrophobic interaction chromatography is able to evaluate the surface hydrophobicity of nanocrystals. Two-dimensional gel electrophoresis (2-D) PAGE is a method employed for the qualitative and quantitative measurements of protein adsorption after intravenous injection of nanosuspension (Gao 2008). Such analysis is imperative to evaluate the *in vivo* biological performance of the fabricated nanocrystals and establish *in-vitro/in-vivo* correlation.

2.4 Administration routes of nanosuspensions

Nanocrystals generated either by top-down or bottom-up approaches are stabilized with surfactants and/or polymer stabilizers in nanosuspensions, which may be processed into solid dosage forms. Thus drug nanocrystals may be administered orally as tablets (or capsules), while drug nanosuspensions may be directly given carefully through *i.v.* administration. In order to transform an aqueous dispersion into a dry powder, lyophilisation or spray-drying may be used (Muller 2004). Spray drying involves the use of high temperatures, which may be a problem for thermolabile drugs. Alternatively, lyophilisation is used, in which a cryoprotective agent (*eg.* mannitol or sucrose) is added to the nanosuspension to prevent aggregation of the nanocrystals in their dried state (Teeranachaideekul 2008). The application of drug nanocrystals is outlined in the next sub-sections.

2.4.1 Oral route

The oral route of administration is preferred to deliver numerous drugs, for its many advantages. However when administered as a nanosuspension there is an increased drug concentration gradient between the gastrointestinal tract and blood vessel, as a result of the increased saturation solubility and dissolution velocity. This leads to less variability in the fed/fasted state. Thus the nanosizing of the drug improves absorption to a large extent and leads to an enhanced bioavailability. In addition, due to their uniquely small size, nanoparticles exhibit increased adhesiveness to the gut wall. A classic example of this is Danazol, a poorly soluble gonadotropin inhibitor. It was shown that an orally administered nanosuspension of this drug, led to an absolute bioavailability of 82.3%, in comparison to the marketed formulation (Donacrine[®]) which displays only 5.2% (Liversidge 1995).

2.4.2 Parenteral Administration

Parenteral administration is an invasive route often related to problems such as limited number of acceptable excipients approved for parenteral use, stringent requirements of aseptic production procedure, patient non-compliance and biological issues such as toxic or allergic reactions (Patravale 2004). In spite of its limitations the parenteral route presents advantages such as *i.v.* administration of a drug results in 100% bioavailability in the body, so only a small dose of drug is required. For *i.v.* administration, the drug particles must be less than 5 μm in diameter in order to avoid blockage and embolism in the blood capillaries (Gao 2008). Nanosuspensions provide an excellent advantage because they only contain very little stabilizers and no added solvents, therefore biological risks associated with excipients and co-solvents are avoided. The nanosuspension may be sterilized by gamma irradiation, filtration sterilization, thermal sterilization or fabricated aseptically (Na 1999). It is important to select the optimal sterilization technique so that the properties of the drug nanosuspension do not change.

2.4.3 Ocular administration route

Suspensions and ointments have been proposed for the ocular delivery of poorly soluble drugs. However their solubility is still limited in lachrymal fluids and effective drug performance is usually not obtained (Patravale 2004). Nanosuspensions of the poorly soluble drugs display a remarkably increased solubility, and provided an effective performance of the drug. Kassem *et al.* fabricated nanosuspensions of three poorly soluble glucocorticoid drugs; hydrocortisone, prednisolone and dexamethasone (Kassem 2007). They investigated ocular bioavailability of the nanosuspensions in comparison to conventional eye drops (solution of microsuspensions), and concluded that nanosuspensions were effective in ophthalmic drug delivery because fewer side effects were observed.

2.4.4 Pulmonary route

Presently, drugs exhibiting poor solubility in pulmonary secretions are formulated as suspension aerosols or dry powder inhalers containing micron sized drug particles (Patravale 2004). The wide particle size distribution of the microparticulate drug causes problems such as: unwanted deposition of the drug particles in the pharynx and mouth, clearance of the drug by cilia movement in the lungs, and limited diffusion and dissolution of the drug at the site of action. Nevertheless, these problems may be resolved by applying nanosuspensions as pulmonary drug delivery systems. The preferred size of inhaled nanoparticles is approximately 1 – 5 μm (Yang 2008). The increased dissolution and subsequent solubility allow for a larger drug concentration in the lung, leading to greater drug levels at the absorption site. Also since nanocrystals have a natural tendency to adhere to mucosal surfaces at the site of absorption, the residence time of the drug increases and it is not easily cleared by the cilia movement (Ponchel 1997).

2.5 Marketed Nanocrystalline drugs

Though nanocrystals are applied through various administration routes, most of the nanocrystalline API on the market are oral dosages forms. Currently there are several marketed pharmaceutical products utilising nanocrystalline drug (Table 2.1). NanoCrystal[®] technology (Elan) is used to fabricate four oral products Rapamune[®], Emend[®], TriCor 145[®] and MegaceES[®] (Merisko-Liversidge 2008). Triglide[™] is marketed as SkyPharma IDD-P technology.

Table 2.1: Summary of nanocrystalline products currently on the market (Junghanns 2008)

Product	Drug compound	Indication	Company	Nanoparticle technology
RAPAMUNE [®]	Sirolimus	Immunosuppressant	Wyeth	Elan Drug Delivery Nanocrystals [®]
EMEND [®]	Aprepitant	Antiemetic	Merck	Elan Drug Delivery Nanocrystals [®]
TriCor [®]	Fenofibrate	Treatment of hypercholesterolemia	Abbott	Elan Drug Delivery Nanocrystals [®]
MEGACE [®] ES	Megestrol acetate	Appetite stimulant	PAR Pharmaceutical	Elan Drug Delivery Nanocrystals [®]
Triglide [™]	Fenofibrate	Treatment of hypercholesterolemia	First Horizon Pharmaceutical	SkyePharma IDD [®] -P technology

Nanonization had allowed these poorly soluble drug compounds to exhibit a faster dissolution rate and solubility and thus an enhanced bioavailability. For instance Tricor[®] marketed by Abbott Laboratories has an active ingredient of fenofibrate; a lipophilic compound and almost insoluble in water (Junghanns 2008). Fenofibrate

may not be converted to a salt because it has no ionisable moiety. Formulation approaches involving lipids and surfactants do enhance the absorption of the drug in fed patients only. However by nanosizing the drug, not only is solubility enhanced, but the drug is bioequivalent in the fed and faster state.

As discussed, there are several advantages of nanocrystal technology. Nanonization is a simple, elegant and universal technique that may be applied to many poorly soluble drugs. The top-down strategies to fabricate nanocrystals are energy intensive and time consuming techniques; however, several drugs have been successfully formulated and marketed based upon such methods. The next chapters describe an alternative technique that has been explored for the fabrication of paclitaxel nanocrystals in the present study.

2.6 References

- Breitenbach, J. (2002). Melt extrusion: from process to drug delivery technology. *Eur J Pharm Biopharm* 54: 107-117.
- Brigger, I., Dubernet C., *et al.* (2002). Nanoparticles in cancer therapy and diagnosis. *Adv. Drug Deliv. Rev.* 54: 631-651.
- Date, A., Patravale V. (2004). Current strategies for engineering drug nanoparticles. *Curr Opin Colloid In* 9: 222-235.
- Devalapally, H., Chakilam, A. *et al.* (2007). Role of nanotechnology in pharmaceutical product development. *J Pharm Sci* 96: 2547-65.
- Gao, L., Zhang, D. *et al.* (2008). Drug nanocrystals for the formulation of poorly soluble drugs and its application as a potential drug delivery system. *J Nanopart Res* 10: 845-862.
- Grau, M. J., Kayser O, *et al.* (2000). Nanosuspensions of poorly soluble drugs -- reproducibility of small scale production. *Int J Pharm* 196: 155-159.
- Haley B., Frenkel E. (2008). Nanoparticles for drug delivery in cancer treatment. *Urol Oncol-Semin Ori*, 26 :57-64
- Horter, D., Dressman J.B (2001). Influence of physicochemical properties on dissolution of drugs in the gastrointestinal tract. *Adv Drug Deliv Rev* 46: 75-87.
- Hu, J., Johnston K. P., *et al.* (2004). Nanoparticle Engineering Processes for Enhancing the Dissolution Rates of Poorly Water Soluble Drugs. *Drug Dev Ind Pharm*, 30: 233-245.
- Junghanns J,. (2008). Nanocrystal technology, drug delivery and clinical applications. *Int J Nanomedicine*. 3: 295-309.
- Keck, C. M., Muller R. H (2006). Drug nanocrystals of poorly soluble drugs produced by high pressure homogenisation. *Eur J Pharm Biopharm* 62:3-16.
- Kesisoglou, F., Panmai S., *et al.* (2007). Nanosizing--oral formulation development and biopharmaceutical evaluation. *Adv Drug Deliv Rev*, 59: 631-44.
- Krause, K., Kayser P. O., *et al.* (2000). Heavy metal contamination of nanosuspensions produced by high-pressure homogenisation. *Int J Pharm*, 196: 169-172.

Merisko-Liversidge, E., Liversidge E., G. G, *et al.* (2003). Nanosizing: a formulation approach for poorly-water-soluble compounds. *Eur J Pharm Sci* 18: 113-20.

Merisko-Liversidge, E., Liversidge G. G. (2008). Drug nanoparticles: formulating poorly water-soluble compounds. *Toxicol Pathol* 36: 43-8.

Müller, R. H., Jacobs C., *et al.* (2001). Nanosuspensions as particulate drug formulations in therapy rationale for development and what we can expect for the future. *Adv. Drug Deliv. Rev.* 47: 3-19.

Müller, R. H., Peters K. (1998). Nanosuspensions for the formulation of poorly soluble drugs I. Preparation by a size-reduction technique. *Int. J. Pharm.* 160: 229-237.

Muller, R. H., Keck C. M. (2004). Challenges and solutions for the delivery of biotech drugs - a review of drug nanocrystal technology and lipid nanoparticles. *J Biotechnol*, 113: 151-170.

Myrdal, P. B., Yalkowsky S. H. (2002). Solubilization of drugs in aqueous media. Encyclopedia of Pharmaceutical Technology. J. Swarbrick and J. C. Boylan. New York, Marcel Dekker.

Rabinow, B. E. (2004). Nanosuspension in drug delivery. *Nat. Rev. Drug Discov.* 3: 785-796.

Rasenack, N., Muller B. W. (2004). Micron Size Drug Particles: Common and Novel Micronization Techniques. *Pharm Dev Technol*, 9: 1-13.

Teeranachaideekul, V., Junyaprasert V. B., *et al.* (2008). Development of ascorbyl palmitate nanocrystals applying the nanosuspension technology. *Int J Pharm* 354: 227-34.

Van Eerdenbrugh, B., Van den Mooter G., *et al.* (2008). Top-down production of drug nanocrystals: Nanosuspension stabilization, miniaturization and transformation into solid products. *Int J Pharm*, 364:64-75.

Wu, Y., A. Loper, *et al.* (2004). The role of biopharmaceutics in the development of a clinical nanoparticle formulation of MK-0869: a Beagle dog model predicts improved bioavailability and diminished food effect on absorption in human. *Int J Pharm*, 285:135-146.

Yang W, Peters JI, Williams Iii RO 2008. Inhaled nanoparticles--A current review. *Int J Pharm* 356 :239-247.

Zhang, Z.-B., Shen Z.-G, *et al.* (2009). Nanonization of Megestrol Acetate by Liquid Precipitation. *Ind Eng Chem Res* 48: 8493-84

CHAPTER 3:

Laser Fabrication of Nanocrystals in Liquid

3.1 Introduction

Pulsed laser ablation (PLA) was introduced in the early 1960s and consists of the collective ejection of material from a target following irradiation by short, intense bursts of light (Yang 2007; Besner 2009 in press). As light does not induce any contamination and is not subject to wear and tear, the technique was naturally adopted for material processing. An important application of PLA is pulsed laser deposition (PLD), which is the growth of thin films in vacuum or low background pressure. In this process, material is removed from the surface of a target by irradiation with a laser beam and collected on a suitably positioned substrate. Over the years, PLD have been used to deposit thin films a wide range of materials, including metals, semiconductors, superconductors, insulators, polymers and biological materials (Jackson 1994; Chrisey 2003).

More recently, several research groups have investigated PLA for the generation of nanoparticles of a variety of materials in gaseous environment. For example, Dolbec *et al.* deposited platinum nanoparticles onto a pyrolytic graphite and a silicon substrate (Dolbec 2004). Mao *et al.* reported mechanical properties of nickel (Ni) nanocrystals which were deposited onto silica and sapphire thin films using pulsed laser deposition (Shan 2004). Steitz *et al.* fabricated silver nanoparticles of predetermined size and very high size uniformity using laser irradiation of large metal clusters (Bosbach 1999). Kabashin *et al.* prepared thin films of photoluminescent silicon nanoparticles (Kabashin 2002). As nanoparticles synthesized by PLA in gaseous environment tend to agglomerate irreversibly, the method is well adapted for the fabrication of thin films of the nanoparticles, but less so when dispersed nanoparticles (such as nanosuspensions in a liquid) are desired. Laser fabrication of nanoparticles in liquid environment proved to be a much better alternative for the production of nanosuspensions.

Laser fabrication of nanoparticles in liquids is a relatively recent, but rapidly growing research field (Barcikowski 2009). The approach encompasses two methods: laser

ablation and laser fragmentation in liquids. In laser ablation, first introduced in the early 1990s, a laser radiation is focused on a solid target immersed in a liquid, resulting in the ablation of the material and dispersion nanoparticles of the solid in the liquid (Figure 3.1 A). In laser fragmentation, on the other hand, the laser is focused on a stirring suspension of the material powder dispersed in a liquid in order to modify (usually to reduce) the size or the shape of the initial particles (Figure 3.1 B) (Sugimori 2000).

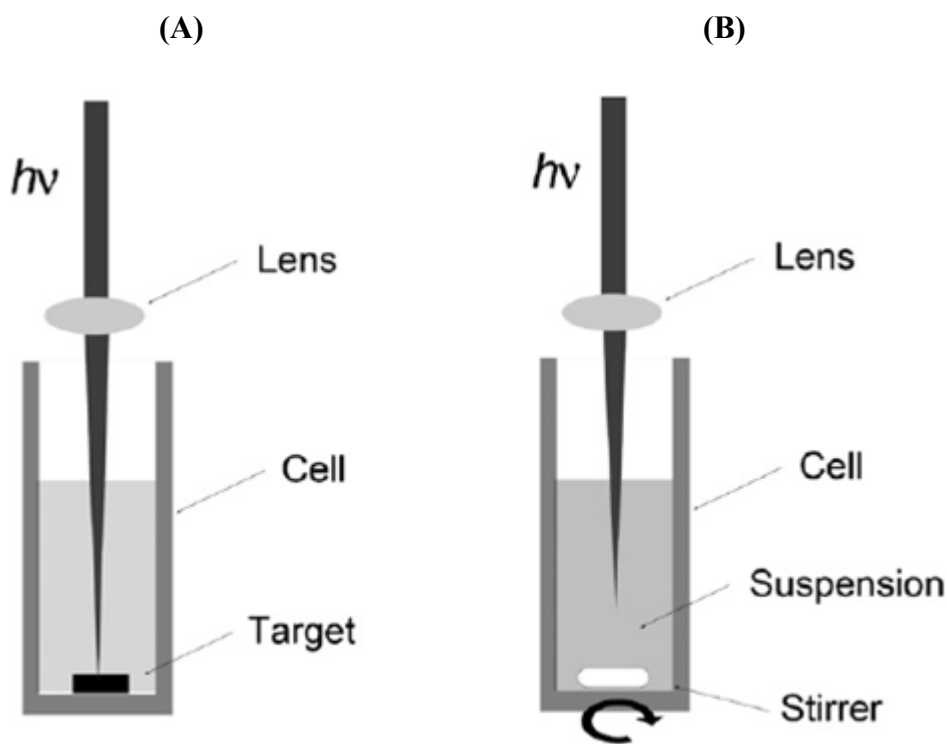


Figure 3.1: (A) Typical experimental set-up for laser ablation at solid-liquid interface and (B) laser fragmentation; irradiation of of suspension by laser (Sugimori 2000).

Laser fabrication in liquids can be applied universally with almost unlimited variety of materials (organic and inorganic alike – see sections 3.2 and 3.3 below) and liquid

matrices (Yang 2007; Barcikowski 2009). A stabilizing agent (*eg.* surfactants, salts and biocompatible molecules) can be incorporated in the liquid in order to control the size of the nanoparticles and improve the stability of the nanosuspension produced.

Several types of lasers, with different wavelengths, average and peak output powers and pulse durations, are now available for the laser processing of materials. The wavelength of the laser, relative to the absorption of the material, and power of the laser radiation are parameters strongly impacting on the amount of energy transferred to the material under treatment. The duration of the laser pulse is also a determinant parameter in the ablation process. Compared to nanosecond and longer pulses, ablation with femtosecond laser pulses provides two major advantages: (1) the reduction of the pulse energy which is necessary to induce ablation for fixed laser wavelength and focusing conditions and (2) a significant reduction or complete removal of heat-affected zones around the laser-treated zone (Yang 2007). It follows therefore, that the energy is more effectively used to break physical bounds, thus limiting the fraction of energy dissipated in the form of heat that could be harmful to the material.

In the following two sections, the laser fabrication of inorganic and organic nanosuspensions in liquids is briefly reviewed. The laser-based approach proposed in this thesis to produce drug nanosuspensions is described in section 3.5.

3.2 Fabrication of inorganic nanosuspensions

Unique electronic, magnetic, optical and catalytic properties of metal (*eg.* Au, Ag, Pt, Co and Cu), metal oxide (FeO, ZnO and TiO₂) and semiconductor (PbS, CdS, Ag₂S and Si) nanoparticles offer great advantages for technological applications and for fundamental research (Katz 2004). Inorganic nanoparticles are promising for application in electronics (Huang 2001), photonics (Law 2004), hierarchical biologically inspired nanocomposites (Fan 2000), biochemical sensing and imaging (Katz 2004) and drug delivery (Salem 2003). For many years gold nanoparticles have been used as contrast agents in electron microscopy (Murphy 2005). More recently gold and silver nanoparticles are being used in biological optical imaging and sensing applications (Eugenii 2004).

Suspensions of inorganic nanoparticles are usually produced by wet-chemical reduction or decomposition of precursors (*eg.* metal salts, metal carbonyls and molecular precursors) (Masala 2004; Besner 2005). These techniques use various chemical steps often involving non-biocompatible chemical products. Furthermore, impurities (including unreacted starting materials, excess reagents, and byproducts resulting from side reactions or degradation pathways) are present in nanoparticle samples and may have a significant impact on properties such as reactivity, stability and toxicity (Dahl 2007). Laser fabrication in liquids offers an interesting alternative for the production of inorganic nanosuspensions in a clean, contamination-free environment, with minimal concentration of surface-active agents. Moreover, when adequate ablation conditions are chosen, metastable materials, not easily attainable otherwise under ambient conditions, can be achieved (Yang 2007). The variety of inorganic nanosuspensions obtained by laser ablation and fragmentation in liquids has been recently reviewed by Yang (Yang 2007).

The ultrashort (femtosecond) pulse laser ablation provides drastically different results from that of the nanosecond laser. When ablation by femtosecond laser near the

threshold was used to produce gold nanoparticles in deionized water, nanoparticle size of 4–5 nm in size were achieved, which is virtually impossible with nanosecond laser ablation. However, the small size and low dispersion was compromised by a very slow production. When ablation efficiency was improved, the average size and size dispersion increased (Kabashin 2003).

The focusing conditions of the femtosecond laser ablation process provides a mean of varying specific conditions which control the size of the particles and efficacy of the procedure (Sylvestre 2005). By varying the position (noted as *z* position) of the target (substance to be ablated), with respect to the focal plane of the focusing objective it is possible to alter the radiation fluence, which is defined as the energy per surface area. At sufficiently high laser fluences, a plasma in the liquid above the surface of the target is formed. Plasma is ionized ‘gas’ and constitutes the fourth state of matter. It may be formed by the highly energetic species ejected from the target, or by optical breakdown in water (formation of a plasma in water by nonlinear absorption of the high power laser pulse). The localized plasma can reach extremely high temperatures and pressures and may further contribute to the ablation (and melting) of the target. Furthermore, as a result of the vaporization of water surrounding the plasma, a cavitation bubble in liquid is formed which expands and then collapses. This mechanical energy impacting on the surface of the target is suggested as another possible ablation mechanism. For the ablation of gold in water, an intense plasma was associated with higher ablation efficiency but larger nanoparticles (Kabashin 2003; Sylvestre 2005).

The addition of stabilizing agents in the liquid environment may profoundly alter the final size distributions of the nanoparticles and stability of the resulting nanosuspension during laser ablation. For example Mafuné *et al.* studied the formation and size control of silver nanoparticles by laser irradiation of a solid target in a solution of sodium dodecyl sulfate (SDS). They found that laser irradiation of the metal immersed in liquid allows for stable suspensions to be provided (Mafuné

2000). It was determined that the average diameter of the nanoparticles decreased as the concentration of SDS increased. Biomolecules, such as CDs had a similar effect during the fabrication of gold by covering the gold nanoclusters obtained, and limiting their growth and interactions (Sylvestre 2004). More recently, Besner *et al.* demonstrated the *in situ* functionalization of gold nanoparticles may be achieved during laser fragmentation in presence of different biocompatible polymers (Besner 2009).

Finally, laser ablation and fragmentation are traditionally used on their own. It was recently demonstrated that the successive application of ablation followed by fragmentation could be an interesting approach to produce narrowly dispersed contaminant-free nanosuspensions. Since gold nanoparticles produced by femtosecond (fs) laser ablation in deionized water at high power were relatively large (few tens of nanometers) and largely dispersed, a second step (fragmentation) was introduced in order to refine the size of the particle (Besner 2007). Further treatment with laser fragmentation for 2h led to reduced to a particle mean size of 20 ± 4 nm from an initial size of 54 ± 36 nm (Besner 2006). Moreover, the fragmentation experiments performed on gold colloidal particles showed that the final size distribution is independent of the initial size and shape of the particles. The latter depends on the radiation parameters (*eg.* power, focusing position and time of irradiation) and on the presence of chemical additives, suggesting that the final size of the nanoparticles depends on the chemical interaction of the fragmented species in solution. It was also shown that fragmentation of gold nanoclusters (previously formed *via* ablation) improved the solution stability. Gold nanoparticles produced by ablation only agglomerated within a few hours, but nanoparticles which were further subjected to laser fragmentation remained stable for several months. Such stability of gold nanoparticles in the absence of chemical additives was never reported before, and so the two-step fs laser assisted method was established as a successful tool to

fabricate small sized stable gold nanoparticles in a chemically pure and contaminant free liquid environment (Besner 2007).

3.3 Fabrication of organic nanosuspensions

The development of laser techniques for fabrication of inorganic nanoparticles has attracted attention to fabricate organic nanoparticles using the similar methods. Recently laser techniques have been explored for the fabrication of organic nanoparticles in suspension (Asahi 2008). The preparation of organic nanoparticles, such as aromatic and dye molecules has drawn increasing attention due to their application as pigments, cosmetics and new materials for optical and electronic devices (Li 2003). A laser fragmentation method for the preparation of organic nanoparticles was developed by Masuhara and coworkers (Masuhara 2003; 2004), in which a nanosecond (ns) laser was applied to micrometer sized vanadyl phthalocyanine (VOPc) dispersed in various solvents suspension to fabricate nanoparticles. They discussed the formation process of the VOPc nanoparticles, and the dependence of laser power as well as the size and morphology of the nanoparticles (Yoshiaki 2003).

The ns laser fragmentation method was also applied to quinadrone (QA, a red pigment) microcrystals in water. It was shown that the crystalline phase and size of the nanoparticles were controlled by the intensity and wavelength of the laser (Jeon 2007). The ns laser fragmentation method established was used to fabricate pentacene nanoparticles and colloidal fullerene (C_{60}) nanoparticles in ethanol solution (Itaya 2006).

In these publications, no accounts of degradation analyses nor complete physico-chemical characterizations were reported. Spectroscopy results suggested that degeneration and decomposition of C_{60} nanocrystals by laser irradiation are insignificant. The authors concluded that there was sign of photodecomposition at higher powers, however they did not provide quantitative data on the extent of degradation nor information on the polymorphic state of the nanoparticles. In another study, ns pulsed radiation was used for the production of 3,4,9,10-

perylene-tetracarboxylic dianhydride (PTCDA) nanoparticles (Hobley 2007). The production of PTCDA nanoparticles was accompanied by formation of polyyne and perylene byproducts in photothermal and multi-photon processes respectively. Once again the degradation and polymorphic state of the nanoparticles was not thoroughly investigated.

The work previously reported utilises a nanosecond laser for the fabrication of nanoparticles, but recently it has been shown that fs laser irradiation of an organic suspension produces smaller nanocrystals. Indeed, Masuhara *et al.* reported that Ti:sapphire fs laser irradiation of bulk VOPc suspended in water produced nanoparticles of smaller size and narrower distribution in comparison with that by nanosecond laser irradiation (Masuhara 2004). However no polymorphic or degradation study was conducted to test the VOPc nanoparticles.

3.4 Fabrication of drug nanosuspensions

As discussed in chapter 2, formulation of poorly water soluble drugs into nanosuspensions can be used to overcome dissolution and bioavailability issues. Considering that the synthesis of a variety of inorganic and organic nanosuspensions could be achieved by laser ablation and fragmentation in liquids (sections 3.2 and 3.3), it is interesting to ask whether the methods could be used for the fabrication of drug nanosuspensions fabrication. To date, only one group has reported the production of drug nanoparticles by laser irradiation, but the laser fabrication was carried in a gaseous rather than a liquid environment. In their studies, PLA was used to break the intermolecular van der Waals force of consolidated phenytoin and indomethacin in order to generate drug nanoparticles with size below 20 nm (Nagare 2004). Laser ablation was performed with a ns pulsed laser, by varying power. More recently, the same group employed PLA, again in a gaseous environment, to form nanostructured indomethacin-bovine serum albumin composites (Nagare 2006). Changes in the crystallinity of indomethacin and in the tridimensional structure of albumin were observed. In both studies, the authors did not examine the dispersibility of the resulting nanoparticles in water. As previously mentioned (section 3.1), the particles produced in a gaseous environment – *eg.* the absence of a dispersing medium and a stabilizing colloid/surfactant, are usually irreversibly agglomerated. Accordingly, the dispersion of the individual nanoparticles in an aqueous medium should be extremely difficult, if not impossible.

3.5 Research proposal & Objectives

The proposed project of this thesis aimed to investigate the use of the recently introduced methods of fs laser ablation and fragmentation in liquids to fabricate drug nanocrystals. The two-steps laser ablation/fragmentation approach previously applied to the fabrication of gold nanosuspensions were investigated. In the first laser ablation step, laser radiation was focused on a solid tablet of the drug immersed in an aqueous solution of a suitable surfactant, resulting in the ablation and dispersion of the product in the liquid (Figure 3.2). The generated dispersion was subjected to a second laser (fragmentation) treatment in which a laser beam is used to irradiate and refined the particles size (Figure 3.3). Alternatively, this two-step approach was substituted by a single laser fragmentation method where the microcrystalline powder of the drug was directly dispersed in an appropriate aqueous medium and treated with the laser radiation. Sterically stabilized drug nanoparticles in a dispersed (non-agglomerated) state were anticipated for all the proposed approaches, and therefore overcoming the redispersion problems associated with the PLA technique. Compared to ns pulses, fs pulses offered the advantage of ablating materials with less energy, thus limiting the possible alteration of the produced drug nanocrystals. Indeed, due to the extremely short laser pulse, the energy was more effectively used to break physical bounds, thus limiting the heat dissipation that could be harmful to the material (Yang 2007). Furthermore, there are evidences that fs laser ablation and fragmentation in liquids of inorganic and organic result in smaller nanoparticles with narrower size distributions compared to the ns processes (sections 3.2 and 3.3). Therefore, we hypothesized that femtosecond laser ablation in an aqueous environment would prove as an efficient and non-destructive production process of drug nanocrystals.

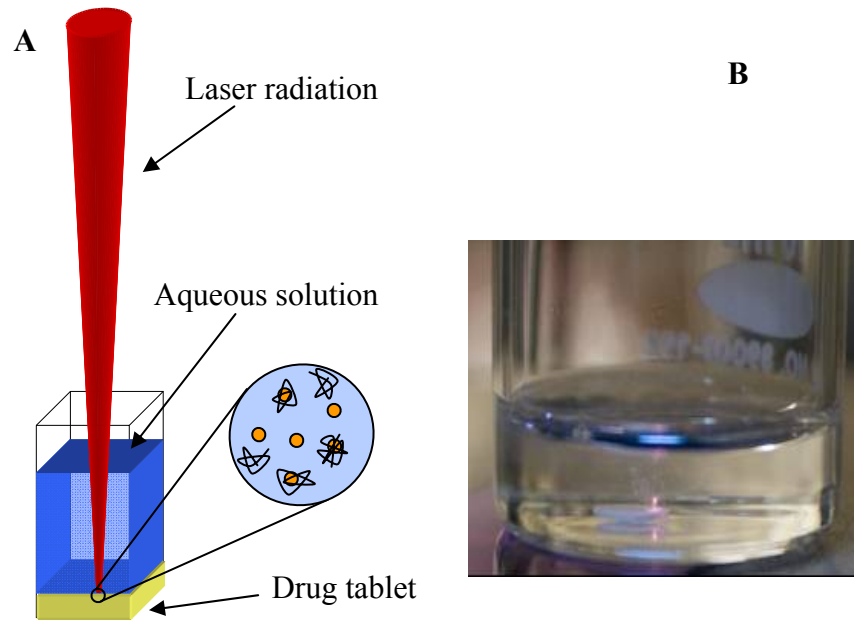


Figure 3.2: (A) Illustration of the production of drug nanoparticles by femtosecond laser ablation; (B) Photography of a paclitaxel tablet immersed in a poloxamer 188 aqueous solution and irradiated by a femtosecond laser

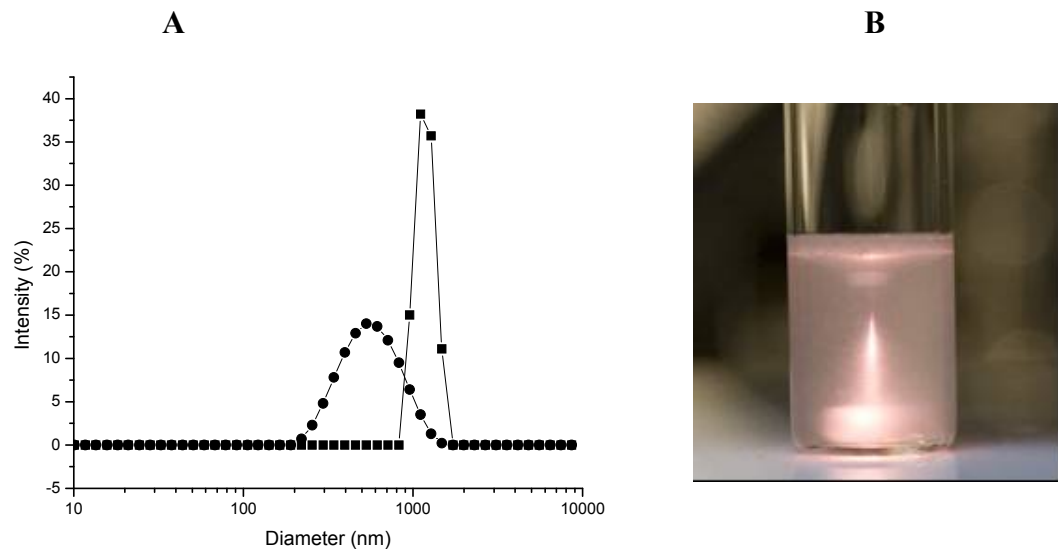


Figure 3.3: (A) Size distribution of drug nanoparticles produced by femtosecond laser ablation before (■) and after (●) the second laser treatment step; (B) illustration of the fragmentation process during the second laser treatment step.

The feasibility of the proposed approach was investigated on paclitaxel, a cytostatic agent. Paclitaxel, a diterpinoid pseudoalkaloid is an important anticancer drug extracted from the bark of Western yew, *Taxus brevifolia* (Panchagnula 1998). With a molecular weight of 853 Da and molecular formula $C_{47}H_{51}NO_{14}$, paclitaxel is a promising anti-tumor agent with poor water solubility ($0.3 \mu\text{g/mL}$) (Figure 4.2)

It is a white crystalline powder, highly lipophilic and insoluble in water, with a melting temperature of $216\text{-}217^{\circ}\text{C}$ (Singla 2002). Paclitaxel is a microtubule-stabilizing agent, such that it binds to the β -subunit of microtubules preventing their depolymerisation. When bound to paclitaxel the microtubules are not only stable, but also dysfunctional, thereby leading to cell death (Panchagnula 1998). Paclitaxel works as an efficient anti-cancer agent and is used to treat breast and ovarian cancer, but also has neoplastic activity against colon, head, non-small cell lung cancer and AIDS related Kaposi's sarcoma (Singla 2002).

To enhance its solubility, paclitaxel is currently formulated in a vehicle of 50:50 blend of Cremophor EL (polyethoxylated castor oil) and ethanol and is known as Taxol[®]. Side effects associated to Cremophor EL, such as hypersensitivity reactions, nephrotoxicity and neurotoxicity, labored breathing, lethargy and hypotension are experienced by patients receiving Taxol[®] chemotherapy (Soga 2005; Miele 2009). Efforts are being made to prepare a stable paclitaxel formulation devoid of Cremophor EL and ethanol with reduced toxicity. Research groups in pharmaceutical sciences have made many efforts to enhance the solubility of paclitaxel, by employing formulation strategies discussed in chapter 1. For instance, liposomes, polymeric micelles and nanoparticles have been developed as carrier systems to solubilize paclitaxel (Liggins 2001; Fonseca 2002; Soga 2005). Other attempts include use of emulsions, cyclodextrin or prodrug formation (Singla 2002). Recently in 2009, Abraxane[®], a novel albumin bound 130 nm particle formulation of paclitaxel marketed by Abraxis Bioscience has been developed for adjuvant treatment of breast cancer. Nyman *et al.* have shown that weekly dosing of Abraxane[®] is safe and

generates minimum toxic effect with objective antitumor responses in patients previously exposed to paclitaxel (Nyman 2005).

The specific objectives of this research project are outlined as follows:

- Firstly, to determine the optimal fabrication conditions to generate water-dispersed paclitaxel nanocrystals (below 500 nm in size with low polydispersity) using the fs laser methodologies. The ablation conditions were optimized (power, time and focusing position), and then the subsequent fragmentation method was studied as a function of laser power.
- The second specific aim was to produce paclitaxel nanocrystals of uniform size distribution, with minimizing chemical degradation.
- Thirdly, the impact of optimal fabrication conditions on the crystallinity and polymorphic state were examined on the finest nanocrystal paclitaxel formulation.

The aims, methodology and results of this project are further discussed in chapter 4 and 5.

3.6 References

- Asahi, T., Sugiyama T., *et al.* (2008). Laser fabrication and spectroscopy of organic nanoparticles. *Acc Chem Res*, 41: 1790-8.
- Barcikowski, S., Devesa F., *et al.* (2009). Impact and structure of literature on nanoparticle generation by laser ablation in liquids. *J Nanopart Res*, 11: 1883-1893.
- Besner, S., Kabashin A. V., *et al.* (2006). Fragmentation of colloidal nanoparticles by femtosecond laser-induced supercontinuum generation. *App Phys Lett*, 89: 233122-3.
- Besner, S., Kabashin A. V., *et al.* (2007). Two-step femtosecond laser ablation-based method for the synthesis of stable and ultra-pure gold nanoparticles in water. *App Phys A-Mater* 88: 269-272.
- Besner, S., Kabashin A. V., *et al.* (2005). Fabrication of functionalized gold nanoparticles by femtosecond laser ablation in aqueous solutions of biopolymers. *Photonic Applications in Biosensing and Imaging*, Toronto, Canada, SPIE.
- Besner, S., M. Meunier (2009 (in press)). Laser synthesis of nanomaterials. *Laser Precision Microfabrication*. K. Sugioka, M. Meunier and A. Pique, Springer.
- Besner, S., Kabashin A. V., *et al.* (2009). Synthesis of Size-Tunable Polymer-Protected Gold Nanoparticles by Femtosecond Laser-Based Ablation and Seed Growth. *J Phys Chem C* 113: 9526-9531.
- Bosbach, J., Martin D., *et al.* (1999). Laser-based method for fabricating monodisperse metallic nanoparticles. *Appl Phys Lett* 74: 2605-2607.
- Chrissey, D. B., Pique A., *et al.* (2003). Laser Deposition of Polymer and Biomaterial Films. *Chem Rev* 103: 553-576.
- Dahl, J. A., Maddux B. L. S., *et al.* (2007). Toward Greener Nanosynthesis. *Chem Rev* 107: 2228-2269.
- Dolbec, R., Irissou E., *et al.* (2004). Growth dynamics of pulsed laser deposited Pt nanoparticles on highly oriented pyrolytic graphite substrates. *Phys Rev B* 70: 201406.
- Dordunoo, S. K., Burt H. M. (1996). Solubility and stability of taxol: effects of buffers and cyclodextrins. *Int J Pharm* 133: 191-201.

- Eugenii, K., Itamar W. (2004). Integrated Nanoparticle-Biomolecule Hybrid Systems: Synthesis, Properties, and Applications. *Angewandte Chemie International Edition* 43(45): 6042-6108.
- Fan, H., Lu Y., *et al.* (2000). Rapid prototyping of patterned functional nanostructures. *Nature* 405:56-60.
- Fonseca, C., Simões S., *et al.* (2002). Paclitaxel-loaded PLGA nanoparticles: preparation, physicochemical characterization and in vitro anti-tumoral activity. *J of Control Release* 83: 273-286.
- Hobley, J. N., Kajimoto T, *et al* (2007). Formation of 3,4,9,10-perylenetetracarboxylicdianhydride nanoparticles with perylene and polyyne byproducts by 355 nm nanosecond pulsed laser ablation of microcrystal suspensions. *J Photoch Photobio A*, 189: 105-113.
- Huang, Y., Duan X., *et al.* (2001). Directed Assembly of One-Dimensional Nanostructures into Functional Networks. *Science* 291: 630-633.
- Itaya, A. K., Masuo S., *et al.* (2006). Nanoparticle Formation of Pentacene by Laser Irradiation in Ethanol Solution. *Jpn J Appl Phys*, 45 : 6501-6507.
- Jackson, T. J., Palmer S. B. (1994). Oxide superconductor and magnetic metal thin film deposition by pulsed laser ablation: a review. *J Phys D:Appl Phys*, 27: 1581-1594.
- Jeon, H.-G., Sugiyama T., *et al.* (2007). Study on Electrophoretic Deposition of Size-Controlled Quinacridone Nanoparticles. *J Phys Chem C*, 111: 14658-14663.
- Kabashin, A. V., Meunier M. (2003). Synthesis of colloidal nanoparticles during femtosecond laser ablation of gold in water. *J Appl Phys*, 94: 7941-7943.
- Kabashin, A. V., Meunier M., *et al.* (2003). Fabrication and characterization of gold nanoparticles by femtosecond laser ablation in an aqueous solution of cyclodextrins. *J. Phys. Chem. B* 107: 4527-4531.
- Kabashin, A. V., Sylvestre J. P., *et al.* (2002). Correlation between photoluminescence properties and morphology of laser-ablated Si/Si nanostructured films. *J Appl Phys*, 91: 3248-3254.
- Katz, E., Willner I. (2004). Integrated Nanoparticle-Biomolecule Hybrid Systems: Synthesis, Properties, and Applications. *Angewandte Chemie International Edition* 43: 6042-6108.

- Law, M., D. Sirbuly J., *et al.* (2004). Nanoribbon Waveguides for Subwavelength Photonics Integration. *Science* 305: 1269-1273.
- Li, B., Kawakami T., *et al.* (2003). Enhancement of organic nanoparticle preparation by laser ablation in aqueous solution using surfactants. *Appl Surf Sci*, 210: 171-176.
- Liggins, R. T., Burt H. M. (2001). Paclitaxel loaded poly(L-lactic acid) microspheres: properties of microspheres made with low molecular weight polymers. *Int J Pharm*, 222: 19-33.
- Mafune, F., Kohno J., *et al.* (2000). Formation and Size Control of Silver Nanoparticles by Laser Ablation in Aqueous Solution. *J Phys Chem B*, 104: 9111-9117.
- Masala, O. Seshadri R. (2004). Synthesis routes for large volumes of nanoparticles. *Annu Rev Mater Res*, 34: 41-81.
- Masuhara, H., Sugiyama T., *et al.* (2004). Formation of 10 nm-sized Oxo(phtalocyaninato) vanadium(IV) Particles by Femtosecond Laser Ablation in Water. *Chem Lett*, 33 :724-725.
- Miele, E., Spinelli G. P., *et al.* (2009). Albumin-bound formulation of paclitaxel (Abraxane ABI-007) in the treatment of breast cancer. *Int J Nanomedicine*, 4: 99-105.
- Murphy, C. J., Sau T. K., *et al.* (2005). Anisotropic Metal Nanoparticles: Synthesis, Assembly, and Optical Applications. *J Phys Chem B*, 109: 13857-13870.
- Nagare, S., Sagawa J., *et al.* (2006). Chemical and Structural Properties of Drug–protein Nanocomposites Prepared by Pulsed Laser Deposition from Conjugated Targets. *J of Nanopart Re,s* 8: 37-42.
- Nagare, S., Senna M. (2004). Reagglomeration mechanism of drug nanoparticles by pulsed laser deposition. *Solid State Ionics*, 172: 243-247.
- Nyman, D. W., Campbell K. J., *et al.* (2005). Phase I and Pharmacokinetics Trial of ABI-007, a Novel Nanoparticle Formulation of Paclitaxel in Patients With Advanced Nonhematologic Malignancies. *J Clin Oncol*, 23: 7785-7793.
- Panchagnula, R. (1998). Pharmaceutical aspects of paclitaxel. *Int J Pharm*, 172 :1-15.
- Salem, A. K., Searson P. C., *et al.* (2003). Multifunctional nanorods for gene delivery. *Nat Mater*, 2: 668-671.

Shan, Z. S., Wiezorek, J. *et al* (2004). Grain Boundary-Mediated Plasticity in Nanocrystalline Nickel. *Science*, 305: 654-657.

Singla, A. K., A. Garg, *et al*. (2002). Paclitaxel and its formulations. *Int J Pharm*, 235: 179-92.

Soga, O., Van Nostrum C. F., *et al*. (2005). Thermosensitive and biodegradable polymeric micelles for paclitaxel delivery. *J Control Release*, 103 : 341-353.

Sugimori, A. (2000). Photochemistry of metalladichalcogenolene complexes. *J Photoch Photobio C*, 1: 33-56.

Sylvestre, J. P., Kabashin A. V., *et al*. (2004). Stabilization and size control of gold nanoparticles during laser ablation in aqueous cyclodextrins. *J. Am. Chem. Soc*, 126: 7176-7177.

Yang, G. W. (2007). Laser ablation in liquids: Applications in the synthesis of nanocrystals. *Prog Mater Sci*, 52: 648-698.

Yang, J., Zhao Y., *et al*. (2007). Ablation of metallic targets by high-intensity ultrashort laser pulses. *Phys Rev B (Condensed Matter and Materials Physics)*, 76: 165430-10.

Yoshiaki T, *et al* (2003). Solvent-Dependent Size and Phase of Vanadyl Phthalocyanine Nanoparticles Formed by Laser Ablation of VOPc Crystal-Dispersed Solution. *Jpn J Appl Phys* 42(Part 1, No. 5A).

CHAPTER 4: Presentation of article

Fabrication of Paclitaxel Nanocrystals by Femtosecond Laser Ablation and Fragmentation

Sukhdeep Kenth^a, Jean-Philippe Sylvestre^b, Kathrin Lueling^c, Michel Meunier^b and Jean-Christophe Leroux^{a,c}

^aCanada Research Chair in Drug Delivery, Faculty of Pharmacy, Université de Montréal, P.O. Box 6128, Downtown Station, H3C 3J7 Montreal, Quebec, Canada;

^bCanada Research Chair in Laser Micro/nano-engineering of materials, Department of Engineering Physics, École Polytechnique de Montréal, P.O. Box 6079, Downtown Station, H3C 3A7, Québec, Canada;

^cInstitute of Pharmaceutical Sciences, ETHZ, 8093 Zürich, Switzerland

Submitted to Pharmaceutical Research on February 23rd 2010. Resubmitted to Journal of Pharmaceutical Science on March 16th 2010.

The experimental work of this article was conducted by Sukhdeep Kenth. Jean-Phillipe Sylvestre helped with the fs laser technique trouble-shooting. Kathrin Lueling was a summer student who helped in the initiation of this project. All authors have assisted in the final proof-reading of the text written by Sukhdeep Kenth.

4.1 Abstract

This study investigated a novel femtosecond (fs) laser technique, previously used to generate fine inorganic nanoparticles in a biologically friendly environment, for the fabrication of paclitaxel nanocrystals in aqueous solution. Two distinct methods of this technology, ablation and fragmentation, have been investigated. The influence of laser power, focusing position and treatment time on the particle size, drug concentration and degradation was studied. Particle size and degradation were evaluated using dynamic light scattering and high performance liquid chromatography respectively. Morphology and chemical composition was correspondingly studied by scanning electron microscopy and Fourier-transform infrared spectroscopy. Differential scanning calorimetry and X-ray diffraction spectroscopy were used to evaluate the polymorphic state of the paclitaxel nanocrystals. Optimal laser conditions generated uniformly sized paclitaxel nanoparticles (<500 nm) with quantifiable degradation. The crystalline morphology of the drug was retained upon nanonization, but the anhydrous crystals were converted to a hydrated form, a phenomenon also observed during bead milling. These findings suggest that drug nanocrystals can be produced with fs laser technology using very little drug quantities, which may be an asset for preclinical evaluation of new drug candidates.

KEYWORDS: nanotechnology, nanoparticles, paclitaxel, femtosecond laser, preclinical development, preformulation, cancer, physicochemical, calorimetry, X-ray powder diffraction, morphology.

4.2 Introduction

Over the recent years, drug design has explored and developed new chemical species resulting in more complex molecules with higher hydrophobicities. It is estimated that 40% or more of active substances being identified through combinatorial screening programs are poorly water-soluble. Consequently, formulation of these drugs presents a major challenge to their clinical development (Rabinow 2004). As a result of their very low aqueous solubility such drugs cannot be injected intravenously and/or often have low oral bioavailability. Classical methods to increase the solubility include micellar solubilization, complexation (*eg.* cyclodextrins) and use of organic solvents. However, these approaches are limited in their success (Muller 2001). A common strategy to enhance dissolution rate of a drug is to decrease the particle size and hence increase the surface area of the drug powder. Nanonization which involves formulating the drug powder as nanometer-sized particles was developed to further improve drug absorption and allow the intravenous injection of insoluble drugs (Merisko-Liversidge 2003). There exist several methods to produce drug nanoparticles, of which at least two are used commercially: NanoCrystal[®] technology (Elan) based on a mechanical process of wet milling and DissoCube[®] (SkyePharma), a high pressure homogenization technique (Muller 2001; Keck 2006). Concerns are often raised regarding the quality and durability of the milling media used in manufacturing and possible contamination of the product following erosion of the grinding material. Disadvantages of the latter method are that prior to preparing the dispersion, the drug needs to be micronized and changes in drug crystallinity have also been reported (Muller 2001).

Laser techniques have been used extensively for the production of metal (Sylvestre 2004) and organic nanoparticles (Asahi 2008; Besner 2008). These methods consist in the irradiation of a solid target or irradiation of a stirring suspension (Nagare 2004; Besner 2008). The high energy from the laser breaks the macroparticles into

nanoparticles. The production of nanoparticles using laser irradiation has proved to be a simple and versatile technique in which stable and contaminant free nanoparticles are generated and thus toxicity problems associated with conventional methods of nanofabrication are avoided (Sylvestre 2005; Besner 2008). Previously, nanosecond (ns) laser fragmentation method, in which a laser beam is focused into a stirring organic microsuspension was developed for the preparation of vanadyl phthalocyanine (VOPc) and quinadron nanoparticles in suspension (Tamaki 2002; Asahi 2008). More recently, this technique was explored to fabricate colloidal fullerene (C_{60}) nanoparticles and 3,4,9,10-perylenetetracarboxylicdianhydride (PTCDA) nanoparticles (Hobley 2007; Asahi 2008). These studies reported very little information on the degradation and on the polymorphic transformation of the organic material upon laser fragmentation. Furthermore, these organic nanoparticles fabricated were for applications in cosmetics and optical/electronic devices and not for drug delivery. Only one group has reported the production of drug (Indomethacin) nanoparticles by ns laser technique (Nagare 2004), where laser ablation (irradiation of a solid target) was performed with a ns pulsed Nd:YAG laser in a dry environment – *i.e.* the absence of a dispersing medium and a stabilizing colloid/surfactant. Some changes in the crystallinity of indomethacin were observed.

Alternatively, femtosecond (fs) laser technology is more favourable than the ns laser because fs pulses offer the advantage of ablating materials with less energy, thus limiting the possible alteration of the ablated drugs nanocrystals. Therefore, fs laser irradiation in liquid could prove as an efficient and non-destructive production process of drug nanocrystals. Additionally, performing fs laser ablation in an appropriate aqueous medium will generate sterically stabilized particles in a dispersed (non-agglomerated) state. Not only has the fs laser recently proven to be effective to produce fine inorganic nanoparticles with narrow size distribution (Besner 2007; 2008), but has confirmed to fabricate smaller sized particles than the ns laser strategy (Masuhara 2004).

Previously described to fabricate gold nanoparticles (Besner 2007), the novel fs laser technology investigated here is based upon two distinct methods: ablation and fragmentation. The first consists of a laser beam focused onto a solid target immersed in a liquid, resulting in the ablation of the material and dispersion of the product into the liquid. The subsequent colloidal suspension is then subjected to a second laser treatment (fragmentation) in order to refine particle size, resulting in smaller and narrower size-distributed nanoparticles (Besner 2008). The presented work thoroughly explores the fabrication of drug nanocrystals by fs-laser ablation/fragmentation in aqueous media with an exclusive characterization and degradation examination of produced nanocrystals, and describes the influence of process parameters on the physicochemical characteristics of the drug. The model poorly soluble drug used is paclitaxel (Figure 4.2), an anticancer agent isolated from the bark of *Taxus brevifolia*. Paclitaxel is generally dissolved in a vehicle of 50:50 Cremophor EL and ethanol blend, which is further diluted with normal saline before intravenous administration. The disadvantage of this formulation is that Cremophor EL causes severe adverse reactions (*eg.* hypertension reactions, nephrotoxicity and neurotoxicity) (Dordunoo 1996; Singla 2002). These side-effects can be substantially alleviated by formulating paclitaxel as a nanoparticulate formulation (Miele 2009).

4.3 Experimental

4.3.1 Materials

Poloxamer 188 was supplied by BASF (Mississauga, ON, Canada). Anhydrous paclitaxel (purity 99.2%) was purchased from Bioxel Pharma (Sainte-Foy, QC, Canada). Dihydrate paclitaxel was purchased from Guanyu Bio-Technology Co., (Xi'an, China). Diphenylhydantoin (DPH) which served as an internal standard and Baccatin III were obtained from Sigma-Aldrich (Oakville, ON). 7-Epipaclitaxel, 7-epi-10-deacetylpaclitaxel and 10-deacetylpaclitaxel were purchased from 21CEC PX Pharm Ltd (East Sussex, UK). Deionised water was generated using Millipore Milli-Q system (Bedford, MA) and all other reagents were of analytical or HPLC grade.

4.3.2 Methods

4.3.2.1 Preparation of paclitaxel tablet and suspension

Pure drug tablets without excipients were prepared in a hydraulic press using 4-mm diameter punches. The applied pressure was $3.9 \times 10^8 \text{ N/m}^2$ (x 25 s). Paclitaxel suspensions (200 $\mu\text{g/mL}$) were prepared by adding paclitaxel powder to freshly prepared poloxamer 188 (8 mg/mL) aqueous solution. The suspension was sonicated (10 min) and stirred vigorously for several hours to obtain a homogenous sample.

4.3.2.2 Fs-laser treatment

Fs-laser radiation was used to ablate a solid paclitaxel tablet placed at the bottom of a 10-mL glass beaker filled with 3.5 mL of poloxamer 188 solution (8 mg/mL) (Figure 4.1*i*). The tablet was held in place within a hole having the size of the tablet performed in a metal disk. The experiments were carried out using a Hurricane, Spectra Physics Ti:sapphire laser (Newport Corporation, Mountain View, CA), providing 120 fs pulses centered at 800 nm with a repetition rate of 1 kHz. The beam

was focused by an objective with the focal length of 7.5 cm. The focusing radiation was moved (0.5 mm/s) using a motorized stage to obtain identical surface conditions during the laser ablation process (Figure 4.1ii). Different parameters were varied, such as the power of ablation (25 to 400 mW), treatment time (10 to 60 min) and different focusing conditions, *i.e.* z positions of 0, 1 and 1.5 mm (Figure 4.1iii). Further size refinement was carried out using laser fragmentation of the produced drug nanocrystal dispersion. The drug suspension was transferred into another glass vial and the laser was focused in the middle of the stirred solution (500 rpm) for 60 min (Figure 4.1iv). Laser power was manipulated from 25 to 400 mW.

Alternatively, single-step fragmentation (no prior ablation) was conducted using prepared paclitaxel suspension (200 µg/mL). Paclitaxel suspension (2.5 mL) was added to a small cuvette with a stir bar, and fragmentation (500 rpm) for 60 min at powers ranging from 50 to 400 mW (Figure 4.1iv).

4.3.2.3 Paclitaxel assay

The amount of paclitaxel and degradation products in suspension, after laser treatments were evaluated by high performance liquid chromatography (HPLC) assay. The sample suspension was first mixed with equal volume of acetonitrile in order to dissolve the particles. After vortexing, the internal standard, DPH (50 µg/mL) was added, and the sample was filtered through 0.2-µm nylon membrane. Injection volume was 70 µL. HPLC was performed using a Waters HPLC system (Waters, Mississauga, ON, Canada) with a C18 column (3.5 mm x 16 mm, dp = 3 µm). The elution was performed using an isocratic mix of water and acetonitrile 3:2 (v/v) for 26 min, continuing with a gradient acetonitrile and mix 0:100 to 43:57 within 21 min, at an elution rate of 1.2 mL/min. UV detection was set at 227 nm and column temperature was maintained at 35°C. Prior to sampling, calibration curves for paclitaxel and all 4 degradation products (baccatin III, 7-epipaclitaxel, 7-epi-10-deacetylpaclitaxel and 10-deacetylpaclitaxel) were established (linearity range 0.3 -

200 µg/mL). The content of paclitaxel and degradation products (µg/mL) was calculated using their respective calibration curves. The % degradation corresponded to the sum of degradation products (µg/mL) divided by the sum of paclitaxel and total degradation products x 100.

4.3.2.4 Particle size analysis and zeta potential measurements

The size of nanocrystals was determined by dynamic light scattering (DLS) using Malvern Zetasizer NanoSeries, with a detection angle of 173° (Malvern, Worcestershire, UK). Each measurement was performed on undiluted suspension in low volume disposable sizing cuvette at 25°C in triplicate. The CONTIN program was used to extract size distributions from the autocorrelation functions. The zeta potential of the nanocrystals was measured by electrophoretic mobility using Zetasizer NanoSeries; samples were prepared by mixing 400 µL of nanocrystal suspension with 500 µL of MilliQ water and 100 µL of saline (0.9% NaCl in water). Each measurement was performed in disposable zeta cells at 25°C in triplicate.

4.3.2.5 Scanning electron microscopy

Morphological evaluation of the optimal paclitaxel nanocrystals was conducted by scanning electron microscopy (SEM). The nanosuspension fabricated by fragmentation was centrifuged to remove the excess surfactant. A drop of suspension was placed on a silicon substrate and dried overnight in a dessicator under vacuum. The sample was observed with a FE-MEB S-4700 field-emission scanning electron microscope (Hitachi, Tokyo, Japan). Paclitaxel control sample (non-fragmented) was prepared by adding pure paclitaxel drug powder to poloxamer 188 solution, sonicated (10 min) and stirred for several hours, but not subjected to laser treatment.

4.3.2.6 Thermal Analyses

For thermogravimetric analysis (TGA) and differential scanning calorimetry (DSC), the nanocrystals and control samples were prepared without poloxamer 188, in order to avoid signal interference from the polymer which degraded before the melting point of paclitaxel. TGA of the anhydrous paclitaxel, dihydrate paclitaxel, nanocrystals and water-exposed non-fragmented drug was performed with a TA Instruments TGA 2950 system (TA Instruments, New Castle, DE). Approximately 3 mg of the paclitaxel sample was weighed in a platinum pan and heated to 700°C at a rate of 10°C/min under nitrogen purge. Thermal properties were obtained by DSC, TA Instruments DSC Q200 system, (TA Instruments, New Castle, DE). Samples of 2-3 mg were placed and sealed in Tzero pinhole pans and analysed at a heating rate of 50°C/min. High heating rate was used in order to avoid decomposition of the drug in the DSC furnace.

4.3.2.7 Spectroscopic Analyses

Paclitaxel samples were analyzed by Fourier transform infrared spectroscopy (FTIR) for chemical composition and by X-ray diffraction (XRD) for crystallinity. Prior to FTIR and XRD analysis, the control sample (raw paclitaxel suspended in poloxamer 188 by sonication and stirring) and the laser fragmented nanocrystals were both cleaned by ultracentrifugation, and then lyophilized. Firstly, the samples were centrifuged for 15 min at 10,600 x g. The sedimented particles were washed with MilliQ water, re-suspended and centrifuged twice more to remove the residual poloxamer 188 and then lyophilized for 72 h. FTIR and XRD spectra were obtained for the lyophilized nanocrystals and control sample (non-fragmented), the raw anhydrous and dihydrate paclitaxel samples. FTIR analysis, with a resolution of 4 cm⁻¹, was performed with a Bio-Rad Excalibur Series spectrometer, FTS3000 (Bio-rad Laboratories, Randolph, MA) using the potassium bromide (KBr) pellet technique. Each 150 mg pellet contained 2 mg of the paclitaxel sample. XRD spectra

were obtained with an X'Pert X-ray PANalytical diffractometer (PANalytical Inc, Montreal, QC, Canada) using the grazing angle method in which the X-ray source was fixed at $\omega = 2^\circ$. Samples of 10-15 mg were used. The x-ray source was $\text{CuK}\alpha$ (50 kV 40 mA). The 2θ range scanned was 5 to 50° at a rate of $0.02^\circ 2\theta/\text{s}$.

4.4 Results & Discussion

In the first part of this work, fs-laser ablation followed by subsequent fragmentation was explored. The ablation process was investigated as a function of power (25 to 400 mW), focusing position ($z = 0, 1$ and 1.5 mm) and ablation time (20 to 60 min). Upon completion of the ablation process, the sample was collected and analyzed by HPLC for paclitaxel concentration and degradation products. Figure 4.3 (top) shows the concentration of paclitaxel particles produced after ablation as a function of laser power for 3 focusing positions. At z positions of 1 and 1.5 mm, increasing the power from 25 to 400 mW resulted in a higher concentration of the suspended paclitaxel particles. Ablation was also more important at z position of 1.5 than 1 mm. In all cases, degradation was relatively low but greater at $z = 1.5$ (ca. 2%). Ablation at the surface of the tablet ($z = 0$ mm) generated the least degradation but also the least concentrated paclitaxel suspensions, thus indicating that ablation on the surface of the tablet was not an efficient method to produce particles. It has been reported that ablation of $z = 0$ mm generates a plasma (partially ionized matter, containing a portion of free electrons) which readily absorbs part of the laser radiation, leaving less energy for the ablation of the target (Sylvestre 2005). The size of the particles was independent of the power since particles ranging from 800-3000 nm were observed at all powers (data not shown). As ablation at $z = 1.5$ mm generated the largest degradation, subsequent experiments were carried out at $z = 1$ mm. The effect of time of ablation was then assessed at a power of 150 mW. As illustrated in Figure 4.3 (bottom), the amount of paclitaxel particles produced increased as a function of exposure time and reached a plateau between 20 and 40 min (~ 50 $\mu\text{g/mL}$). After 20 min ablation, the suspension became relatively turbid, thereby decreasing the ablation efficiency. The turbidity of the suspension caused the laser beam to be scattered, thereby reducing the energy available to ablate the tablet. Ablation for over 20 min also generated more degradation (data not shown). The optimal ablation condition was selected as: $z = 1$ mm, treatment time of 20 min and power of 150 mW. Next, a

stock suspension prepared via optimal ablation was subjected to fragmentation from 25 to 400 mW. This second laser treatment did refine the mean diameter of the particles; particles as small as 50 nm were obtained, however the particle size distribution remained considerably large (Table 4.2). Degradation also increased with laser power, reaching important levels (>4%) above 150 mW. The zeta potential was almost neutral and did not change with fragmentation conditions.

As the overall efficiency of the two step ablation/fragmentation process was limited by the amount of drug ablated in the initial step, an alternative strategy based upon fragmentation alone was explored. A paclitaxel suspension ($\sim 200 \mu\text{g/mL}$) was prepared directly by adding the drug powder to the poloxamer 188 solution. The suspension was fragmented at powers ranging from 50-400 mW, and size and degradation were measured (Table 4.3). As the power increased, smaller particles with acceptable polydispersities ($\text{PDI} \sim 0.3$) were obtained, however higher degradation was observed (up to 23% at 400 mW). This trend in particle size was reported in other studies involved in the production of C60 and VOPc nanoparticles using a ns-laser fragmentation method (Tamaki 2002; Asahi 2008), suggesting that higher laser power provides greater energy to fragment particles, thus smaller nanocrystals are obtained. This single step fragmentation process yielded a smaller size distribution in comparison to the ablation/fragmentation method. The morphology assessment by SEM confirmed that significant nanonization occurred during laser fragmentation. The original needle-like shape was retained upon fragmentation at 400 mw for 60 min, and size was reduced from micro- to nanoparticles (Figure 4.4). In previous studies, it was demonstrated that laser irradiation of VOPc microcrystals dispersed in solvent changed the morphology of the initial crystals (Tamaki 2002). Such morphological change was not observed when paclitaxel was fragmented using the fs laser technique.

Following the size and degradation examination of the paclitaxel particles, further characterization was carried to evaluate the hydration and crystalline states of the

drug upon laser fragmentation. The fs-laser generated nanoparticles were compared to anhydrous paclitaxel, dihydrate paclitaxel and a non-fragmented water exposed sample which was fabricated by suspending the anhydrous drug in the aqueous solution followed by lyophilization.

FTIR spectroscopy was used to characterize the hydration state of the various paclitaxel samples (Figure 4.5). The peak shapes of anhydrous paclitaxel and the water-exposed non-fragmented paclitaxel were similar at 3500 cm^{-1} and 1700 cm^{-1} . At these wavenumbers the dihydrate paclitaxel and the laser fragmented sample displayed broadened and less defined peaks, suggesting hydration of the drug upon laser fragmentation. A general trend was observed: the peaks became less defined (eg. loss of doublet peak around 1700 cm^{-1}) and broadened as the sample becomes more hydrated. This phenomenon of doublet to singlet peaks upon hydration of paclitaxel has been reported before (Pyo 2007).

As expected, DSC analysis showed that the anhydrous paclitaxel and water-exposed non-fragmented sample exhibited a sharp melting point at ca. 225°C (Liggins 1997). This melting endotherm was also observed in the dihydrate paclitaxel sample, but was not seen in the laser fragmented sample (Figure 4.6). DSC analysis depicted the degradation of the fragmented sample at temperatures above 220°C , this correlated with the TGA analysis which demonstrated that degradation occurred at a lower temperature in comparison to the other paclitaxel samples (Figure 4.S1). Dihydrate paclitaxel exhibited a broad endotherm from approximately $50\text{-}125^{\circ}\text{C}$ corresponding to water evaporation (Gi 2004). A similar endotherm, but less broad was observed in the fragmented sample, indicating that this sample displayed a hydrated nature. Additionally, a significant endothermic peak at 170°C (relevant to a solid-solid transition), was observed in the dihydrate paclitaxel and to a lesser extent in the laser fragmented sample (Gi 2004).

In order to obtain more insight into the possible polymorphic transformation occurring upon fs-laser fragmentation, XRD analysis was performed on the drug samples (Figure 4.7). Anhydrous paclitaxel exhibited characteristic XRD peaks at $2\theta = 5.6^\circ, 9.1^\circ, 10.4^\circ, 12.7^\circ$ and 21.1° (Liggins 1997). Anhydrous and dihydrate paclitaxel demonstrated different XRD patterns, and thus there was a polymorphic transformation upon hydration of anhydrous paclitaxel (Liggins 1997; Pyo 2007). Five new peaks (6.2, 9.8, 11.2, 13.3 and 16.7), which were all absent in the anhydrous paclitaxel appeared in the water-exposed control, laser-fragmented and dihydrate samples, thus suggesting partial hydration of paclitaxel. As the anhydrous paclitaxel was suspended in water it became slightly hydrated as evidenced by the apparition of peaks characteristic of the dihydrate form. As fragmentation was performed, the hydration of the drug augmented and thus displayed similar XRD patterns to dihydrate paclitaxel (Figure 4.7). Moreover, the paclitaxel suspension (700-800 nm sized particles) prepared by bead-milling displayed similar features to the laser fragmented sample suggesting that nanonization of paclitaxel in water transforms anhydrous drug into the hydrated state (Fig 4.7 and Fig 4 S2).

By compiling the calorimetry and spectroscopy results, it appears that the anhydrous drug underwent crystalline change into dihydrate form after fs laser treatment in water. The slight differences between the laser fragmented and the dihydrate samples may be due to the presence of degradation products or small size of the nanocrystals. These two paclitaxel forms both exhibit needle shaped crystal habit (Liggins 1997). In previous work reporting the laser fragmentation of organic suspensions, quantitative degradation studies were not performed (Hobley 2007; Sugiyama 2009). Sugiyama *et al.* assessed the photoproducts of C_{60} by ^{13}C NMR. They revealed that no appreciable photoproduct was formed under specific ns-laser irradiation conditions, although decomposition of C_{60} was induced at a higher fluence (Sugiyama 2009). Hobley *et al.* used the similar pulsed ns-laser technique to fabricate PTCDA nanoparticles (Hobley 2007). Byproducts of PTCDA were indentified but no

quantitative degradation study was conducted. In the present work, nanoparticles of a complex drug molecule were prepared by fs laser method and the production of degradation products was monitored. The fs laser treatment was previously shown to generate smaller particles than ns-laser (Masuhara 2004). However, as can be seen in Tables 4.2 and 4.3, the fabrication of particles of less than 1000 nm was associated with significant degradation of paclitaxel. The latter is a labile molecule (Jiaher 2008; Jiaher 2009) and therefore it can be expected that chemically less complex and more stable drugs would be better suited for nanonization by fs laser treatment. In order to decrease the degradation process, fragmentation was performed under an inert atmosphere (argon), in the presence of antioxidants (L-cysteine) or with other stabilizing agents (polysorbate 80, polyvinylpyrrolidone). However, these approaches proved unsuccessful (data not shown).

4.5 Conclusion

In this work, fs laser irradiation was explored for the fabrication of paclitaxel nanocrystals. Narrowly-dispersed paclitaxel nanoparticles of approximately 400 nm were obtained by single-step fragmentation. However they were associated with significant degradation. The polymorphic transformation of paclitaxel into the dihydrate state is not associated with the fs laser conditions, but rather is characteristic of any nanonization method performed in water. Paclitaxel is perhaps not the best drug candidate for this nanonization technique, nevertheless work in progress for other hydrophobic drugs, *eg.* megestrol acetate, suggests that fs laser fragmentation may be an alternative route for the production of nanoparticles of other poorly water soluble and less sensitive drugs (Sylvestre 2009). Though several studies have reported use of laser technology for the development of organic nanoparticles, this is the first investigation where a novel fs-laser fragmentation technique is used for the fabrication of paclitaxel nanocrystals in aqueous medium, and in which the nanocrystals have been fully characterised. A current limitation of the fs-technique as presented here is that the efficiency of the process is limited by the increase in turbidity of the suspension as more particles are produced. However, this problem could be easily solved by implementing a continuous flow system, which may also eventually lead to lower degradation of the drug. This work may translate into successful future avenues for the production of drug nanocrystals for an array of pathologies including cancer and infectious diseases. In addition, this fs-laser technology presented here may be valuable in the preclinical development. In the pre-formulation and late discovery stage, compound availability is scarce and thus examining numerous formulation approaches is difficult (Van Eerdenbrugh 2008; 2009). Using the fs-laser technology on minute amounts of drug (μg) to fabricate nanoparticles may be advantageous as an *in vivo* screening approach. If the nanocrystal formulation appears to be promising (*eg.* displays good bioavailability),

then more conventional techniques may be applied for the production of greater amounts of nanocrystals without degradation.

4.6 Acknowledgements

Financial support was provided by the Natural Sciences and Engineering Research Council of Canada (NSERC), the Canadian Institutes of Health Research (CIHR), the Groupe de Recherche Universitaire sur le Médicament (GRUM), and Fonds de la recherche en santé du Québec (FRSQ). Special thanks to Dr Marc Gauthier for proof-reading the text.

Figure 4.1: Representation of fs-laser ablation (top) and fragmentation (bottom) methods.

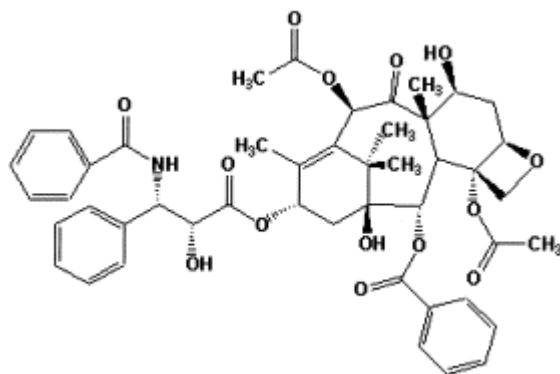


Figure 4.2: Chemical Structure of paclitaxel (5 β ,20-epoxy-1,2 α ,4,7 β ,13 α -hexahydroxytax-11-en-9-one 4,10-diacetate-2-benzoate 13-ester with (2*R*,3*S*)-*N*-benzoyl-3-phenylisoserine). (Singla 2002)

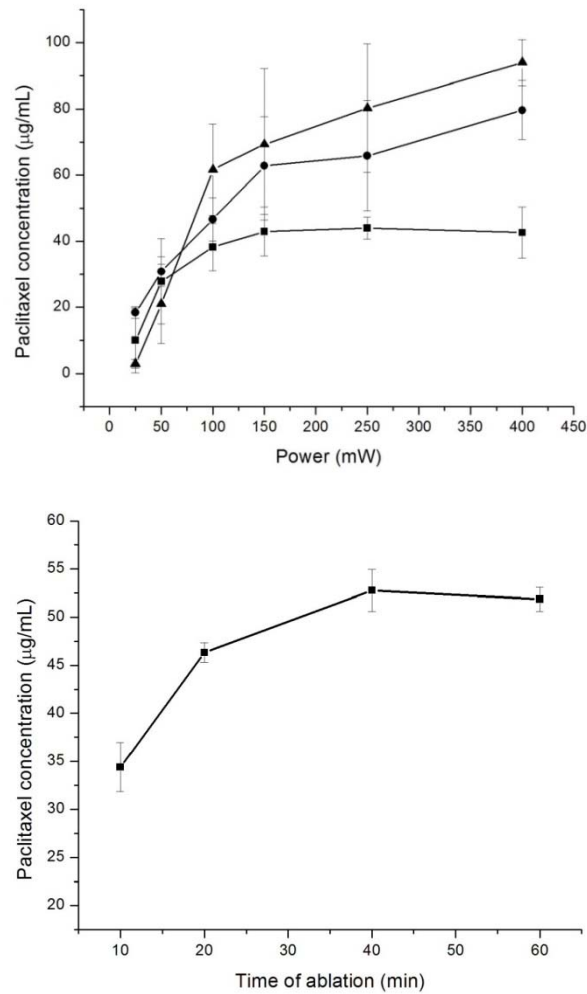


Figure 4.3 (Top) : Paclitaxel concentration of the suspensions prepared by fs-laser ablation at focusing positions of $z = 0$ mm (squares), 1 (circles) and 1.5 (triangles), at power ranging from 25 to 400 mW. Mean \pm SD ($n=3$). **(Bottom) :** Paclitaxel concentration of the colloidal suspensions prepared by fs-laser ablation at focusing positions $z = 1$, 150 mW, and time ranging from 10 to 60 min. Mean \pm SD ($n=3$).

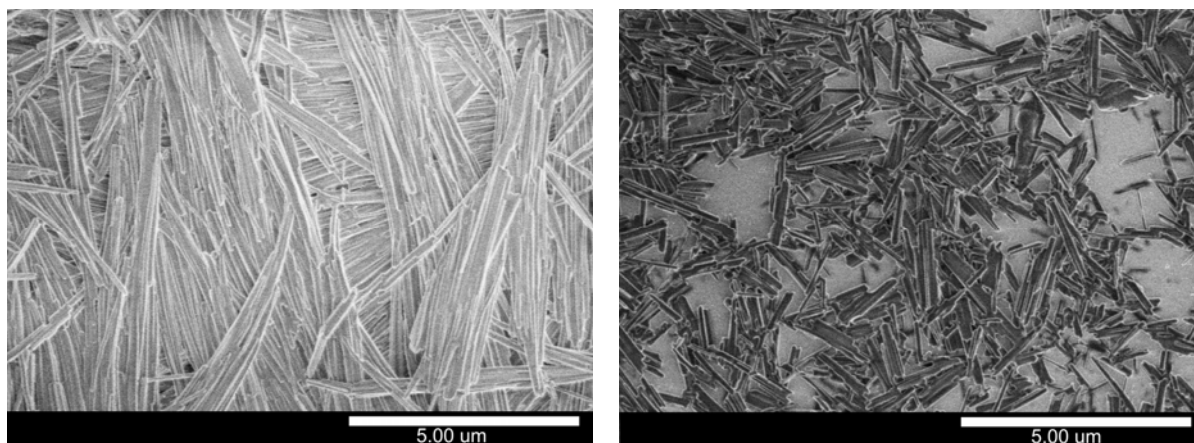


Fig 4.4: Scanning electron micrographs of **(right)** water-exposed non fragmented paclitaxel and **(left)** laser fragmented paclitaxel nanocrystals (400 mW, 60 min).

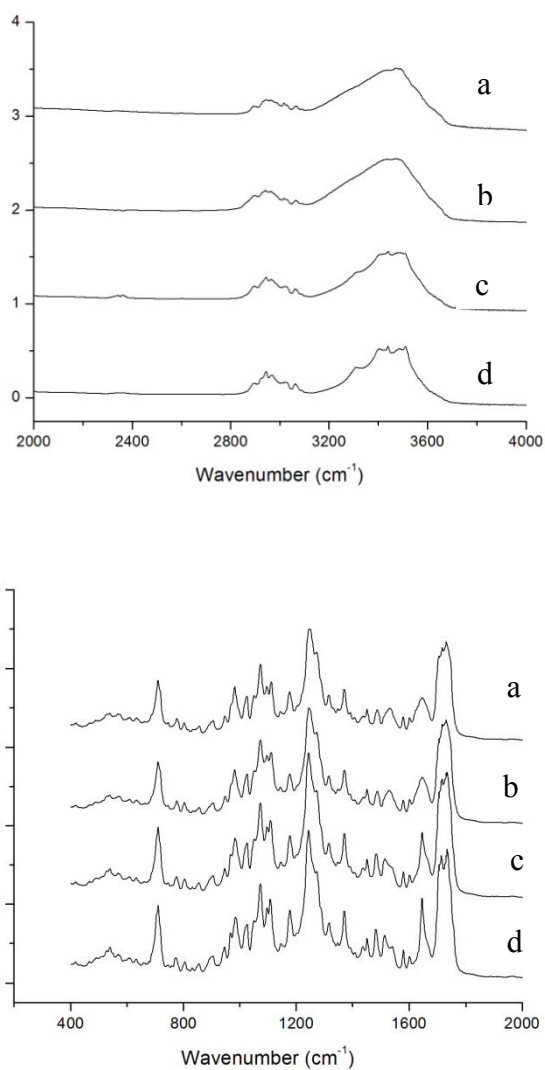


Fig 4.5 :FTIR spectra of anhydrous paclitaxel (**d**), water exposed non-fragmented paclitaxel (**c**), laser fragmented nanocrystals (**b**) and dihydrate paclitaxel (**a**)

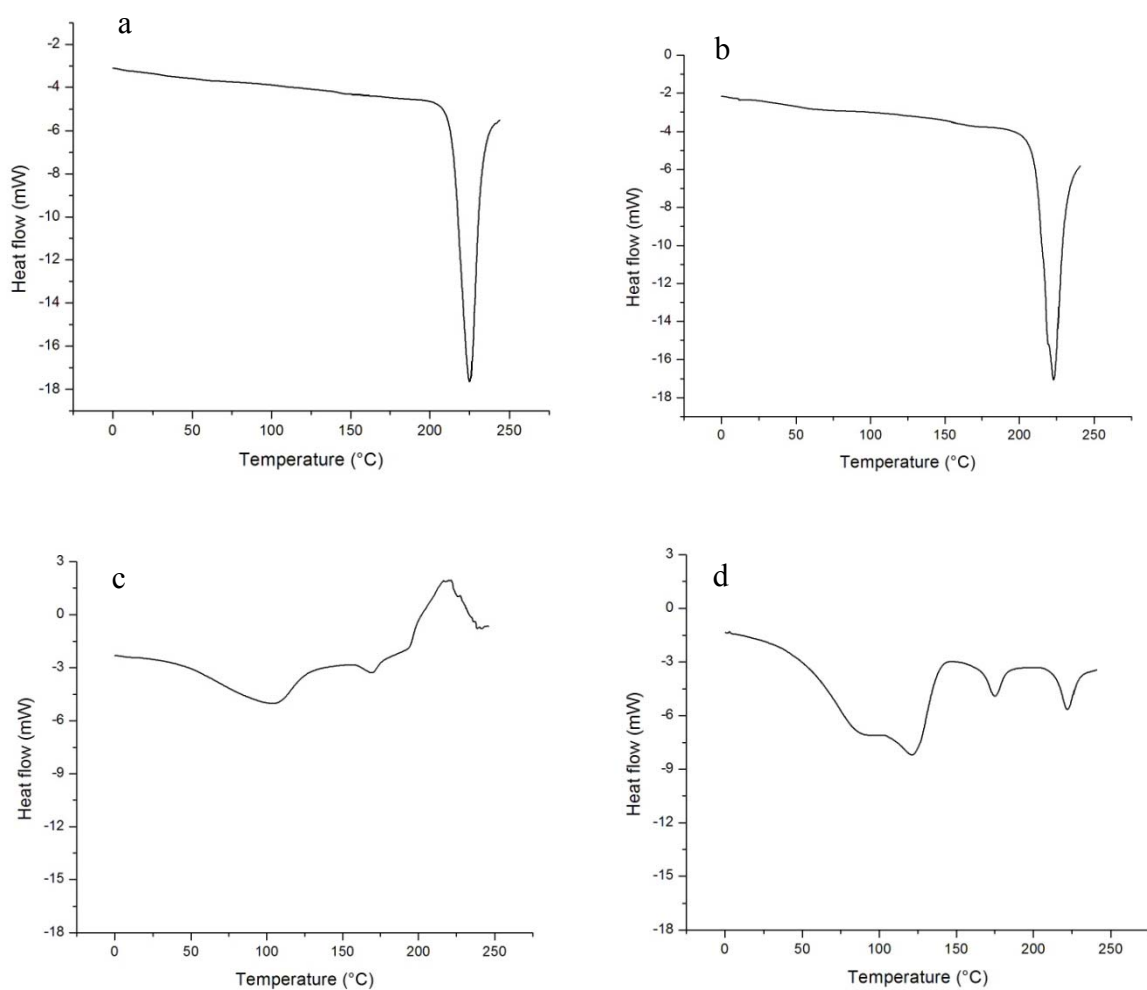


Figure 4.6: DSC thermograph of anhydrous paclitaxel **(a)**, water exposed non-fragmented paclitaxel **(b)** laser fragmented (400 mW, 60 min) nanocrystals **(c)** and dihydrate paclitaxel **(d)**.

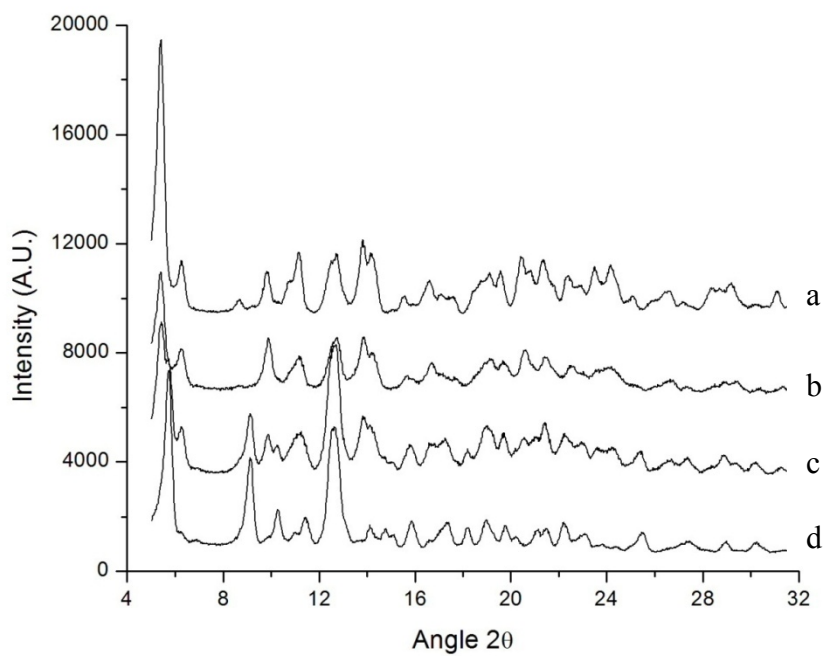


Figure 4.7: XRD analysis of anhydrous paclitaxel (**d**), water exposed non-fragmented paclitaxel (**c**), laser fragmented (400 mW, 60 min) paclitaxel nanocrystals (**b**) and dihydrate paclitaxel (**a**).

Table 4.1: Degradation of the paclitaxel colloidal suspensions generated by ablation at three focusing conditions. Mean \pm SD (n=3).

Power (mW)	Degradation (%)		
	z = 0 mm	z = 1 mm	z = 1.5 mm
25	0.7 \pm 1	0.3 \pm 0.2	1.8 \pm 1.7
50	0.3 \pm 0.4	0.5 \pm 0.3	2.9 \pm 1.9
100	0.5 \pm 0.5	1.0 \pm 0.5	2.2 \pm 0.7
150	0.8 \pm 0.4	0.8 \pm 0.1	2.3 \pm 1.3
250	0.8 \pm 0.3	1.1 \pm 0.2	2.8 \pm 1.1
400	0.8 \pm 0.4	1.8 \pm 0.7	2.1 \pm 0.5

Table 4.2: Chemical degradation, size distribution and surface charge of paclitaxel suspensions prepared by two-step fs-laser ablation and fragmentation. Mean \pm SD (n=3).

Power (mW)	[PTX] ($\mu\text{g/mL}$)	Degradation (%)	Size (nm)	PDI	Zeta potential (mV)
0	37.3 ± 3	1.6 ± 1	2700 ± 800	0.9 ± 0.2	-6.0 ± 3.0
25	34.5 ± 4	4.0 ± 1	2000 ± 500	0.7 ± 0.2	-5.6 ± 0.4
50	32.3 ± 3	3.3 ± 2	2200 ± 600	0.9 ± 0.1	-6.8 ± 0.5
100	33.2 ± 2	2.8 ± 1	1500 ± 450	0.7 ± 0.3	-6.2 ± 0.3
150	30.8 ± 1	3.8 ± 2	1100 ± 400	0.3 ± 0.2	-4.4 ± 0.2
250	14.1 ± 2	9.7 ± 1	300 ± 100	0.6 ± 0.2	-5.8 ± 0.9
400	10.3 ± 1	8.0 ± 3	50 ± 15	0.7 ± 0.2	-1.0 ± 0.6

Table 4.3: Chemical degradation and size distribution of paclitaxel particles obtained by fragmentation (60 min) Mean \pm SD (n=3)

Power (mW)	Size (nm)	PDI	Degradation (%)
50	3000 \pm 160	0.29 \pm 0.20	1.2 \pm 0.14
100	1100 \pm 70	0.34 \pm 0.07	8.3 \pm 0.41
150	800 \pm 30	0.32 \pm 0.05	12.6 \pm 1.3
250	600 \pm 50	0.31 \pm 0.04	17.1 \pm 1.7
400	400 \pm 60	0.29 \pm 0.07	23.1 \pm 2.0

Supporting Information

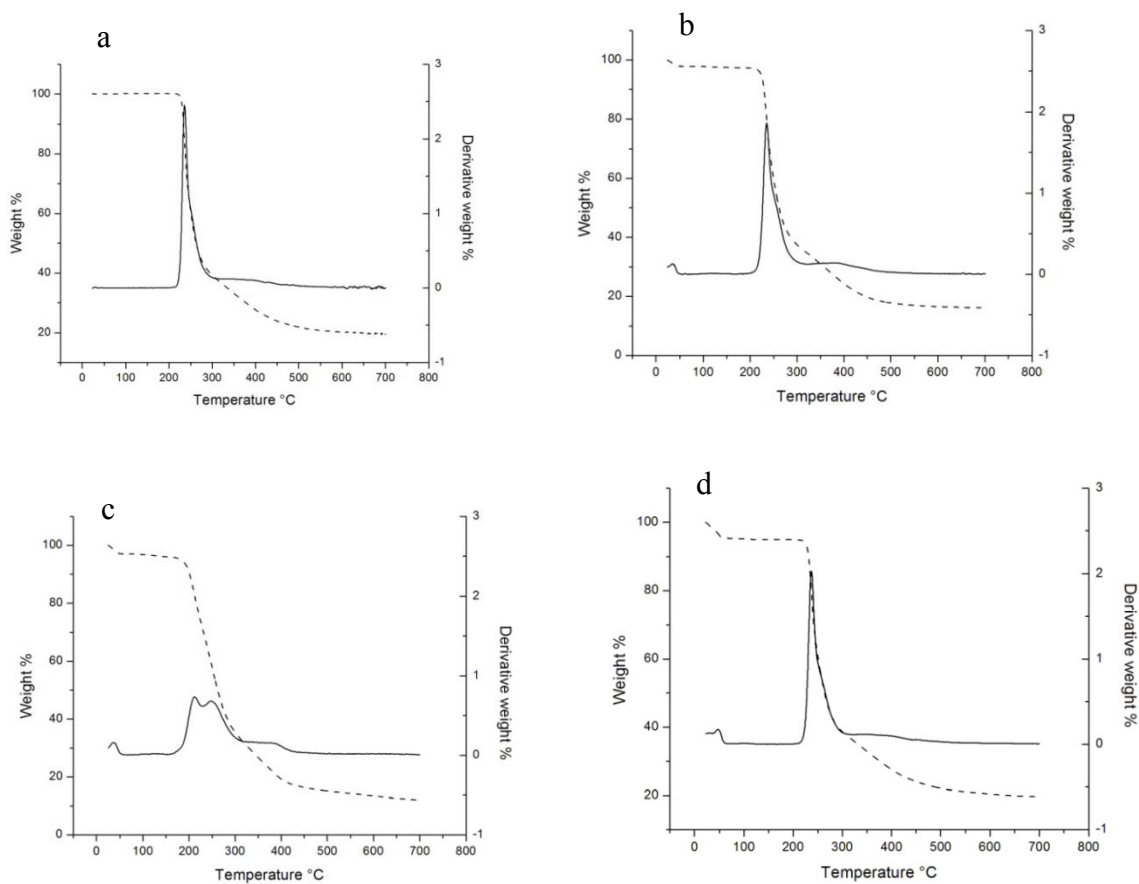


Figure 4.S1: TGA thermograph of paclitaxel anhydrous powder **(a)**, water exposed non-fragmented paclitaxel **(b)** laser fragmented (400 mW, 60 min) nanocrystals **(c)** and dihydrate paclitaxel **(d)**. Weight percent is expressed in solid line and derivative weight percent is expressed as dashed line

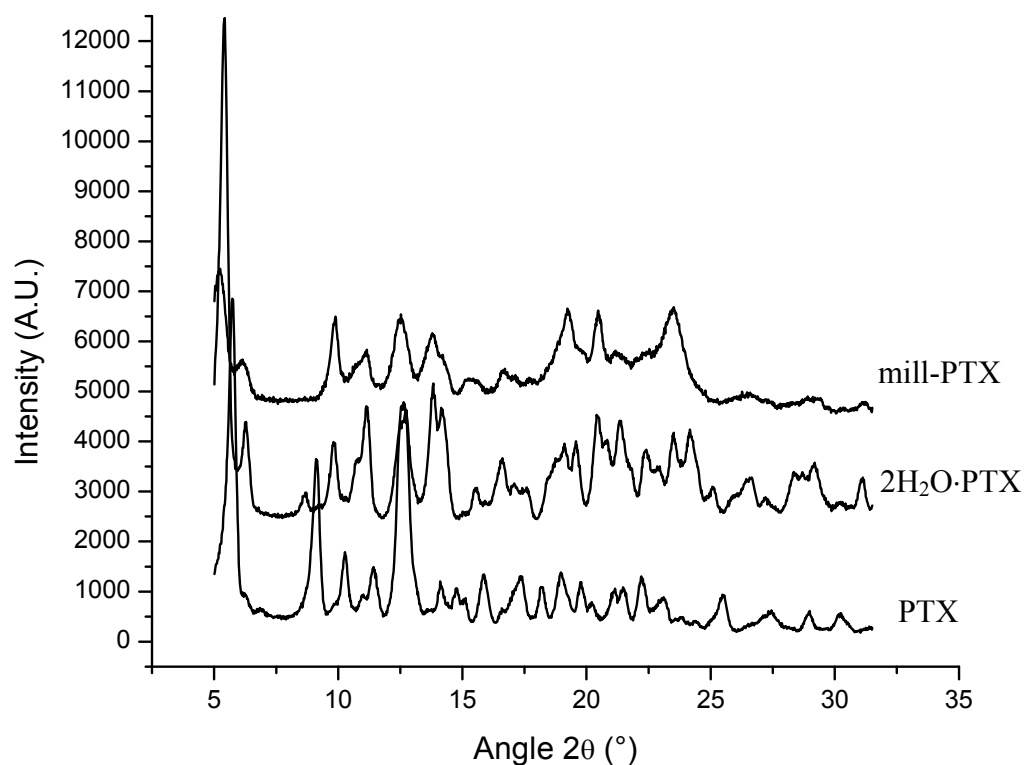


Fig. S2. XRD analysis of milled paclitaxel (mill-PTX), dihydrate paclitaxel (2H₂O-PTX) and anhydrous paclitaxel (PTX).

The milled paclitaxel sample was prepared by bead milling. 0.5%(w/w) of paclitaxel was suspended in a 0.125% (w/w) Poloxamer 707 solution in ultrapure water. This suspension was added to a glass vessel with zirconium oxide beads (3 mm diameter) and placed on a roller mill. After 4h of agitation at 220 rpm, the beads were separated and size of the drug particles was measured by DLS. The suspension was washed by centrifugation and lyophilized before XRD analysis.

Table 4.S1 : XRD peaks (angle 2θ) comparison of anhydrous paclitaxel, water-exposed paclitaxel, laser fragmented nanocrystals and dihydrate paclitaxel.

Raw PTX	Control PTX	Fragmented PTX	Dihydrate PTX
5.73	5.45	5.44	5.43
	6.27	6.25	6.25
9.11	9.13		
	9.87	9.85	9.87
10.27			
	11.25	11.17	11.13
11.43			
12.63	12.69	12.75	12.71
	13.89	13.83	13.83
14.11			
14.77			
15.87	15.79	15.67	15.55
	16.71	16.71	16.61
17.37	17.25		
18.21	18.19		
18.97	18.97		
		19.25	19.11
19.75	19.67	19.67	19.57
		20.59	20.45
21.15			
21.39	21.43	21.51	21.39
22.21	22.25	22.45	22.41
	22.95		22.95
	23.63		23.51
	24.21	24.19	24.17
25.55	25.39		25.11
	26.71	26.79	26.65
27.11	27.35		27.31
28.99	28.81	28.89	28.35
	29.09		28.75
30.25			29.01
		31.23	29.19
			31.13
	34.33		34.33

4.7 References

- Asahi, T., Sugiyama T., *et al.* (2008). Laser Fabrication and Spectroscopy of Organic Nanoparticles. *Acc Chem Res* 41: 1790-1798.
- Besner, S., Kabashin A. V., *et al.* (2007). Two-step femtosecond laser ablation-based method for the synthesis of stable and ultra-pure gold nanoparticles in water. *Appl Phys A: Mater Sci* 88: 269-272.
- Besner, S., Winnik, F. *et al* (2008). Ultrafast laser based “green” synthesis of non-toxic nanoparticles in aqueous solutions. *Appl Phys A: Mater Sci* 93: 955-959.
- Dordunoo, S. K., Burt H. M. (1996). Solubility and stability of taxol: effects of buffers and cyclodextrins. *Int J Pharm* 133: 191-201.
- Gi, U.-S., Bumchan M., *et al.* (2004). Preparation and characterization of paclitaxel from plant cell culture. *Korean J Chem Eng* 21: 816-820.
- Hobley, J. N., Kajimoto T., *et al* (2007). Formation of 3,4,9,10-perylenetetracarboxylicdianhydride nanoparticles with perylene and polyne byproducts by 355 nm nanosecond pulsed laser ablation of microcrystal suspensions. *J Photoch Photobio A*, 189: 105-113.
- Jiaher, T., Valentino J. S. (2008). Degradation of paclitaxel and related compounds in aqueous solutions I: Epimerization. *J Pharm Sci* 97: 1224-1235.
- Jiaher, T., Valentino J. S (2009). Degradation of paclitaxel and related compounds in aqueous solutions III: Degradation under acidic pH conditions and overall kinetics. *J Pharm Sci* 99: 1288-1298.
- Keck, C. M., Muller R. H. (2006). Drug nanocrystals of poorly soluble drugs produced by high pressure homogenisation. *Eur J Pharm Biopharm* 62: 3-16.
- Liggins, R. T., Hunter W. L., *et al.* (1997). Solid-state characterization of paclitaxel. *J Pharm Sci* 86: 1458-63.
- Masuhara, H., Sigiyama T., *et al.* (2004). Formation of 10 nm-sized Oxo(phtalocyaninato)vanadium(IV) Particles by Femtosecond Laser Ablation in Water. *Chem Lett* 33: 724-725.
- Merisko-Liversidge, E., Liversidge G. G., *et al.* (2003). Nanosizing: a formulation approach for poorly-water-soluble compounds. *Eur J Pharm Sci* 18: 113-20.

- Miele Evelina, G., Ermanno P. S *et al* (2009). Albumin-bound formulation of paclitaxel (Abraxane® ABI-007) in the treatment of breast cancer. *Int J Nanomedicine* 4: 99-105.
- Muller, R. H., Jacobs C., *et al.* (2001). Nanosuspensions as particulate drug formulations in therapy. Rationale for development and what we can expect for the future. *Adv Drug Deliv Rev* 47: 3-19.
- Nagare, S., Senna M. (2004). Reagglomeration mechanism of drug nanoparticles by pulsed laser deposition. *Solid State Ionics* 172: 243-247.
- Pyo, S.-H., Cho, J-S, *et al* (2007). Preparation and Dissolution Profiles of the Amorphous, Dihydrated Crystalline, and Anhydrous Crystalline Forms of Paclitaxel. *Dry Technol* 25: 1759-1767.
- Rabinow, B. E. (2004). Nanosuspensions in drug delivery. *Nat Rev Drug Discov* 3 : 785-96.
- Singla, A. K., Garg A., *et al.* (2002). Paclitaxel and its formulations. *Int J Pharm* 235(: 179-92.
- Sugiyama, T. R., *et al.* (2009). Nanosecond laser preparation of C60 aqueous nanocolloids. *J Photoch Photobio A*, 207 :7-12.
- Sylvestre, J.-P. (2009). Fabrication of dispersed megestrol acetate nanocrystals by laser fragmentation in water. 2009 AAPS Annual Meeting and Exposition Los Angeles.
- Sylvestre, J. P. Meunier, M. *et al* (2005). Femtosecond laser ablation of gold in water: influence of the laser-produced plasma on the nanoparticle size distribution. *Appl Phys A: Mater Sci* 80: 753-758.
- Sylvestre, J. P., Meunier, M. *et al.* (2004). Stabilization and size control of gold nanoparticles during laser ablation in aqueous cyclodextrins. *J Am Chem Soc* 126: 7176-7177.
- Tamaki, Y., Asahi T., *et al.* (2002). Nanoparticle Formation of Vanadyl Phthalocyanine by Laser Ablation of Its Crystalline Powder in a Poor Solvent. *J Phys Chem A* 106: 2135-2139.
- Van Eerdenbrugh, B., Van den Mooter G., *et al.* (2008). Top-down production of drug nanocrystals: Nanosuspension stabilization, miniaturization and transformation into solid products. *Int J Pharm* 364: 64-75.

Van Eerdenbrugh, Bernard B. S., *et al.* (2009). Downscaling Drug Nanosuspension Production: Processing Aspects and Physicochemical Characterization. *AAPS PharmSciTech* 10: 44-53.

CHAPTER 5:

Discussion

The general objective of this research project has been accomplished such that uniformly small sized paclitaxel nanocrystals have been generated using the femtosecond laser technology previously employed for gold nanoparticles (Besner 2008). Ideally the fabrication of drug nanocrystals with little chemical degradation and polymorphic transformation were anticipated. However, laser fragmentation at high powers generated hydrated paclitaxel nanocrystals with considerable degradation (Table 4.2 and 4.3).

Firstly the aim to produce paclitaxel nanocrystals with diameters below 500 nm and low polydispersity (<0.3) was achieved by optimizing femtosecond laser methods. It was shown that laser ablation of the paclitaxel tablet did not generate monodisperse particles, and generally the sizes of 800 to 1500 nm were obtained. Though the two step (ablation and subsequent fragmentation) method produced desired nanocrystal size, the degradation of the drug was significant. Finally the single step fragmentation generated nanocrystals below the size of 500 nm at high powers.

Secondly, the objective of studying the impact of fabrication conditions on chemical degradation was achieved. The effect of ablation and fragmentation power on the chemical integrity of paclitaxel was monitored by an optimized HPLC assay. Even though high laser powers generated small sized nanocrystals, the integrity of the drug was compromised such that higher degradation was observed.

Thirdly, the study of the impact of fabrication conditions on morphology and polymorphic state was realized. It was established that femtosecond laser fragmentation of anhydrous paclitaxel at high power, generated hydrated nanocrystals with crystalline character.

Before the production and evaluation of the drug nanocrystals, an HPLC assay was standardized (Appendix III). In the following sections, the key aspects of this research project: the optimization of ablation and fragmentation methods, attempt to decrease degradation and finally the characterisation of the optimal nanocrystals are discussed in further detail.

5.1 Optimization of laser ablation procedure

The parameters investigated to obtain optimal laser ablation conditions included power, focusing condition (z position) and time. By changing the laser power it was possible to alter the energy provided to ablate the tablet, thus affecting the ablation rate, the plasma formation over the surface and the cavitation dynamics in water. The variation of the position of the tablet with respect to the focal plane of the focusing objective (z position) allowed for the irradiation fluence to be varied (section 3.2) influencing the size and degradation of the drug particles. In addition, the time of ablation was varied to determine the optimal duration of ablation for the least degraded and smallest sized particles.

Firstly, femtosecond laser ablation was studied as a function of power and focusing conditions. All three focusing positions ($z = 0, 1$ and 1.5 mm), demonstrated that as the power increased from 25 to 400 mW, the concentration of the paclitaxel nanocrystals in suspension also increased (Figure 4.3 top). At higher powers, stronger ablation occurred resulting in greater amounts of drug particles being generated in suspension. With this increase in drug amount, an increase in degradation was also observed (data not shown). This could be explained as follows, as femtosecond radiation acted on a solid target (paclitaxel tablet), the energy was absorbed by the target. Then, several picoseconds after the laser pulse, the radiation-related ablation of material occurred, resulting in the ejection of small clusters (Sylvestre 2005). The nano-clusters coalesced during their subsequent cooling in the ambient medium, forming particles in the nanometer size range. Moreover, as the laser power increased, the water layer just above the target surface strongly absorbed the radiation (referred to as optical breakdown), and became ionized forming a hot plasma. Heat transfer from the plasma to the target and shock wave production generated by the plasma expansion etched the surface and caused the ejection of large nanoclusters. This mechanism was previously proposed for the fabrication of gold nanoparticle by femtosecond laser ablation in water. In addition, it was previously

suggested that the formation and collapse of the cavitation bubble (section 3.2) also lead to ablation of the gold surface. In this project, the ablation of paclitaxel tablet probably took place in the similar manner.

The size of the particles was independent of the laser power, since particles ranging from 800-1500 nm were observed. Previously femtosecond laser ablation of a gold target in suspension generated smaller nanoparticles at lower laser fluences (Kabashin, 2003). This was not the case for the generation of paclitaxel nanocrystals and the difference may be due to the friability of the drug tablet.

To better understand the ablation process, the surface of the tablets ablated at a low and high power were analysed by SEM (Figure 5.1). The crater formed at low power (50 mW) displayed fine lines depicting the path of the laser beam, whereas ablation at higher power (250 mW) displayed a uniform circle on the surface of the tablet, showing that the ablated area increased with the laser fluence (power), thus resulting in overlap at the ablated regions from one line to the next. Augmentation of the ablated area with laser power was also observed for the production of gold nanoparticles using the same femtosecond laser technique and was attributed to greater heating effects at higher powers (Kabashin, 2003).

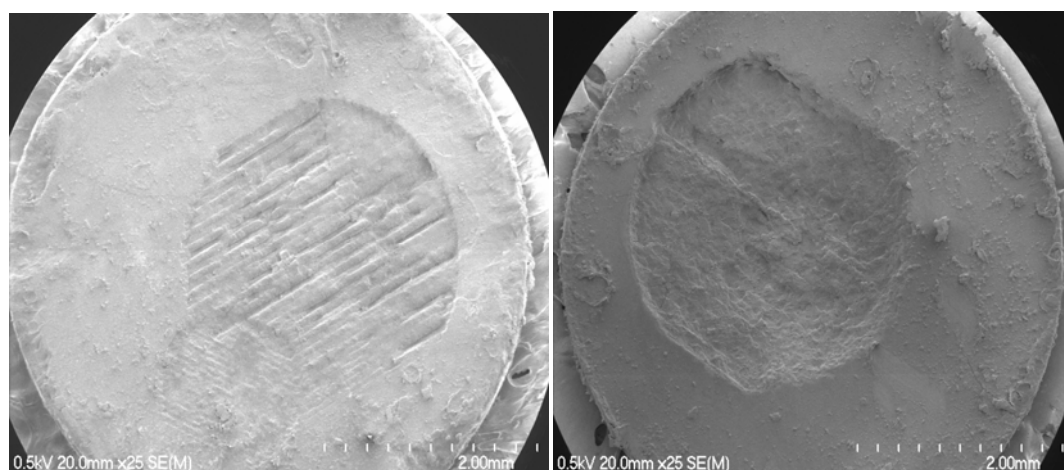


Figure 5.1: SEM images of craters formed with ablation ($z = 1$ mm, 20 min) on the surface of paclitaxel tablet at 50 mW (Left) and 250 mW (Right).

Ablation at position $z = 1.5$ mm produced higher concentrated drug suspensions because of the enlargement of the irradiation spot on the tablet surface (Figure 4.1iii). Previously, for the ablation of gold nanoparticles by fs laser ablation, it was shown that an enlargement of irradiation spot size due to change in focusing condition (z position) led to lower amount ablated as a result of reduced laser fluence. However, in our study, it was observed that as z position increased, a larger irradiation spot led to more drug being ablated and thus more particles in suspension (Figure 4.3 top). This result suggested that ablation of paclitaxel can be achieved at lower fluences than gold. This was perhaps not surprising considering that only intermolecular interactions between the paclitaxel molecules need to be broken, rather than the stronger bonds between the gold atoms, for ablation to occur. Moreover, the paclitaxel tablet was much more friable than gold, which made it more prone to mechanical erosion due to cavitation effects. Ablation at $z = 0$ mm generated the least amount of paclitaxel nanoparticles as well as the least degradation (Table 4.1). The low amounts of drug ablated at the surface may be due to the smaller irradiation spot size ablating the tablet, and to a significant laser energy loss due to absorption in water (optical breakdown) above the drug tablet, a phenomenon observed during ablation of gold (Sylvestre 2005).

Ablation at 150 mW and $z = 1$ mm resulted in the highest amount of drug concentration with the least amount of degradation (Table 4.2). By focusing the laser beam at 1 mm into the tablets, the time of ablation was evaluated as a function of power (Figure 4.3 bottom). Indeed 20 min was the optimal time of ablation because it provided the highest amount of drug with the least degradation. It was observed that the paclitaxel concentration reached a plateau after 20 min of ablation. This may be explained by the fact that as more particles were generated the suspension became opaque, thereby scattering the laser beam and reducing the intensity of the laser

energy reaching the tablet surface. Due to the decreased energy, ablation of the tablet was inefficient after 20 min; therefore the concentration of the drug remained constant. Though it was suspected that ablation efficiency decreased after 20 min, there was an increase in degradation as time of ablation increased. The particles in suspension (produced *via* ablation) interacted with the laser energy more frequently and thus degradation increased as a function of time.

5.2 Optimization of fragmentation (following ablation)

Once the ablation process was optimized at $z = 1$ mm, for 20 min at 150 mW, further size refinement of the drug particles was carried by fragmentation. A stock colloidal suspension was prepared *via* ablation and from this suspension; samples were withdrawn and fragmented at individual power ranging from 25-400 mW. Large nanocrystals generated by laser ablation interacted more strongly with the radiation and fragmented, resulting in a narrower and smaller size distribution. As fragmentation power increased, smaller sized particles were obtained, but degradation increased once again (data not shown).

The effect of the concentration and type of surfactant on the size and degradation of paclitaxel was studied (Table 5.1). Ablation was performed at the optimal conditions described above and fragmentation was performed at 150 mW for 60 min. Increasing the poloxamer 188 (Pluronic F68[®]) concentration had no significant effect on the final size and degradation of the nanoparticles. Ablation and fragmentation in Solutol HS-15 (polyethylene glycol 660 hydroxystearate) generated particles with much lower degradation however very large particles were obtained. It was suspected that the larger particles had less interaction with the laser irradiation and thus degraded to a lesser extent.

Table 5.1: Degradation and size analysis of paclitaxel particles generated by ablation and fragmentation in two different surfactants at various concentrations $n=1$.

Surfactant Concentration (μM)	% Degradation		Final size distribution	
	Ablation	Fragmentation	Size (nm)	PDI
<i>Pluronic F68</i>				
0.238	10.4	14.3	1000 ± 100	0.2 ± 0.06
0.952	9.5	11.1	980 ± 10	0.4 ± 0.07
1.785	8.9	10.3	950 ± 50	0.5 ± 0.04
<i>Solutol HS-15</i>				
0.238	4.1	7.32	5400 ± 200	0.4 ± 0.1
0.952	6.9	8.6	4600 ± 550	0.5 ± 0.2
1.785	6.5	8.2	2900 ± 250	0.3 ± 0.04

5.3 Optimization of single-step fragmentation strategy

The two-step femtosecond laser strategy: (ablation followed by fragmentation) was inconvenient in generating small sized paclitaxel nanoparticles (≤ 500 nm) with low degradation ($\leq 2\%$). In addition, the concentration of paclitaxel in suspension was limited by the amount of drug ablated in the first step. Hence, an alternative fragmentation single step fragmentation method was introduced, in which a paclitaxel suspension was prepared directly by adding drug to a surfactant solution. Poloxamer 188 was selected as a suitable surfactant because it proved to fabricate smaller particles in comparison to other surfactants (Table 5.1). Four different drug suspensions were prepared and subjected to fragmentation at 400 mW. The size and degradation of the fragmented suspension were evaluated to determine which concentration provided homogenous nanocrystals (Table 5.2). The least concentrated suspension (177 $\mu\text{g/mL}$) demonstrated the least degradation and the smallest sized nanoparticles. The higher concentrated paclitaxel suspensions were not homogenous, therefore all further experimentation was performed using paclitaxel suspensions with a concentration less than 200 $\mu\text{g/mL}$.

Table 5.2: Degradation and size analysis of fragmented paclitaxel suspension, n=1

[Paclitaxel] ($\mu\text{g/mL}$)	% Degradation	Size (nm)	PdI
177.6	0.2	311 ± 6	0.6 ± 0.05
312.5	1.1	288 ± 21	0.5 ± 0.05
793.4	0.9	321 ± 20	0.5 ± 0.02
642.7	1.1	272 ± 2.8	0.4 ± 0.03

Paclitaxel suspensions (≈ 200 $\mu\text{g/mL}$) were fragmented for 60 min at powers ranging from 50-400 mW (Table 4.3). At lower power, microcrystals (≈ 3 μm) were obtained with acceptable degradation ($\approx 1\%$). As the laser power was increased, smaller particles were generated, resulting in nanocrystals (400 nm) with substantial degradation ($\approx 23\%$). Though this single step fragmentation process yielded good

size distribution, the degradation was relatively high and therefore various strategies were investigated to reduce the oxidation.

Suspecting that the degradation may be due to oxidation, fragmentation studies were conducted using anti-oxidant (L-cysteine), however no change in degradation was observed. Further, fragmentation was performed under inert conditions using argon in a closed system. The paclitaxel suspensions were bubbled under argon for 10 min prior to fragmentation, and then kept in the inert environment during the laser treatment. Once again, no difference in degradation was observed, suggesting that degradation of paclitaxel was not a result of oxidation induced by reactive oxygen species present in solution. Suspecting that the degradation products might be of a different size than the paclitaxel nanocrystals or in solution, size exclusion chromatography was performed. Several fractions were collected and assayed *via* HPLC for degradation products and DLS for size. The degradation products were not separable from paclitaxel, and so it was concluded that fragmentation at high power produced nanocrystals with degradation on the surface of the drug crystal.

The possible explanation for the generation of paclitaxel degradation upon high power laser fragmentation was based upon the formation of a localized hot plasma in the aqueous environment. Indeed, during laser fragmentation, optical breakdown (generation of a plasma accompanied by cavitation effects) in water occurred in a small volume near the focal point of the lense. As the power increased, the intensity of the plasma increased, thereby increasing the thermal and mechanical effects (Sylvestre 2005; Besner 2006). It is likely that this thermal and mechanical energy (cavitation, also suggested as a size reduction mechanism in homogenization, see Chapter 2) produced in the water through optical breakdown is transferred to the nearby drug particles thereby fragmenting them into nanoparticles. In the process, the thermal energy could however induce chemical degradation of the drug. Consequently, as the laser power was increased, smaller particles were obtained due to increased fragmentation efficiency, but larger degradation was observed (Table 4.3).

5.4 Optimization of fragmentation in larger volume

As characterization tests required a substantial amount of sample (*eg.* 15 mg for XRD) a “scale up” process for the generation of paclitaxel nanocrystals was attempted. Previously laser fragmentation was carried in volume of 2.5 mL, consisting of 500 µg of paclitaxel. To obtain a minimum of 20 mg of dried paclitaxel nanoparticles for characterization studies, fragmentation (400 mW) in a 10 mL volume was employed. The larger volume fragmentation generated large sized particles with much lower degradation in comparison to the traditional method (Table 5.3). In order to refine the size, an additional hour of fragmentation was performed which reduced particle size to 1800 nm, however degradation of the drug increased. As the volume of fragmentation increased, the likelihood of the particles interacting with the laser decreased. Even though the energy of the system remained constant at 400 mW, the larger volume caused the fragmentation efficiency to decrease, thus generating larger sized particles. Since the particles were not being fragmented as much due to decreased contact with the laser beam, less degradation took place.

Table 5.3: Fragmentation process in large volume (10 mL) at 400 mW, n=1.

Time	Volume (ml)	% degradation	Size (nm)	PDI
0	0	0	17000 ± 3000	0.4 ± 0.2
1 h	2.5	25.1	400 ± 60	0.30 ± 0.07
1 h	10	2.3	2200 ± 60	0.3 ± 0.08
2 h	10	4.4	1800 ± 200	0.4 ± 0.3

By these preliminary results, it was decided that a larger volume fragmentation method was not a successful strategy to fabricate nanoparticles of 400 nm, therefore several small batches of 2.5 mL were produced in order to produce over 20 mg of lyophilized paclitaxel nanocrystals.

5.5 Characterization of paclitaxel nanocrystals

After several attempts of reducing the degradation of paclitaxel nanoparticles, characterization was carried on the optimized formulation (400 nm in size, 23 % degradation). The nanocrystals remained stable and did not agglomerate for four weeks. SEM analysis confirmed the significant size reduction and showed that the needle-like morphology of the drug remained intact after fragmentation at high powers (Figure 4.4). The needle-like morphology signified that the sizes obtained by DLS (where spherical particles are assumed) reported in this thesis should be interpreted with care. While the sizes reported cannot reflect the exact dimensions of the ‘needles’, they can be used to differentiate the size reduction efficiency of the different laser processing conditions tested.

Since the fragmentation process was carried in water, it was suspected that there may be some hydration of the drug, therefore dihydrate paclitaxel was investigated in parallel to the paclitaxel nanocrystals. DSC analysis demonstrated that the laser-treated paclitaxel nanocrystals displayed a different polymorphic state than the pure anhydrous paclitaxel, since the characteristic melting endotherm at 225°C was absent (Figure 4.6). The thermal events of the laser treated sample were similar to the ones of dihydrate paclitaxel. XRD analysis further confirmed the fact that indeed femtosecond laser fragmentation at high powers generated hydrated paclitaxel (Figure 4.7). Many of the characteristic paclitaxel XRD peaks disappeared in the laser-treated sample, suggesting that the polymorphic state changed (Table 4.S1). The laser treated sample displayed peaks analogous XRD peaks to the dihydrate paclitaxel, thus confirming the fact that anhydrous drug was transformed into a hydrated form upon femtosecond laser treatment in water. Considering that the transformation of anhydrous paclitaxel into the hydrated form in presence of water is documented (Liggins 1997) and that partial hydration of the drug was observed in absence of laser treatment (Chapter 4), it is likely that any wet nanonization method would result in the hydrated form of the drug, although experimental confirmation would be required.

By analyzing the polymorphic state of the laser treated nanocrystals it was concluded that anhydrous paclitaxel became hydrated upon femtosecond laser fragmentation at high powers. The degree of hydration was questionable because there were differences in the polymorphic analysis of dihydrate and laser treated samples. The slight dissimilarity between the two samples may be due to the extensive degradation of the drug. Paclitaxel is a very sensitive compound and is susceptible to solvolysis (Dordunoo 1996). It degrades easily at high temperatures and thus suspected to be an inappropriate candidate for femtosecond laser fragmentation.

Another limitation of this technique was that the amount of drug nanocrystals produced was low. This could be resolved by employing a flow through system, in which the drug nanocrystals are transferred to another vessel for collection once the desirable size is obtained. At the same time, more drug suspension is added to the stirring fragmentation vial for nanocrystal production. By simultaneously removing the drug nanocrystals and adding new suspension to be fragmented, there is a faster generation of nanocrystals. An optimized flow through system may possibly help reduce degradation because the produced nanocrystals will be removed from the system, and avoid further laser treatment and subsequent degradation.

5.6 References

- Besner, S., Kabashin A. V, *et al.* (2006). Fragmentation of colloidal nanoparticles by femtosecond laser-induced supercontinuum generation. *Appl Phys Lett*, 89: 233122-3.
- Besner, S. Winnik, F. *et al.* (2008). Ultrafast laser based “green” synthesis of non-toxic nanoparticles in aqueous solutions. *Appl Phys A: Mater Sci*, 93: 955-959.
- Brigger, I., Dubernet C., *et al.* (2002). Nanoparticles in cancer therapy and diagnosis. *Adv. Drug Deliv. Rev*, 54 631-651.
- Date, A. A, Patravale V. B. (2004). Current strategies for engineering drug nanoparticles. *Curr Opin Colloid In*, 9: 222-235.
- Dordunoo, S. K., Burt H. M. (1996). Solubility and stability of taxol: effects of buffers and cyclodextrins. *Int J Pharm*, 133: 191-201.
- Gao, L., Zhang D., *et al.* (2008). Drug nanocrystals for the formulation of poorly soluble drugs and its application as a potential drug delivery system. *J Nanopart Res*, 10 845-862.
- Grau, M. J., Kayser O., *et al.* (2000). Nanosuspensions of poorly soluble drugs -- reproducibility of small scale production. *Int J Pharm*, 196: 155-159.
- Hu, J., K. Johnston P., *et al.* (2004). Nanoparticle Engineering Processes for Enhancing the Dissolution Rates of Poorly Water Soluble Drugs. *Drug Dev Ind Pharm*, 30: 233-245.
- Junghanns JU, *et al* (2008). Nanocrystal technology, drug delivery and clinical applications. *Int J Nanomedicine*, 3: 295-309.
- Kabashin, A. V., Meunier M. (2003). Synthesis of colloidal nanoparticles during femtosecond laser ablation of gold in water. *J Appl Phys* 94: 7941-7943.
- Keck, C. M., Muller R. H. (2006). Drug nanocrystals of poorly soluble drugs produced by high pressure homogenisation. *Eur J Pharm Biopharm*, 62: 3-16.
- Kesisoglou, F., Panmai S., *et al.* (2007). Nanosizing--oral formulation development and biopharmaceutical evaluation. *Adv Drug Deliv Rev* 59: 631-44.

- Krause, K. P., Kayser, O. *et al.* (2000). Heavy metal contamination of nanosuspensions produced by high-pressure homogenisation. *Int J Pharm*, 196: 169-172.
- Merisko-Liversidge, E., G. G. Liversidge, *et al.* (2003). "Nanosizing: a formulation approach for poorly-water-soluble compounds." *Eur J Pharm Sci*, 18: 113-20.
- Merisko-Liversidge, E. M. and G. G. Liversidge (2008). Drug nanoparticles: formulating poorly water-soluble compounds. *Toxicol Pathol* 36: 43-8.
- Mosharraf, M., Nyström C. (1995). The effect of particle size and shape on the surface specific dissolution rate of micro-sized practically insoluble drugs. *Int. J. Pharm*, 122: 35-47.
- Müller, R. H., Jacobs C., *et al.* (2001). Nanosuspensions as particulate drug formulations in therapy rationale for development and what we can expect for the future. *Adv. Drug Deliv. Rev*, 47: 3-19.
- Müller, R. H., Peters K (1998). Nanosuspensions for the formulation of poorly soluble drugs I. Preparation by a size-reduction technique. *Int. J. Pharm*, 160: 229-237.
- Muller, R. H., Keck C. M. (2004). Challenges and solutions for the delivery of biotech drugs - a review of drug nanocrystal technology and lipid nanoparticles. *J Biotechnol*, 113: 151-170.
- Patravale, V. B., Date A. A., *et al.* (2004). Nanosuspensions: a promising drug delivery strategy." *J Pharm Pharmacol* 56: 827-840.
- Rabinow, B. E. (2004). Nanosuspension in drug delivery. *Nat. Rev. Drug Discov* 3: 785-796.
- Singla, A. K., A. Garg, *et al.* (2002). Paclitaxel and its formulations. *Int J Pharm* 235:179-92.
- Sylvestre, J. P., Kabashin A. V, *et al.* (2005). Femtosecond laser ablation of gold in water: influence of the laser-produced plasma on the nanoparticle size distribution. *Appl Phys A: Mater Sci* 80: 753-758.
- Teeranachaideekul, V. Junyaprasert V. B, *et al.* (2008). Development of ascorbyl palmitate nanocrystals applying the nanosuspension technology. *Int J Pharm*, 354: 227-34.

Van Eerdenbrugh, Van den Mooter B., G., *et al.* (2008). Top-down production of drug nanocrystals: Nanosuspension stabilization, miniaturization and transformation into solid products. *Int J Pharm*, 364(1): 64-75.

Zhang, Z.-B., Shen Z.-G., *et al.* (2009). Nanonization of Megestrol Acetate by Liquid Precipitation. *Ind Eng Chem Res* 48: 8493-8499.

CHAPTER 6:

Conclusion and Perspectives

To our knowledge, this was the first study in which active pharmaceutical ingredient was used for the fabrication of nanocrystals using a femtosecond laser technology, and complete characterization was conducted. Small sized and stable paclitaxel nanocrystals were produced in a contamination-free aqueous environment. The limitation of this technique was the considerable degradation of paclitaxel, however this could have been reduced by substituting with less sensitive drugs. It was suspected that degradation of the drug was a consequence of the thermal effects generated by the plasma at high powers. Further investigation on the generation of plasma would have confirmed this theory.

Despite the degradation observed in this study, the femtosecond laser fragmentation could be an efficient tool for preclinical evaluation of many drug candidates. Early identification of formulation strategies help guide drug molecules through preclinical development. Often times limited amounts of the compound are available therefore formulation approaches using minute amounts of drug are necessary for evaluation. The conventional methods used to fabricate drug nanocrystals typically require large amounts of drug. Therefore the femtosecond laser fragmentation may be utilized to investigate the formulation of the drug as nanocrystals, using scarce amounts (μg to mg). If the screening tests (*eg.* bioavailability study) prove the nanocrystal formulation to be successful in enhancing the solubility of the drug, then conventional (*eg.* Nanocrystal[®] technology by Elan) methods may be applied to produce greater amounts of drug nanocrystals (Gao 2008).

Other projects in the lab; fragmentation of less sensitive drugs (*eg.* megestrol acetate) suggests that fs laser fragmentation may be an alternative route for the production of nanoparticles of other poorly water soluble and less sensitive drugs (Sylvestre 2009). Suggestions to improve this project involve the nanonization of several less sensitive drugs using fs laser fabrication. The oral bioavailability, pharmacokinetics and anticancer activity of the reformulated drugs would then be investigated. In addition, it would be interesting to design a continuous flow cell to enhance the efficiency of the fs-laser fragmentation method for the fabrication of

nanocrystals. Upon successful achievement, this work may translate into successful future avenues for the production of drug nanocrystals for an array of pathologies including cancer and infectious diseases.

References

- Besner, S., Kabashin A. V., *et al.* (2006). Fragmentation of colloidal nanoparticles by femtosecond laser-induced supercontinuum generation. *Appl Phys Lett* 89: 233122-3.
- Besner, S., Winnik, F. *et al* (2008). Ultrafast laser based “green” synthesis of non-toxic nanoparticles in aqueous solutions. *Appl Phys A: Mater Sci* 93(4): 955-959.
- Gao, L., Zhang D., *et al.* (2008). Drug nanocrystals for the formulation of poorly soluble drugs and its application as a potential drug delivery system. *J Nanopart Res* 10: 845-862.
- Sylvestre, J.-P. (2009). Fabrication of dispersed megestrol acetate nanocrystals by laser fragmentation in water. 2009 AAPS Annual Meeting and Exposition, Los Angeles
- Sylvestre, J. P., Meunier, M. *et al* (2004). Stabilization and size control of gold nanoparticles during laser ablation in aqueous cyclodextrins. *J Am Chem Soc* 126: 7176-7177.

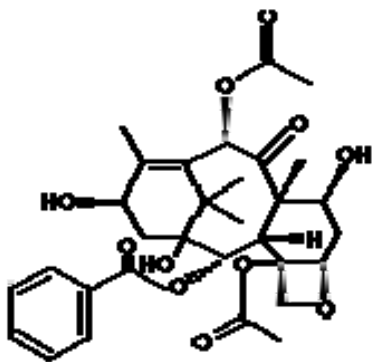
Appendix I: Mononuclear phagocyte system

The mononuclear phagocyte system (MPS) (also referred to as the reticuloendothelial system) is a network of macrophages and their precursors in the body's tissues, which is concentrated in the bone marrow, liver, spleen, and lymph nodes. Macrophages are large phagocytic cells that clear the blood, lymph and tissues of particles (*eg.* bacteria, cell debris etc..).

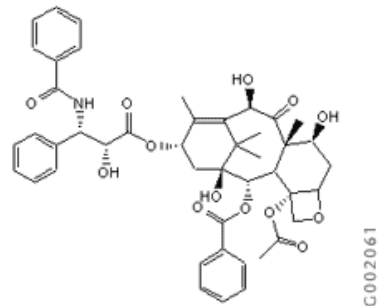
Hume, D. A., Ross, I. L. *et al.* (2002). The mononuclear phagocyte system revisited. *J Leukoc Biol* 72: 621-627

Appendix II : Degradation products of paclitaxel

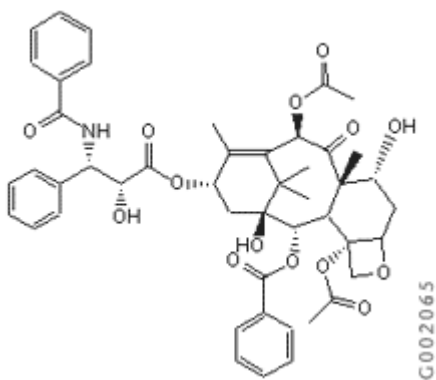
Bacattin



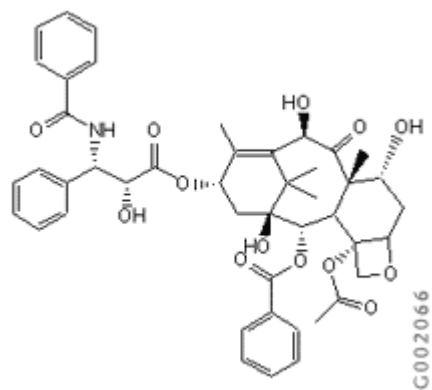
10-deacetyl paclitaxel



7-epi paclitaxel



10-deacetyl-7-epi paclitaxel



Appendix III: HPLC Assay

The chemical integrity of paclitaxel was monitored by HPLC using a C18 reverse phase column and an eluent mixture containing acetonitrile and water using procedures previously validated for paclitaxel (www.uspnf.com). Calibration curves for paclitaxel and the degradation products; Baccatin III (Bac), 10-Deacetylpaclitaxel (DPTX), 10-Deacetyl-7-epipaclitaxel (DEPTX), 7-Epipaclitaxel (EPTX) were established prior to the testing of nanocrystals generated by the femtosecond laser. The products were assayed according to the tests described in the United States Pharmacopoeia respective monographies. The paclitaxel content ($\mu\text{g/mL}$) was calculated based upon an established calibration curve [$y = mx + b$], where y is the area of paclitaxel divided by the area of DPH, and x is the concentration ($\mu\text{g/mL}$) of paclitaxel in the sample. The concentration of each degradation product was calculated in the similar manner using calibration curves. The sum of degradation products ($\mu\text{g/mL}$) was divided by the sum of paclitaxel and total degradation, and then multiplied by 100 to obtain the percent degradation. Below are the chromatographic profiles of paclitaxel and the degradation products.

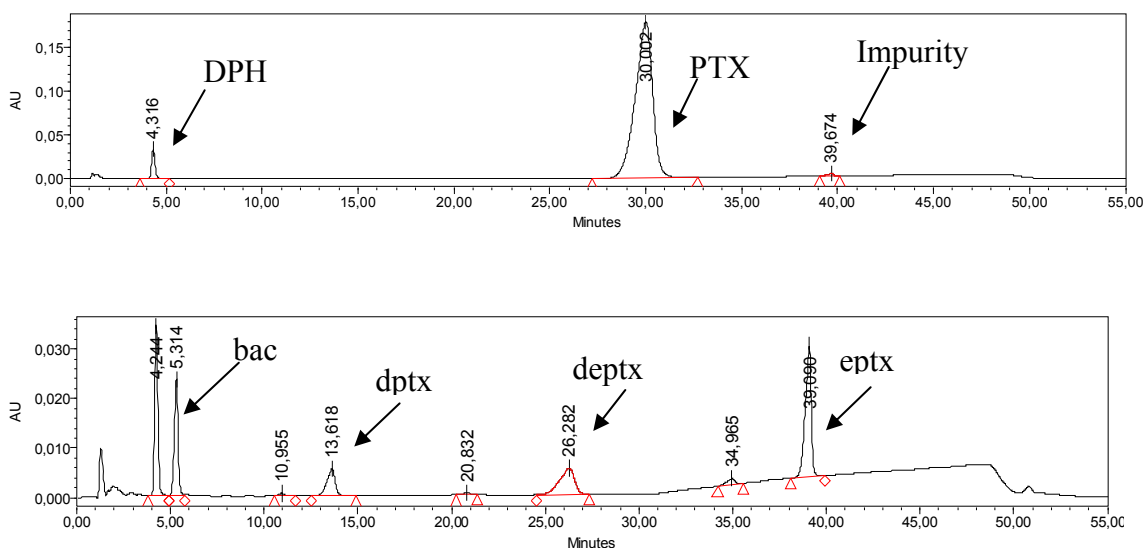


Figure A3: HPLC assay of paclitaxel (top) and degradation products (bottom).

The impurity of paclitaxel was calculated as 0.5 %, which was in agreement of the manufacture's certificate of analysis. The additional peaks observed in the chromatograph of the degradation products results from minor impurities which were present in the drug as purchased.

The calibration curves were carried every month to ensure the adequate calculation of the degradation in the fragmented samples.